NASA TECHNICAL MEMORANDUM NASA TM-76703

THE ANALYSIS OF TURBULENT FLOW BY HOT WIRE SIGNALS

M. Bartenwerfer

Translation of "Zur Analyse von Hitzdrahtsignalen turbulenter Strömungen," Physikalische Ingenieurwissenschaft der Technischen Universität Berlin, Berlin (West Germany), Doctoral Dissertation, 1981, pp. 1-142

NATIONAL AERONAUTICS AND SPACE ADMINISTRATION
WASHINGTON, D.C. 20546 APRIL 1982

STANDARD TITLE PAGE

1. Report No. NASA TM-76703	2. Government Accession No.	3. Recipient's Catalog No.
4. Title and Subtitle THE ANALYSIS OF TURBULENT FLOW BY HOT WIRE SIGNALS		5. Report Date April 1982 6. Performing Organization Code
7. Author(s) M. Bartenwerfer		8. Performing Organization Report No. 10. Work Unit No.
9. Performing Organization Name and Address Leo Kanner Associates Redwood City CA 94063		11. Contract or Grant No. NASW-3541 13. Type of Report and Period Covered Translation
12. Sponsoring Agency Name and Address National Aeronautics and Space Administration, Washington DC 20546		14. Sponsoring Agency Code

15. Supplementary Notes

Translation of "Zur Analyse von Hitzdrahtsignalen turbulenter Strömungen," Physikalische Ingenieurwissenschaft der Technischen Universität Berlin, Berlin (West Germany), Doctoral Dissertation, 1981, pp. 1-142.

16. Abstract

When measuring velocities in turbulent gas flows, one must rely on approximation-signal analysis with hot-wire anemometers having one and two-wire probes. By a numeric test of standard analyses it can be shown that the resulting systematic error increases quickly with increasing turbulent intensity. Since it also depends on the turbulence structure it cannot be corrected. The use of such probes is thus restricted to low turbulence. By means of three-wire probes (in two-dimensional flows with X-wire probes) in principle instantaneous values of velocity can be determined, and an asymmetric arrangement of wires has a theoretical advantage.

17. Key Words (Selected by Author(s))	18. Distribution Statement
	Unclassified - Unlimited

19. Security Classif. (of this report)	20. Security Classif. (of this page)	21. No. of Pages	22.
Unclassified	Unclassified		

CONTENTS

Symbols

/4*

A_1	1=1,2,3; fluctuation amplitude of component 1 (eq. 45)
A_{1m}	1,m = 1,2,3; orthogonal 3x3-matrix which represents a rotation
$\underline{\underline{A}}$	Brief notation for the matrix (the tensor) A_{1m}
a_o	Speed of sound in air
$a_{1m}(\alpha,\beta)$	1,m = 1,2,3; symmetric, positively defined quadratic form (equation 4)
$\underline{\underline{B}}$	Brief notation for the matrix B_{1m}; 1,m = 1,2,3 (eq. 53)
$b_{1m}(\alpha_i,\beta_i)$	1,m = 1,2,3; i=1,...,6; coefficients (eq. 7.1-7.9 & app. C)
C	Coefficient (eq. 48.3)
C_1	$\overline{\quad}^{2}$ (eq. 46)
C_1	$= \overline{u_1'^2}/\overline{u_1'^2}$; 1 = 2,3; (eq. 46)
C_{1m}	$= \frac{\overline{u_1' u_m'}}{\sqrt{\overline{u_1'^2}}\sqrt{\overline{u_m'^2}}}$; 1, m = 1,2,3; 1≠m (eq. 46)
c	$= e^2$ (equations 43)
$\overline{c_{i/j}}^2$	$= \frac{1}{2}(\overline{c_i}^2 + \overline{c_j}^2)$ (eq. 43.8)
d	Wire diameter
$\underline{\hat{d}}$	Unit vector ($\hat{d}^2$=1) representing the wire direction
$\overline{d_{i/j}}$	$= \overline{c_i} - \overline{c_j}$ (eq. 43.8)
det($\underline{\underline{A}}$)	Determinant of matrix $\underline{\underline{A}}$
E, E_o	Electric output voltage of an anemometer
e	= E/K
$\tilde{e}_1^2$, $\tilde{e}_1$	1 = 1,2,3; see eq. (12) and (14)
$\check{e}_1$	1 = 1,2,3; see eq. (17)
F	Correction factor for conventional analysis (eq. 36)
F_q	Correction factor for analysis via squared signals (eq.43.9)
Fkt(...)	Monotone function of an argument

*Numbers in the margin indicate pagination in the foreign text.

f	Frequency
$g(t',s,\sigma)$	Periodic stair function to simulate a turbulent speed fluctuation (equation 44)
h	≈ 1, factor of cooling by flows perpendicular to the hot wire and perpendicular to the prongs (eq. 3)
K	>0, proportionality constant (unit Vs/m; eq. 2)
k	$1>>k\geq 0$. Factor of tangential cooling (eq. 1)
l	(effective) length of a hot wire
l'	Ratio of effective length of a hot wire to its total length
$0((...)^n)$	Remainder n-th order of a Taylor expansion
p	Pressure
s	Jump point of a stair function in the interval (0,1)(eq.44)
$\text{sign}(...)$	Sign of the argument
T	Periodicity of a periodic fluctuation
t	Time
t'	$=t/T$
$\underline{u}$, $\underline{u}(t)$	Vector of instantaneous speed
u_l	$l=1,2,3$; orthogonal components of the speed vector $\underline{u}$
u_l'	$l=1,2,3$; orthogonal components of average speed
U	≥ 0, absolute value of average speed
$u_\perp$, $u_\parallel$	Components of speed $\underline{u}$ orthogonal or parallel to the hot wire respectively.
u_{eff}	$=\sqrt{u_\perp^2+k^2u_\parallel^2}$, effective speed
$u_{l\omega}'$	$l=1,2,3$; frequency component of u_l' at the frequency $f=\omega/2\pi$ (narrow-band filtered signal $\Delta u_l'/\sqrt{\Delta\omega}$)
$v_{1/2}$	$=\sqrt{a_{11}}u_1 \mp \sqrt{a_{22}}u_2$, see equation (22)
v_l	$l=1,2,3$; speed components of $\underline{u}$ with respect to an orthogonal coordinate system $\hat{y}_l$ $(l=\bar{1},2,3)$

$w_1(u_1)$	1=1,2,3; probability distributions for the speed components u_1 /6
w_j	j=1,...,6; abbreviations (eq. 66.1-66.6)
$\underline{x}$	Space point (local vector)
$\underline{\hat{x}}_1$	1=1,2,3; base vectors of a right-hand oriented orthogonal coordinate system
$\underline{\hat{y}}_1$	1=1,2,3; base vectors of a flow-line-related right-hand oriented orthogonal coordinate system
α	Polar angle with respect to the x_1-axis
α_1, β_1	Fourier coefficients; 1,m = 0,1,2; equation (63)
Γ	$= \overline{u'^4}/\overline{u'^2}^2$, convexity (bulging) factor
γ	Adjusted angle of the probe
Δ	Angle between the instantaneous flow direction and probe axis
Δ_{1m}	$= \left(\frac{\overline{u_1' u_m'}}{\overline{u^2}}\right)_{\text{approx.}} / \left(\frac{\overline{u_1' u_m'}}{\overline{u^2}}\right)_{\text{exact}} - 1$
ϑ	$=54.7^\circ$, angle between the edge of a cube and its space diagonals
δ_{1k}	Kronecker symbol (=1 for 1=k, otherwise = 0)
$\varepsilon_{1/2}$	$= \left(\overline{(e_2'-e_1')^2}/4\,\bar{e}_{1/2}^2\right)^{1/2}$
θ	Azimuth angle (in the x_2x_3-plane, related to x_2)
ξ, η^2	Abbreviations for fluctuation terms in eq. (28)
λ, μ, ν	Anisotropy factors (eq. 34)
λ_q, μ_q, ν_q	Anisotropy factors in an analysis via the squared signals (eq. 43)
ρ	Air density
σ	Jump point of a stair function in the interval (0,1)(eq.44)
ϕ	Angle between the direction of (u_1,u_2) and the x_1-axis (equation 25)
ϕ, ϕ_p	Angle between certain lines and the x_1-axis (eq. 23 & 24)
Ω_D	Angular velocity of a rotating hot-wire
$.....'$	Fluctuation
$\overline{.....}$	Time average

$\|....\|$	Absolute value of a scalar or vector
$=$	Equality
$\equiv$	Identity
$-$	Asymptotic equivalence (Taylor series)
$=:$ $:=$	Definition equivalence character (the quantity to be defined is on the side of the colon)
$\leftrightarrow$	Equivalence

/7

THE ANALYSIS OF TURBULENT FLOW BY HOT WIRE SIGNALS

M. Bartenwerfer

1. Most technically important flows of gases or liquids are turbulent flows. As a rule, these flows are stationary in a time-average, so that the quantities of state of the flow medium are composed of time-independent averages and stochastic fluctuations, for instance: /8

$$\left.\begin{array}{l}\text{Pressure}\\ \text{Velocity}\end{array}\right| \begin{array}{l} p(\underline{x},t) = \overline{p}(\underline{x})+p'(\underline{x},t) \text{ with } \overline{p}'=0,\\ \underline{u}(\underline{x},t) = \overline{\underline{u}}(\underline{x})+\underline{u}'(\underline{x},t) \text{ with } \overline{\underline{u}}'=0\ . \end{array}$$

Flow fields can only be described phenomenologically and theoretically when the speed is measurable. In contrast to laminar flows, for turbulent flows, not only is the average speed $\overline{u}$ to be determined, but the fluctuations must be characterized, e.g. by specific time averages. Depending on the type of theoretical description, these can be correlations $\overline{u_i' u_j'}$ $(i,j=1,2,3)$ as important quantities of the Reynolds stress tensor $\rho\overline{u_i'u_j'}$ or even correlations of higher order, e.g. $\overline{u_i'u_j'u_l'}$, $\overline{u_i'u_j'u_l'u_m'}$ $(i,j,l,m=1,2,3)$.

Many measurement methods suitable for laminar stationary flows, for instance, for the Prandtl static tube, are not suitable for measurements in turbulent flows, since the correct, average speed is not measured and since average values of the fluctuations cannot be measured at all.

Now it is a known fact that a warm body in a cooler, flowing gas cools off faster the "stronger the wind" and the greater the temperature difference between the body and the gas. According to this principle, hot-wire anemometers measure speeds and their fluctuations in flowing media. The potential measurement of temperature fluctuations will not be discussed here, rather--except for the small, turbulent temperature fluctuations--a constant temperature shall be assumed at the measurement location.

A thin wire tied between two prongs is heated electrically. /9
In order to keep the temperature of the wire constant over time during the initially laminar flow, more heat per time unit must be generated, the greater the rate of flow of the moving gas. The heat removal is affected significantly by the speed component perpendicular to the wire, and only a little by the component parallel to the wire--if it is not neglected entirely. At any rate, the heat flow grows uniformly with these two components, if we neglect any possible influence of the prongs and/or the probe shaft.

Through suitable electronic circuits--summaries e.g. in Bradshaw [1], Strickert [2], Comte-Bellot [3]--it is possible to keep the wire temperature or heating current of the wire constant in a chronologically changing speed, or in a turbulent flow, and a starting voltage of the anemometer will increase uniformly with the heat flow, or uniformly with the speed. Through comparison measurements, advantages and disadvantages of the constant-temperature or constant-current anemometer were derived, e.g. by Helland and van Atta [4]. At present, the anemometers with constant wire temperature seem to be preferred.

As already mentioned, as a rule the hot-wire is cooled much more by a perpendicular flow than by a parallel one. If the wire diameter d ratio to the effective wire length l is sufficiently small (d|l < 1|200), then for many probes or anemometers, a good approximation is:

$$E^2 - E_o^2 = Fkt\,(u_\perp^2 + k^2 u_\parallel^2) \qquad (1)$$

with E = operating voltage of the anemometer,
E_o = operating voltage of the anemometer at u = 0,
Fkt() = monotonous function of the argument, Fkt(0) = 0
$u_\perp$ = velocity component perpendicular to the hot wire
$u_\parallel$ = velocity component parallel to the hot wire (see fig. 1)
k^2 = Velocity-independent constant $k^2 \ll 1$, $k^2 \approx 0.04$ for $d/l \approx 1/200$.

For other probes, using an accurate observation of the heat transfer over a large velocity range or when noting the prong-influence, in the literature equations other than (1) are given, e.g. by Hinze [5], Webster [6], Corrsin [7], Champagne et al. [8], Davies and Bruun [9], Friehe and Schwarz [10]. /10

Surprisingly, regarding the used equation (1), the parallel component $u_\parallel$ cools the wire much less ($k^2 \ll 1$) than the perpendicular component $u_\perp$, but it acts with the same exponent 2. Simmons and Bailey [11] found in 1927 that the heat loss of an electrically-heated filament increases linearly with the rate of flow in a parallel-flowing stream, but in a perpendicular stream, it increases linearly with the square-root of the speed. Accordingly, if an additive composition of these different cooling effects is possible, instead of (1), a relation

$$E^2 - E_o^2 = Fkt\,(u_\perp^2 + k^2 u_\parallel'')$$

would be expected. Probably, the relation (1) still proved useful because in most cases, the tangential cooling represents only a correction. In particular, in modern hot-wire probes, the tangential cooling can be neglected as a rule.

If eq. (1) is true, then by using an analogous linearization step or by using a digital computer, even a proportional relation can be expected between the output signal E^2 and the square u_{eff}^2 of the "effective" velocity $u_{eff.} = \sqrt{u_\perp^2 + k^2 u_\parallel^2}$:

$$E^2 = K^2 \cdot (u_\perp^2 + k^2 \cdot u_\parallel^2) \qquad (2)$$

K = velocity-independent constant, K > 0 (unit: V_s/m).

This linearization simplifies the analysis of hot-wire signals in turbulent flows.

The experimental validation of the functional relation (1), the setting of the linearization and the determination of the constants k and K is usually performed as a calibration in a laminar or slightly /11

turbulent flow. In measurements in turbulent flows, it is assumed that the equations (1) or (2) also apply for instantaneous values of the speed and of the signals, even though the speed in a turbulent flow can change very quickly. This assumption presumes that the electronic control of the anemometer can follow the fluctuations at sufficient speed--in order to keep the wire temperature or the heating current constant--and also that the cooling of the wire can be described as quasi-stationary.

Thus, by using one point as an example, it is clear that the hot-wire measuring method is not as simple in practice as indicated by the summary presentation of measurement methods. Actually, this method is based on decades of testing, use and development. A bibliography by Freymuth [12] contains about 1300 publications on the subject of thermo-anemometry and this illustrates the scope of research work in this area in the period from 1900 to 1978.

Like all measuring methods, hot-wire measuring has its own sources of error and limitations. In the course of time, many problems have been corrected by refinement of probes and electronic equipment, but rising expectations of measuring accuracy and utility are also noted. If we presume the validity of a relation (1) or (2), we limit ourselves to incompressible, turbulent flows of constant temperature (except for the turbulent temperature fluctuations), or to low flow speeds (flow mach-number $<<1$). Vagt [13] reported on the state of the art of hot-wire probes for just this case and also discussed the occurring sources of error in detail. Thus, a summary of possible errors will suffice here for illustrating the prerequisites for further investigations.

2. Errors

/12

As for all probe measurements, it must first be assumed that the probe does not affect the flow. In general, this assumption is correct when both the sensor (hot wire) and its mount (prong, shaft) are sufficiently small or thin. The meaning of "sufficiently small" in this case, the best shape of the prongs and shaft and the size of the remaining error, must all be determined by experiment.

A sufficiently small spatial size of the hot wire is also a prerequisite for a local measurement. The speed along the wire must be viewed as constant. A velocity gradient perpendicular to the wire may not be allowed to deform it. In multi-wire probes, the speed in the entire measured volume containing all wires, must be the same. On the other hand, interaction between the wires must be excluded. The optimum hot-wire lengths and spacing will depend on the turbulence structure of the measured flow field. For incompressible flows, the diameter of the measured volume should not exceed ca.*1 mm (Hinze [5]). Figure 2 shows the outline of a modern X-wire probe which meets these requirements.

*Translator's note: ca. = about.

Even for optimized prongs and shafts, they will still disturb the axial symmetry of the stretched wire. It may then happen that the sensitivity of the wire will depend on the angle of incidence (of the probe) γ. In simpler cases, for $\gamma<\frac{\pi}{2}$ (see fig. 1), we have the following expression instead of (2):

$$E^2 = K^2 \cdot (u_{\perp 1}^2 + h^2 u_{\perp 2}^2 + k^2 u_{\parallel}^2) \quad ; \qquad (3)$$

$$k^2 \ll 1 \quad , \quad |h^2 - 1| \ll 1 \quad .$$

Neglecting this directional characteristic leads to errors when $h \neq 1$.

Due to the flow, the wire or prongs can start to vibrate; naturally this will falsify the signal compared to a fixed wire. Prong vibrations are usually recognized because they occur at a certain speed-independent Eigen frequency. Through suitable prongs, an appropriate prestretching of the hot-wire and through a useful alignment of the probe, these vibrations can be prevented, but in case of doubt, a control measurement is needed. /13

When taking measurements in boundary layers, or when the average speed depends on the location, and when as a rule turbulence quantities are to be determined, the hot-wire must be positioned with great accuracy. Both its local position and its direction with respect to a specified coordinate system must be known with sufficient accuracy. Turbulence quantities can be erroneous by an inaccurate angular setting, especially when signals of a hot-wire in various orientations are needed for their calculation.

If the probe is set near a wall, then wall influences can impede the measurement. First, the probe in connection with the wall, can disturb the flow so much that it will be changed significantly. This must be prevented by a suitable probe design and a favorable alignment of the shaft. Secondly, for heat-conducting walls, the heat is removed from the wire by differing physical laws than in a free field of flow. If this effect is ignored, very large errors can be made in the signal analysis. Wall influences cannot be determined theoretically today. It remains to be explained what minimum distance from the wall is needed to permit neglecting of the wall influences on the hot-wire signal (see Vagt [13] and works cited there).

The characteristic line of an anemometer $E=E(\underline{u}_{\perp}, \underline{u}_{\parallel}, \ldots)$ depends on many parameters which must remain constant during calibration and measurement. One of the critical quantities is the ratio of wire temperature to the surrounding temperature. The electronic control itself can be not quite stable under some circumstances--it may drift. As long as these changes are not completely understood, only a calibration before and after the measurement is of any use. /14

It was already mentioned that the hot-wire anemometer is "statically calibrated" as a rule, and that the resulting heat-transfer law also applies for instationary flows. By comparitive "dynamic calibration" using soundwaves or shaking table, this assumption has been verified by experiment; see Bechert [14], Bremhorst

and Gilmore [15], but only for low frequencies.

To measure turbulence quantities it is recommended to use a linearization step, since the analytic relation E(u) is then simple. A linearization can increase the noise level and the drift of the entire system; frequent calibration is thus indespensible. The linearization is as a rule only accurate for a certain speed range, whereby the low velocities are critical. In high-turbulence flows, the instantaneous values of speed can lie outside the "calibration range", even when the average speed lies within in. An ideal linearization is assumed here.

In the analysis of hot-wire signals of turbulent flows, low turbulence intensity is presumed throughout and a series expansion of the signal E by the small relative fluctuations u_1'/U is used. It is clear that through this restrictive condition, a systematic error increasing with increasing turbulence can occur in the speeds and their fluctuations.

This long and yet incomplete list of sources of error illustrates that only very carefully performed hot-wire measurements will give reasonable results. For a more accurate discussion of the individual errors, refer to Vagt [13] and to the works cited there. A part of the error is probe-related and development-induced, e.g. the prong influence; another part is of a fundamental nature. But over-all, the number of possible errors is very large, and many of them cannot be estimated realistically. These facts impede a quantitative error computation and thus one is not available. Experiments have shown that several errors can be of considerable magnitude and can vary greatly. This can be the reason why systematic errors have not been taken into account very much. /15

In this paper, the analysis of hot-wire signals is discussed with regard to the named systemmatic errors which follow from the series expansion of the speed fluctuations. Possibilities for an exact signal evaluation are also sought. Furthermore, we evaluate the size of the error in the relative fluctuations $\overline{u_1' u_m'}/U^2$ resulting from the use of one- or two-wire probes after the unavoidable series expansion. All other measurement errors presented above are ignored. It will be shown that the use of one- and two-wire probes is subject to fundamentally lower limits due to high turbulence than has been previously assumed.

It is also assumed that the frequently used equation:

$$E^2 = K^2 \cdot (u_\perp^2 + k^2 \cdot u_\parallel^2) \quad ; \qquad (2)$$

K,k=speed-independent constants ,

and that it applies for*:

*One could also begin from eq. (3), but essentially the same results are obtained under the standard conditions $k^2 \ll 1$ and $|h^2-1| \ll 1$.

-the instantaneous values of starting voltage and flow speeds,
-any incident-flow direction to the probe,
-all speeds below the maximum speed of $u_{max} \ll a_o$, (a_o= speed of sound).

Physically this means that ideal, linearized, hot-wire probes must be studied which /16

-are not subject to prong influences, wall influences and undergo no prong or wire vibrations,
-operate at constant temperature,
-are found in an incompressible, turbulent or laminar flow of constant temperature.

These extensive prerequisites must be met in order to obtain quantitative results. The discussed, system errors may be just as important in more general cases.

3. Exact Analyses /17

Let:

$$E = K \cdot (u_\perp^2 + k^2 u_n^2)^{n/2} \qquad (2')$$

In a rectangular, right-handed oriented coordinate system, $\hat{x}_1$, $\hat{x}_2$, $\hat{x}_3$ will now describe the direction of a hot wire by the unit vector $\hat{d}$ in polar coordinates with respect to the x_1-axis:

$$\hat{d} = \cos\alpha \hat{x}_1 + \sin\alpha \cos\theta \hat{x}_2 + \sin\alpha \sin\theta \hat{x}_3 ,$$

$$0 \leq \alpha \leq \frac{\pi}{2} ,$$

$$-\pi < \theta \leq \pi .$$

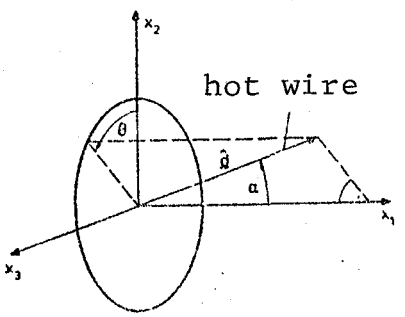

The polar angle α is the angle between the x_1-axis and the wire. It lies in a range $0 \leq \alpha \leq \frac{\pi}{2}$ which will describe all possible wire directions.

The speed $\underline{u}$ is broken down into components:

$$\underline{u} = \sum_{i=1}^{3} u_i \underline{\hat{x}}_i$$

$$\sum_{i=1}^{3} u_i^2 = \underline{u}^2 = u_1^2 + u_2^2 .$$

With:

$$u_1 = \underline{u} \cdot \underline{\hat{d}} = u_1 \cdot \cos\alpha + u_2 \cdot \sin\alpha \cdot \cos\theta + u_3 \cdot \sin\alpha \cdot \sin\theta$$

there follows for the quotient e=E/K from (2'):

$$e^2 = \sum_{l,m=1}^{3} a_{lm} \cdot u_l \cdot u_m \quad , \qquad (4)$$

$$a_{11} = 1 + (k^2-1) \cdot \cos^2\alpha \quad ,$$

$$a_{22} = 1 + (k^2-1) \cdot \sin^2\alpha \cdot \cos^2\theta \quad ,$$

$$a_{33} = 1 + (k^2-1) \cdot \sin^2\alpha \cdot \sin^2\theta \quad ,$$

$$a_{12} = (k^2-1) \cdot \cos\alpha \cdot \sin\alpha \cdot \cos\theta \quad ,$$

$$a_{23} = (k^2-1) \cdot \sin^2\alpha \cdot \cos\theta \cdot \sin\theta \quad ,$$

$$a_{31} = (k^2-1) \cdot \cos\alpha \cdot \sin\alpha \cdot \sin\theta \quad ; \quad a_{lm} = a_{ml} .$$

/18

The other goal of an exact analysis must be to obtain a system of equations

$$e_i^2 = \sum_{l,m=1}^{3} a_{lm}(\alpha_i, \theta_i) \cdot u_l \cdot u_m \quad ; \quad i = 1, \ldots, N \qquad (5)$$

through selection of several directions (α_i, θ_i): i=1,...,N which can be resolved by the three quantities:

$$u_1 = U_1 + u_1' \quad , \quad u_2 = U_2 + u_2' \quad , \quad u_3 = U_3 + u_3'$$

If this resolution were to succeed, then we would have complete information about the velocity, namely the time history profile of orthogonal velocity components. From these, one could derive any time-averages, especially the components of average velocity, U_1, U_2, U_3, the turbulence quantities $\overline{u_1'^2}, \overline{u_2'^2}, \overline{u_3'^2}, \overline{u_1'u_2'}, \overline{u_2'u_3'}, \overline{u_3'u_1'}$, and also time averages of any order.

If we select the usual orientations for X-wires, $\alpha=\frac{\pi}{4}$; $\theta=0,\pi$; $\pi/2, -\pi/2$; $\pi/4, -3\pi/4$; $3\pi/4, -\pi/4$ and denote the signals in this sequence as e_1 to e_8, then we obtain the following system of equations (derivation of these equations and explanation of matrix notation in Appendix A).

/19

$$(6.1) \quad (1-k^2)(U_1+u_1')(U_2+u_2') = (e_2^2-e_1^2)/2 = (e_8^2-e_7^2+e_6^2-e_5^2)/2\sqrt{2} \quad ,$$

$$(6.2) \quad (1-k^2)(U_2+u_2')(U_3+u_3') = (e_8^2+e_7^2)/2 - (e_6^2+e_5^2)/2 \quad ,$$

$$(6.3) \quad (1-k^2)(U_3+u_3')(U_1+u_1') = (e_4^2-e_3^2)/2 = -(e_8^2-e_7^2-e_6^2+e_5^2)/2\sqrt{2} ,$$

$$(6.4) \quad \begin{pmatrix} \frac{1+k^2}{4} & \frac{1+k^2}{4} & \frac{1}{2} \\ \frac{1+k^2}{4} & \frac{1}{2} & \frac{1+k^2}{4} \\ \frac{1+k^2}{4} & \frac{3+k^2}{8} & \frac{3+k^2}{8} \end{pmatrix} \cdot \begin{pmatrix} (U_1+u_1')^2 \\ (U_2+u_2')^2 \\ (U_3+u_3')^2 \end{pmatrix} = \begin{pmatrix} \frac{e_2^2+e_1^2}{4} \\ \frac{e_4^2+e_3^2}{4} \\ \frac{e_6^2+e_5^2}{8} + \frac{e_8^2+e_7^2}{8} \end{pmatrix} .$$

The system of equations (6.4) is not solvable because the equations are not linearly independent. In appendix B it is shown that a complete resolution of the linear equation system (5) by the formal six unknowns $u_1 \cdots u_m$ will not succeed as long as α is held constant and only θ is varied. Equations (6.1) to (6.3) give exact formulas for $U_1U_2+\overline{u'_1u'_2}$, $U_2U_3+\overline{u'_2u'_3}$, $U_3U_1+\overline{u'_3u'_1}$, which will be needed again later.

Now if we choose six suitable orientations for the hot-wire, e.g. $(\alpha,\theta)=(\pi/6,0)$; $(\pi/3,\pi)$; $(\pi/6,\pi/2)$; $(\pi/3,-\pi/2)$; $(\pi/6,\pi/4)$; $(\pi/3,-3\pi/4)$ we can actually resolve the system of equations (5):

$$(7.1)-(7.3)\qquad (U_l+u'_l)^2 = \sum_{i=1}^{6} b_{ll}(\alpha_i,\theta_i)\cdot e_i^2 \quad , \quad l=1,2,3 \, ,$$

$$(7.4)\qquad (U_1+u'_1)\cdot(U_2+u'_2) = \sum_{i=1}^{6} b_{12}(\alpha_i,\theta_i)\, e_i^2 \, ,$$

$$(7.5)\qquad (U_2+u'_2)\cdot(U_3+u'_3) = \sum_{i=1}^{6} b_{23}(\alpha_i,\theta_i)\, e_i^2 \, ,$$

$$(7.6)\qquad (U_3+u'_3)\cdot(U_1+u'_1) = \sum_{i=1}^{6} b_{31}(\alpha_i,\theta_i)\, e_i^2 \, .$$

The coefficients $b_{lm}(\alpha_i,\theta_i)$ are given explicitely for k=0 in appendix C. We see there that all $b_{ll}(\alpha_i,\theta_i)\neq 0$, so that in equations (7.1) to (7.3), all six e_i^2 actually occur. Assuming that at any time $U_l+u'_l\geq 0$ is true*, then by time averaging the primary sought quantities can be found: /20

$$(8.1)-(8.3)\qquad U_l = \Big(\sum_{i=1}^{6} b_{ll}(\alpha_i,\theta_i)\cdot \overline{e_i^2}\Big)^{1/2} \quad , \quad l=1,2,3,$$

$$(8.4)-(8.6)\qquad \overline{u'^2_l} = \sum_{i=1}^{6} b_{ll}(\alpha_i,\theta_i)\,\overline{e_i^2} - U_l^2 \quad , \quad l=1,2,3,$$

$$(8.7)\qquad \overline{u'_1u'_2} = \sum_{i=1}^{6} b_{12}(\alpha_i,\theta_i)\,\overline{e_i^2} - U_1U_2 \, ,$$

$$(8.8)\qquad \overline{u'_2u'_3} = \sum_{i=1}^{6} b_{23}(\alpha_i,\theta_i)\,\overline{e_i^2} - U_2U_3 \, ,$$

$$(8.9)\qquad \overline{u'_3u'_1} = \sum_{i=1}^{6} b_{31}(\alpha_i,\theta_i)\,\overline{e_i^2} - U_3U_1 \, .$$

If the average speed components U_1, U_2, U_3 are known, then equations (8.4) to (8.9) provide all elements of the Reynolds stress tensor. Only the time averages $\overline{e_i^2}$ of the hot-wire signals are needed, but no correlations $\overline{e_ie_j}$, $i\neq j$. For stationary signals, these averages do not have to be measured simultaneously, rather, they can be determined in sequence. But the determination of the average speeds U_1 is difficult since it seems as if the signals of six hot-wires are needed simultaneously. On the other hand, equations (7.4) to (7.6) are entirely dispensable if from (7.1) to 7.3) it follows:

$$U_l + u'_l = \Big(\sum_{i=1}^{6} b_{ll}(\alpha_i,\theta_i)\, e_i^2\Big)^{1/2}$$

so that from this, U_l $(l=1,2,3)$ and $\overline{u'_lu'_m}$ $(l,m=1,2,3)$ can be derived directly. The system of equations (7.1) to (7.6) is thus overestimated (likewise the system of equations (6.1) to (6.4)). One can thus hope that an accurate analysis is possible with fewer than six simultaneous hot-wire signals.

*The sign problem is discussed in section 3.2.1.1.

3.1 Laminar Flow

If the velocity field is time-constant $(u_1' \equiv u_2' \equiv u_3' \equiv 0)$ then so also are the hot-wire signals. Equations (6.1) to (6.3) in this case give:

/21

$$\begin{aligned}(1-k^2)\,U_1 U_2 &= (e_2^2 - e_1^2)/2\,,\\ (1-k^2)\,U_2 U_3 &= (e_8^2 + e_7^2)/2 - (e_4^2+e_5^2)/2\,,\\ (1-k^2)\,U_3 U_1 &= (e_7^2 - e_8^2)/2\,.\end{aligned}$$

Thus one can easily find a coordinate system by using the criteria:

$$e_2^2 = e_1^2\,,\quad e_4^2 = e_3^2\,,\quad e_8^2 + e_7^2 = e_4^2 + e_6^2$$

with $U_2 = U_3 = 0$ and $U_1 = U > 0$. From (6.4) it follows:

$$\frac{1+k^2}{4}\,U^2 = \frac{e_i^2}{2} \quad \text{or}$$

$$U^2 = \frac{2}{1+k^2}\,e_i^2 \qquad (i = 1, \ldots, 8)\,. \tag{9}$$

For a single hot-wire which is sloped by the angle α to the speed, in general:

$$U^2 = \frac{1}{\sin^2\alpha + k^2\cos^2\alpha}\cdot e^2 \tag{10}$$

3.2 Turbulent Flow

Initially it seemed that a hot-wire probe with six wires would be needed for a precise calculation of the average speeds. But actually we do not have 6 unknowns, but only three:

$$u_1 = U_1 + u_1'\,,\quad u_2 = U_2 + u_2'\,,\quad u_3 = U_3 + u_3'\,.$$

This suggests that in principle, three different hot-wire orientations will suffice for an exact analysis. The general case of a three-wire probe with three different hot-wire directions does not have a closed solution, but this is not an insurmountable obstacle, since we can find many special cases in which the desired resolution by velocity components is possible: namely, probes whose three hot-wires are perpendicular to each other or those which lie in a plane. These cases will be discussed below.

3.2.1 Orthogonal Three-Wire Probes

/22

Now imagine three hot-wires in the direction of the orthogonal coordinate axes $\hat{x}_1, \hat{x}_2, \hat{x}_3$ and their signals denoted as e_1, e_2, e_3. The system of equations (5) is simplified into the linear system:

$$\begin{pmatrix} k^2 & 1 & 1 \\ 1 & k^2 & 1 \\ 1 & 1 & k^2 \end{pmatrix} \cdot \begin{pmatrix} (U_1+u_1')^2 \\ (U_2+u_2')^2 \\ (U_3+u_3')^2 \end{pmatrix} = \begin{pmatrix} e_1^2 \\ e_2^2 \\ e_3^2 \end{pmatrix} . \tag{11}$$

The solution to this system of equations gives:

$$\begin{pmatrix} (U_1+u_1')^2 \\ (U_2+u_2')^2 \\ (U_3+u_3')^2 \end{pmatrix} = \frac{1}{(2+k^2)(1-k^2)} \cdot$$

$$\begin{pmatrix} -(1+k^2)\,e_1^2 + e_2^2 + e_3^2 \\ e_1^2 - (1+k^2)\,e_2^2 + e_3^2 \\ e_1^2 + e_2^2 - (1+k^2)\,e_3^2 \end{pmatrix} =: \begin{pmatrix} \tilde{e}_1^2 \\ \tilde{e}_2^2 \\ \tilde{e}_3^2 \end{pmatrix} \tag{12}$$

Let us assume for the moment that for all times t:

$$u_1(t) = U_1 + u_1' \geq 0 \qquad (1 = 1,2,3) \tag{13}$$

thus, the velocity vector $\underline{u} = (u_1, u_2, u_3)$ does not leave the octanden $u_1, u_2, u_3 > 0$. Then we have:

$$U_1 + u_1' = +\sqrt{\tilde{e}_1^2} =: \tilde{e}_1 =: \overline{\tilde{e}_1} + \tilde{e}_1' \quad , \tag{14}$$

and furthermore:

$$U_1 = \overline{\tilde{e}_1} \quad , \tag{15.1}$$

$$u_1' = \tilde{e}_1' \quad , \tag{15.2}$$

$$\overline{u_1' u_m'} = \overline{\tilde{e}_1' \tilde{e}_m'} \quad ; \qquad 1,m = 1,2,3 \, . \tag{15.3}$$

This result is formally quite simple. It was derived without approximations; the condition (13) is an easier condition than that needed for a series expansion $|u_1'| \ll U$, but also means a restriction on turbulent intensity. Since the equation (14) is a linear relation between the fluctuations in speed and those in the hot-wire signals, eq. (15.2) does not apply precisely to frequency components. /23

The turbulence intensity $\overline{u_1'^2}$ and the correlation $\overline{u_1' u_m'}$ $(1 \neq m)$ were computed with respect to a coordinate system which is defined by the three orthogonal hot-wires. This coordinate system may not

coincide with the flow-line-related coordinate system (y_1, y_2, y_3-axis = tangent, normal, binormal of the flow line). Now if a component U_1 disappears, then the corresponding condition (13) is violated even for low turbulence. It is most useful to place the main flow direction into the symmetry axis $(\hat{x}_1+\hat{x}_2+\hat{x}_3)$ of the coordinate intersection, so that $\tilde{e}_1 = \tilde{e}_2 = \tilde{e}_3$

and thus $|u_1 = u_2 = u_3$

Now if the speed fluctuations are to be determined with respect to a flow-line or a fixed coordinate system, they have to be transformed again after measurement (see section 8).

3.2.1.1. The Sign Problem, Probe Symmetry

Now when is $u_1(t) \geq 0$ at all times? What are the consequences if an existing change in sign is ignored? How can one find the correct sign?

Viewed statistically, there can be sign changes in every turbulent flow in the velocity components. When the average velocity components $U_1 > 0$, then only in case of low turbulence is the time interval with $u_1 < 0$ negligible. In general, from equation (12) it follows:

$$\tilde{e}_1 = |u_1 + u_1'|$$

and not:

$$\tilde{e}_1 = u_1 + u_1'$$

If u_1+u_1' changes sign in the time history profile, then this is not noticed by a single hot-wire or by an orthogonal three-wire probe; both "see" a speed fluctuation where negative velocity values are handled as positive values of the same amount: /24

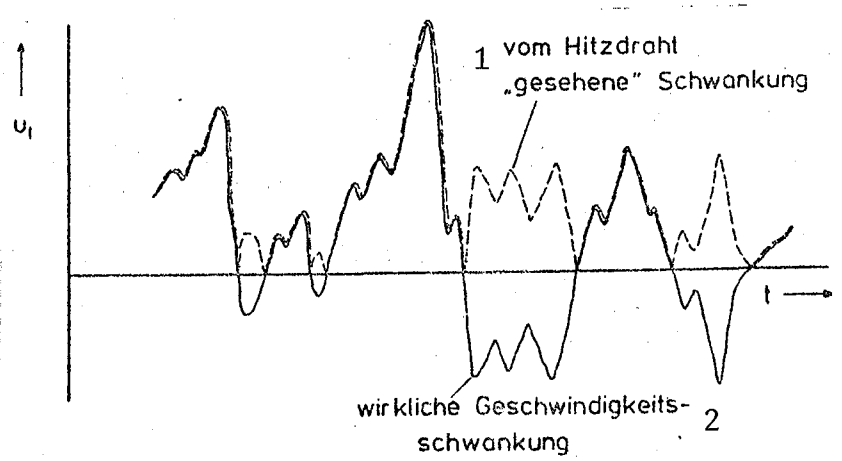

Key: 1-fluctuation "seen" by the hot wire
2-actual velocity fluctuation

Using the example of a simple periodic step function, one can see how the average value and the signal scattering are invalidated by this reflection:

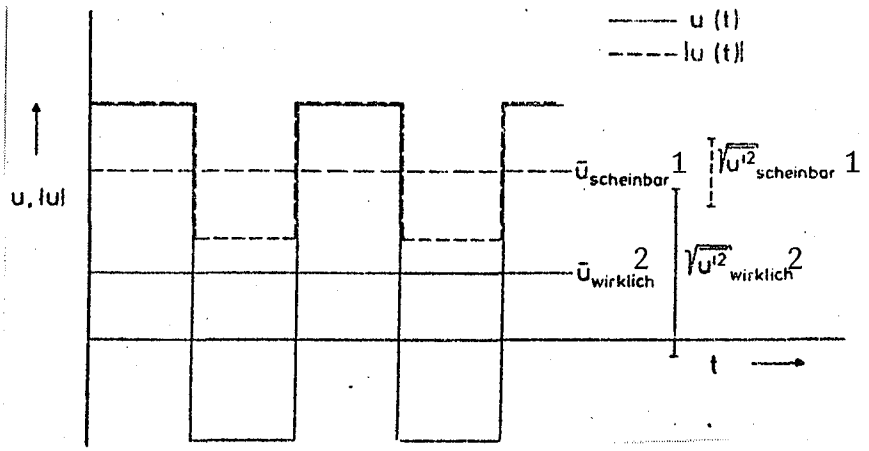

Key: 1-apparent 2-actual

In general it can be proven that the absolute value of the signal $|u(t)|$ has a higher average value and a smaller fluctuation than the actual signal u(t), when it assumes positive and negative values. /25

The system of equations:

$$e_i^2 = \sum_{l,m=1}^{3} a_{lm}(\alpha_i, \theta_i) \cdot u_l \cdot u_m \qquad (5)$$

is invariant against sign reversal of $\underline{u}=(u_1,u_2,u_3)$. Thus, there can be no unique solution to the system of equations by $\underline{u}$, rather with $\underline{u}$ a $-\underline{u}$ is also a solution of eq. (5). When the quadratic forms $a_{lm}(\alpha_i,\theta_i)$ are diagonal, i.e. $a_{lm}=0$ for $l\neq m$, then (5) is also invariant to sign reversal for each individual component. With $\underline{u}=(u_1,u_2,u_3)$ then also $(\pm u_1,\pm u_2,\pm u_3)$ are solutions of (5), so that there are $2^3=8$ solutions. This is the case for the orthogonal three-wire probe. The ambiguity of the solution thus has to do with the symmetry level of the probe: A very symmetric probe gives less information than a less-symmetric probe. For this reason, it is recommended to examine non-orthogonal, asymmetric probes (sec. 3.2.2), although the solution of (5) is more difficult for these probes than for orthogonal probes. Naturally, the ambiguity of solutions is limited since the speed components are continuous functions of time.

Also note that the ambiguity of the functional relation between hot-wire signals and the speed components plays a role when using one- and two-wire probes when they are used in flows of high turbulence intensity. In theoretical investigations by Tutu and Chevray [16] and by Bradbury [17], whose results are presented in section 6, this so-called rectification error was estimated and recognized as important in high turbulence.

3.2.1.2 Alignment of Orthogonal Three-Wire Probes

/26

Theoretically, only the wire directions are specified, but not their precise local position. The three hot wires must be close together in order to resolve even small turbulence structures; on the other hand, they must be spaced far enough apart so that they do not interfere with each other, e.g. one wire should not lie in the wake of another--related to the average flow. Figures 3 and 4 show possible probe designs. These probes are invariant against rotations by 120° or 240° about the $\hat{x}_1$-axis (probe axis). The wire directions are perpendicular to each other, the angle ϑ between the wire directions and the probe axis is 54.7° (precisely: $\vartheta = \arccos(3)^{-1/2} = \arcsin((2/3)^{1/2})$ the same angle as between the edges of a cube and the spatial diagonal. As long as the angle Δ between the instantaneous flow direction and the probe axis is sufficiently small, at no time will one wire lie in the wake of another:

$$\Delta \leq \arccos\left(\frac{1'}{(1'^2 + 0.5\,(1-1')^2)^{1/2}} \right)$$

for the "triangular" probe (fig. 3), e.g. $\Delta \leq 35.5°$ for $1'=0.5$; $\Delta \leq \vartheta = 54.7°$ for the "tripod probe" (fig. 4), regardless of $1'$.

The linear transformation between the base vectors $\hat{x}_1$ ($1=1,2,3$) of the orthogonal coordinate system specified by the hot wires and the base vectors $\hat{y}_1$ ($1=1,2,3$) with $\hat{y}_1$ as probe axis, is defined by:

$$\begin{pmatrix} \hat{x}_1 \\ \hat{x}_2 \\ \hat{x}_3 \end{pmatrix} = \begin{pmatrix} 1/\sqrt{3} & 0 & 2/\sqrt{6} \\ 1/\sqrt{3} & -1/\sqrt{2} & -1/\sqrt{6} \\ 1/\sqrt{3} & +1/\sqrt{2} & -1/\sqrt{6} \end{pmatrix} \cdot \begin{pmatrix} \hat{y}_1 \\ \hat{y}_2 \\ \hat{y}_3 \end{pmatrix} \qquad (16)$$

for the "triangular probe" or by

/27

$$\begin{pmatrix} \hat{x}_1 \\ \hat{x}_2 \\ \hat{x}_3 \end{pmatrix} = \begin{pmatrix} 1/\sqrt{3} & -2/\sqrt{6} & 0 \\ 1/\sqrt{3} & 1/\sqrt{6} & -1/\sqrt{2} \\ 1/\sqrt{3} & 1/\sqrt{6} & 1/\sqrt{2} \end{pmatrix} \cdot \begin{pmatrix} \hat{y}_1 \\ \hat{y}_2 \\ \hat{y}_3 \end{pmatrix} \qquad (17)$$

for the "tripod probe". In both cases, we have: $\hat{x}_1 + \hat{x}_2 + \hat{x}_3 = \sqrt{3}\,\hat{y}_1$ i.e. the probe axis is a symmetry axis.

Building such three-wire probes is surely not much more difficult than building X-wire probes. Whether and to what extent they can be used to advantage, must also be determined experimentally. But it is already obvious that the presence of prongs can greatly invalidate the analysis in high turbulence, when the instantaneous speed direction deviates so much from the probe axis that hot wires lie in the wake of the prongs.

3.2.2 Non-orthogonal Three-Wire Probes

For non-orthogonal three-wire probes, the system of equations (5) generally leads to 2nd, 4th and 8th degree equations for the velocity components, so that as a rule, no analytic solution can be found. The equation system is simplified for the case of a three-wire probe where the wires lie in a plane.

A special case is discussed here, namely of a plane three-wire probe in the form of an isoceles right triangle:

/28

$$\hat{\underline{d}}_1 = (\hat{\underline{x}}_2 - \hat{\underline{x}}_3)/\sqrt{2} \quad , \quad \hat{\underline{d}}_2 = \hat{\underline{x}}_2 \quad , \quad \hat{\underline{d}}_3 = \hat{\underline{x}}_3$$

or

$$\alpha_1 = \alpha_2 = \alpha_3 = \frac{\pi}{2} \quad ;$$

$$\theta_1 = -\frac{\pi}{4} \quad , \quad \theta_2 = 0 \quad , \quad \theta_3 = \frac{\pi}{2}$$

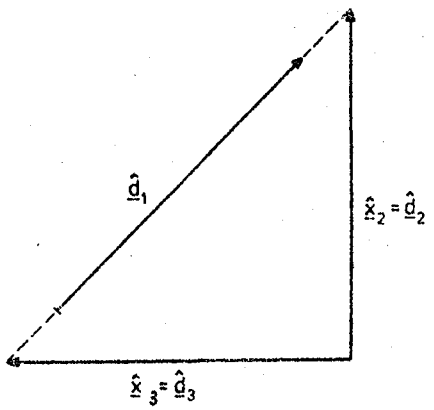

We obtain

$$\begin{pmatrix} 1 & (1+k^2)/2 & (1+k^2)/2 & (1-k^2)/2 \\ 1 & k^2 & 1 & 0 \\ 1 & 1 & k^2 & 0 \end{pmatrix} \circ \begin{pmatrix} u_1^2 \\ u_2^2 \\ u_3^2 \\ 2\,u_2 u_3 \end{pmatrix} = \begin{pmatrix} e_1^2 \\ e_2^2 \\ e_3^2 \end{pmatrix}$$

and, from this:

$$\begin{pmatrix} 1 & 0 & 1+k^2 & 0 \\ 0 & -1 & 1 & 0 \\ 0 & 0 & 0 & 1 \end{pmatrix} \circ \begin{pmatrix} u_1^2 \\ u_2^2 \\ u_3^2 \\ u_2 u_3 \end{pmatrix} = \begin{pmatrix} \frac{1}{1-k^2}\,(e_2^2 - k^2 e_3^2) \\ \frac{1}{1-k^2}\,(e_2^2 - e_3^2) \\ \frac{1}{1-k^2}\,(e_1^2 - \frac{1}{2} e_2^2 - \frac{1}{2} e_3^2) \end{pmatrix} =: \begin{pmatrix} \check{e}_1 \\ \check{e}_2 \\ \check{e}_3 \end{pmatrix},$$

/29

in conventional notation

$$u_1^2 + (1+k^2)\,u_3^2 = \check{e}_1 \quad , \qquad (18.1)$$

$$-u_2^2 + u_3^2 = \check{e}_2 \quad , \qquad (18.2)$$

$$u_2 u_3 = \check{e}_3 \quad . \tag{18.3}$$

Solving the system of equations (18) gives:

$$u_1^2 = \check{e}_1 - (1+k^2)\left[\tfrac{1}{2}\check{e}_2 + \sqrt{(\tfrac{1}{2}\check{e}_2)^2 + \check{e}_3^2}\right] =: \tilde{e}_1^2 \quad , \tag{19.1}$$

$$u_2^2 = -\tfrac{1}{2}\check{e}_2 + \sqrt{(\tfrac{1}{2}\check{e}_2)^2 + \check{e}_3^2} =: \tilde{e}_2^2 \quad , \tag{19.2}$$

$$u_3^2 = +\tfrac{1}{2}\check{e}_2 + \sqrt{(\tfrac{1}{2}\check{e}_2)^2 + \check{e}_3^2} =: \tilde{e}_3^2 \quad . \tag{19.3}$$

The System of equations (18) is invariant to sign reversal of (u_1,u_2,u_3), (u_2,u_3), u_1 but not to sign reversal of u_2 or u_3 alone. Consequently, the probe can be used advantageously in two ways:

-In sufficiently low turbulence, as for the orthogonal probe, the $\hat{y}_1$ axis can be chosen as the main flow direction, fig. 5. We then have:

$$U_1 = +U_2 = +U_3 = \frac{1}{\sqrt{3}}\,U$$

and

$$u_1 = +\sqrt{\tilde{e}_1^2} \quad ,$$

$$u_{2/3} = +\sqrt{\tilde{e}_{2/3}^2} \quad .$$

The linear transformation of the base vectors $\hat{x}_1, \hat{y}_1$ is:

$$\begin{pmatrix} \hat{x}_1 \\ \hat{x}_2 \\ \hat{x}_3 \end{pmatrix} = \begin{pmatrix} 1/\sqrt{3} & 2/\sqrt{6} & 0 \\ 1/\sqrt{3} & -1/\sqrt{6} & +1/\sqrt{2} \\ 1/\sqrt{3} & -1/\sqrt{6} & -1/\sqrt{2} \end{pmatrix} \cdot \begin{pmatrix} \hat{y}_1 \\ \hat{y}_2 \\ \hat{y}_3 \end{pmatrix} \tag{20}$$

-In severe turbulence, sign reversal of u_1 is expected. In this case, it is better to choose the x_1-axis as the main flow direction, so that the probe triangle is perpendicular to the main flow direction, fig. 6. The signs of u_2 and u_3 can then be determined from equation (18.3), if we presume the fluctuations as constant in time, if we know the signs at any given time, and if u_2 and u_3 do not disappear simultaneously. We then obtain: /30

$$u_1 = +\sqrt{\tilde{e}_1^2} \quad , \qquad (\text{sign } u_1 > 0 \text{ is presumed})$$

$$u_2 = \text{sign } u_2 \cdot \sqrt{\tilde{e}_2^2} \quad , \qquad (\text{sign } u_2, \text{ sign } u_3 \text{ from 18.3 and one starting condition})$$

$$u_3 = \text{sign } u_3 \cdot \sqrt{\tilde{e}_3^2} \quad .$$

Similarly, a plane three-wire probe could be used, whose hot wires form an equilateral triangle. The instantaneous speed vectors may only lie in the half-space $u_1 > 0$ in both cases.

From a theoretical standpoint, it would be desirable to use the least symmetric possible probe, since this provides as much information as possible about the flow direction. That the

system of equations (5) cannot be resolved analytically in this case, need not be an obstacle. If we are satisfied with a numeric solution, a fast computer time-signal can give the speed components and with the correct sign (sign u_2·sign u_1 and sign u_3·sign). The sign u_1 must be obtained from an initial value and the continuous profile of u_1 or by other means (e.g. by an additional hot wire).

Three-wire probes of different type for an improved measurement of speeds in highly-turbulent flows were also suggested by other authors. Rodi [18] points out that in principle, the instantaneous speed component could be determined from the signals of a three-wire probe by means of a digital data analysis. But he considers this method to be very cumbersome and fears strong interferences between the three wires. Gaulier [19] uses an orthogonal "triple-probe" by DISA Co., whose wire arrangement resembles the orthogonal probe in fig. 3, but with a different prong design. Since Gaulier does not use a linearization of hot wire signals, he cannot use the advantage of the triple probe over an X-wire probe, since he needs a series expansion using small fluctuation quantities. In addition, in the analysis, wrong relations are used between the average speed components and averages of the cooling rate (eq. (7) in [19]). The same triple probe of Gaulier is used by MOffat, Yavuszkurt and Crawford [20] to determine the instantaneous orthogonal speed components in highly-turbulent flows. The real time analysis makes use of analog techniques here. The sign problem in high turbulence is not discussed. Acrivlellis [21] suggests a triple probe as per fig. 6; he also states explicitely how the square of the speed components $u_1^2=(u_1+u_1')^2$ are calculated for linearized signals, but also does not discuss the sign reversal in higher turbulence. Fabris [22] developed a four-wire probe and a method of signal processing and analysis which is supposed to permit simultaneous determination of the speed components and temperature in turbulent boundary layers with temperature gradients. Of the three hot-wires which measure the speed components, two form an orthogonal X as in standard X-wire probes, whereas the third lies at a 45° angle to the lines of this X, and the fourth--to measure temperature fluctuations--is parallel to this perpendicular. By using extremely thin platinum-rhodium hot-wires (0.625 µm diameter), the wires should be "interference-free". If the angle between the probe axis and the instantaneous speed is greater than 30°, then even for these wires, distortion of signals by the prongs or the thicker, silver-coated wire ends cannot be avoided.

/31

3.3 Two-Dimensional Unsteady Flow

In isotropic, turbulent flows or in boundary layers, the speed fluctuations in the direction of three orthogonal coordinate axes are of the same magnitude, so that no component can be neglected. But there are flows in which large speed fluctuations occur, not because of turbulence, but through other mechanisms and the speed vector revolves almost exclusively in a plane. Examples for this are the entrainment region of a planar or round free-jet, the flow at the outlet of radial impellers in ventilators or compressors, or

/32

the flow in the wake of axial-symmetric or two-dimensional bodies. These are simultaneously cases in which the instantaneous, local velocity vector cannot be restricted to a half-space or quadrant, but instantaneous back-flow occurs. Conventional hot-wire measurements will have to fail here since the standard formulas for analysis of the signals ignore the occurring sign changes of the speed components. But it is expected that an accurate hot-wire analysis in two-dimensions will be much simpler than in three dimensions and that no three-wire probes will be needed, but X-wire probes will suffice.

Let an X-wire (not necessarily orthogonal) lie symmetric to the x_1-axis according to the assumptions in section 3:

$$\alpha_1 = \alpha_2 =: \alpha \quad , \quad 0 < \alpha < \pi/2 \quad ;$$

$$\theta_1 = \theta_2 - \pi =: \theta \quad , \quad 0 \leq \theta \leq \pi/2 \quad ,$$

and let $u_3 \equiv 0$. Then for the two signals e_1, e_2, we have:

$$a_{12} = (k^2-1)\cos\alpha \cdot \sin\alpha \cdot \cos\theta \neq 0 \quad ; \tag{21}$$

with

$$a_{11} = 1 + (k^2-1)\cos^2\alpha > 0 \quad ,$$

$$a_{22} = 1 + (k^2-1)\sin^2\alpha \cdot \cos^2\theta > 0 \quad ,$$

$$a_{12} = (k^2-1)\cos\alpha \cdot \sin\alpha \cdot \cos\theta \neq 0$$

By substitution we see that eq. (21) has the solutions:

$$v_{1/2}^2 := \left(\sqrt{a_{11}}\,u_1 \mp \sqrt{a_{22}}\,u_2\right)^2 = \tag{22}$$

$$= \tfrac{1}{2}\left(1 - \frac{\sqrt{a_{11}\cdot a_{22}}}{a_{12}}\right) e_{1/2}^2 + \tfrac{1}{2}\left(1 + \frac{\sqrt{a_{11}\cdot a_{22}}}{a_{12}}\right) e_{2/1}^2$$

Now the choice of α, θ is basically open:

- $\alpha = \frac{\pi}{4}$ is an orthogonal X-wire probe
- $\alpha > \frac{\pi}{4}$ is a blunt-angle X-wire probe (related to the opening angle, with the x_1-axis as angle bisector)
- $\alpha < \frac{\pi}{4}$ an acute angle X-wire probe /33
- $\theta = 0$ means that the X lies in the x_1x_2-plane
- $\theta \neq 0$ (regardless of the author's reservations $0<\theta<\frac{\pi}{2}$) describes an X-wire probe inclined by the angle θ to the x_1x_2-plane, even though speed components are measured only in this plane.

$a_{22} = a_{11}$ is true when $\cot^2\alpha = \cos^2\theta$ thus applies only for blunt or right-angle X ($\alpha \geq \frac{\pi}{4}$). In the case where $\cot^2\alpha > \cos^2\theta$ (always true for acute-angle X), then $a_{11} < a_{22}$.

In general the lines: $u_1 \mp u_2 = 0$ (45°-lines)

$\sqrt{a_{11}}u_1 \mp \sqrt{a_{22}}u_2 = 0$ (zero lines of $v_{1/2}$)

$\tan\alpha \cdot \cos\theta u_1 \mp u_2 = 0$ (projection of hot wires in x_1x_2-plane

do not coincide.

Example with $a_{11} < a_{22}$, $k = 0$, $\theta \neq 0$:

$$\tan\phi = \sqrt{a_{11}/a_{22}} = \sqrt{\frac{\sin^2\alpha}{1 - \sin^2\alpha \cdot \cos^2\theta}} \quad , \tag{23}$$

$$\tan\phi_p = \tan\alpha \cdot \cos\theta \quad . \tag{24}$$

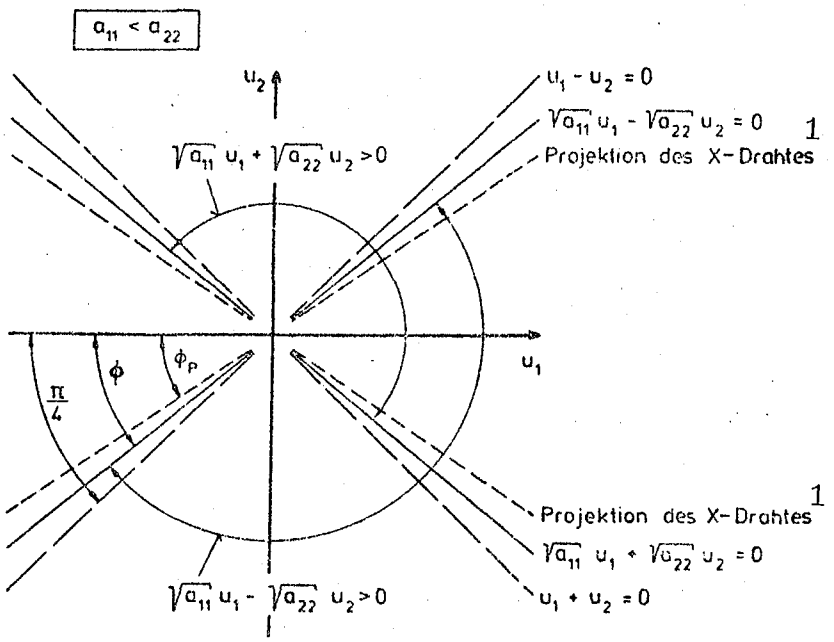

/34

Key: 1-projection of the X-wire

As above, a sign problem occurs: We obtain equations only for $v_{1/2}^2$ but not for $v_{1/2}$. In the case of $a_{11} \neq a_{22}$ the sign can be determined if it is known at a beginning time and if v_1 and v_2 do not disappear simultaneously (or u_1 and u_2 simultaneously). Now if we look at

$$\frac{v_2^2 - v_1^2}{u_1^2 + u_2^2} = \frac{4\sqrt{a_{11}a_{22}}\,u_1u_2}{u_1^2 + u_2^2} = 2\sqrt{a_{11}a_{22}} \cdot \sin 2\Phi \tag{25}$$

with $\cos\Phi = \frac{u_1}{u_1^2+u_2^2}$, $\sin\Phi = \frac{u_2}{u_1^2+u_2^2}$,

then we find that this function has extreme values at $\Phi = \pm\frac{\pi}{4} \pm n\frac{\pi}{2}$ (i.e. $u_1 = \pm u_2$) and no extreme values at $\pm\phi \pm n\pi$, when $\phi \neq \frac{\pi}{4}$. So when θ and α are selected so that $\phi \neq \frac{\pi}{4}$, then the following method gives the correct sign--at least in principle. Let $v_1 > 0$, $v_2 > 0$ at $t = t_0$. If $t_1 > t_0$ is the first zero point following v_1 or v_2, then for $t_0 \leq t < t_1$ we also have $v_1, v_2 > 0$ for continuity reasons. If at t_1

/35

$$(v_2^2 - v_1^2)/(u_1^2 + u_2^2)$$

has no extreme value as a function of the time, then v_1 or v_2 changes sign, otherwise not. A fast computer thus could solve equations (22) with the correct sign of u_1 and u_2.

With two-wire probes, in principle the instantaneous values of speed of a two-dimensional unsteady flow could be determined. The same applies, as shown above with minor restrictions regarding sign, for suitable three-wire probes in a 3-dimensional unsteady flow. From the time history of the speed components, in both cases the average speeds and fluctuations of any, high order can be determined, even when the fluctuations are very large. The suggested probes and the type of signal analysis are however, not in practical testing, so it is not known in what cases they are practically superior to conventional one and two-wire probes and the corresponding signal analysis. As long as one- and two-wire probes are used to measure unsteady flows, it is useful to consider conventional analysis of hot-wire signals more closely, in order to estimate the systematic errors in larger fluctuations.

4. Conventional Analyses of X-Wire Signals

/36

In sufficiently small turbulent flows, the average velocity is large compared to the velocity fluctuations at nearly all times. In this case, from eq. (2') by a series expansion of the square root, approximation formulas can be obtained. Such approximations have been given by various authors, but many of these series expansions are cumbersome. One attempt to derive approximation formulas from a consistent series expansion by Bartenwerfer [23], gave in the second approximation previously non-standard correction factors for the turbulence quantity $\overline{u_l' u_m'}/U^2$ $(l,m=1,2,3)$.

In order to have fewer unknowns, one tries here to set the axis intersection so that $U_2 = U_3 = 0$, or the x_1-axis coincides with the main flow direction. Finding a criterion for this is the first problem; the second problem to determine the average velocity U_1 and the turbulence quantity $\overline{u_l' u_m'}$. In symmetric flows, one will naturally take the symmetry into account in the selection of the coordinate system: So for axial-symmetric flows without spin, the azimuth component of average velocity is zero, likewise the third component in two-dimensional flow.

If the main direction of flow is not known precisely for reasons of symmetry, then it must be known at least approximately for this method, so that an axis intersection $\hat{x}_1, \hat{x}_2, \hat{x}_3$ can be selected so that the following equation applies to the speed components:

$$U_1 \gg |u_1'|, |u_2|, |u_3| \quad ; \quad u_{2/3} = U_{2/3} + u_{2/3}' \tag{26}$$

Then equation (2') applies in the following form:

$$e = \sqrt{a_{11}} \cdot U_1 \cdot \left[1 + 2\xi + \eta^2 \right]^{1/2} \qquad (27)$$

with the abbreviations:

$$\xi = \frac{u_1'}{U_1} + \frac{a_{12}}{a_{11}} \frac{u_2}{U_1} + \frac{a_{13}}{a_{11}} \frac{u_3}{U_1}$$

$$\eta^2 = \frac{u_1'^2}{U_1^2} + \frac{a_{22}}{a_{11}} \frac{u_2^2}{U_1^2} + \frac{a_{33}}{a_{11}} \frac{u_3^2}{U_1^2} + \qquad /37$$

$$+ 2 \frac{a_{12}}{a_{11}} \frac{u_1' u_2}{U_1^2} + 2 \frac{a_{13}}{a_{11}} \frac{u_1' u_3}{U_1^2} + 2 \frac{a_{23}}{a_{11}} \frac{u_2 u_3}{U_1^2}$$

In ξ are the first-order terms, and in η^2 are the second-order terms (η^2 not necessarily >0). According to:

$$\sqrt{1+x} = 1 + \frac{1}{2} x - \frac{1}{8} x^2 + \frac{1}{16} x^3 - \frac{5}{128} x^4 + O(x^5)$$

the root in (27) can be developed consistently when a_{11} is not small compared to 1. Normally, these developments (expansions) are given only down to the lowest orders for the sake of simplicity. But since in the literature sometimes 4th-order terms are found, the general expansion is performed to the fourth order as a check. With

$$\sqrt{1 + 2\xi + \eta^2} = 1 + \xi + \frac{1}{2}(\eta^2 - \xi^2) - \xi \cdot \frac{1}{2}(\eta^2 - \xi^2) - \frac{1}{8}(\eta^2 - \xi^2)\cdot(\eta^2 - 5\xi^2) + O((\xi,\eta)^5)$$

we obtain:

$$e = \sqrt{a_{11}}\, U_1 \cdot \left[1 + \xi + \frac{1}{2}(\eta^2 - \xi^2) - \xi \cdot \frac{1}{2}(\eta^2 - \xi^2) - \frac{1}{2}(\eta^2 - \xi^2)\cdot\frac{1}{4}(\eta^2 - 5\xi^2) + O((\xi,\eta)^5) \right] \qquad (28)$$

with

$$\xi = \frac{u_1'}{U_1} + \frac{a_{12}}{a_{11}} \frac{u_2}{U_1} + \frac{a_{13}}{a_{11}} \frac{u_3}{U_1}$$

$$\eta^2 = \frac{u_1'^2}{U_1^2} + \frac{a_{22}}{a_{11}} \frac{u_2^2}{U_1^2} + \frac{a_{33}}{a_{11}} \frac{u_3^2}{U_1^2} + 2 \frac{a_{12}}{a_{11}} \frac{u_1' u_2}{U_1^2} + 2 \frac{a_{13}}{a_{11}} \frac{u_1' u_3}{U_1^2} + 2 \frac{a_{23}}{a_{11}} \frac{u_2 u_3}{U_1^2}$$

$$\frac{1}{2}(\eta^2 - \xi^2) = \frac{1}{2}\left(\frac{a_{22}}{a_{11}} - \left(\frac{a_{12}}{a_{11}}\right)^2 \right) \cdot \frac{u_2^2}{U_1^2} + \frac{1}{2}\left(\frac{a_{33}}{a_{11}} - \left(\frac{a_{13}}{a_{11}}\right)^2 \right) \cdot \frac{u_3^2}{U_1^2} +$$

$$+ \left(\frac{a_{23}}{a_{11}} - \frac{a_{12}\, a_{13}}{a_{11}} \right) \cdot \frac{u_2 u_3}{U_1^2}$$

$$\frac{1}{4}(\eta^2 - 5\xi^2) = -\frac{u_1'^2}{U_1^2} + \frac{1}{4}\left(\frac{a_{22}}{a_{11}} - 5\left(\frac{a_{12}}{a_{11}}\right)^2 \right) \frac{u_2^2}{U_1^2} + \frac{1}{4}\left(\frac{a_{33}}{a_{11}} - 5\left(\frac{a_{13}}{a_{11}}\right)^2 \right) \frac{u_3^2}{U_1^2} -$$

$$- 2 \frac{a_{12}}{a_{11}} \frac{u_1' u_2}{U_1^2} - 2 \frac{a_{13}}{a_{11}} \frac{u_1' u_3}{U_1^2} + \frac{1}{2}\left(\frac{a_{23}}{a_{11}} - 5 \frac{a_{12}\, a_{13}}{a_{11}^2} \right) \frac{u_2 u_3}{U_1^2}$$

Since it is already clear that hot wires in various orinetations are needed to determine the speed fluctuations, let us handle only the orthogonal X-wire probe below. For such an X-wire, lying /38

symmetric to the x_1 axis, we thus have $\alpha_1=\alpha_2=\frac{\pi}{4}$ and $\theta_2=\theta_1\pm\pi$. Due to

$$\begin{aligned} a_{11}(\alpha_2,\theta_2) &= a_{11}(\alpha_1,\theta_1) \quad , \; 1=1,2,3 \; , \\ a_{12}(\alpha_2,\theta_2) &= -a_{12}(\alpha_1,\theta_1) \; , \\ a_{13}(\alpha_2,\theta_2) &= -a_{13}(\alpha_1,\theta_1) \; , \\ a_{23}(\alpha_2,\theta_2) &= +a_{23}(\alpha_1,\theta_1) \end{aligned}$$

there follows from (28):

$$\bar{e}_1-\bar{e}_2=\sqrt{a_{11}}\,U_1\cdot\left[2\frac{a_{12}}{a_{11}}\frac{U_2}{U_1}+2\frac{a_{13}}{a_{11}}\frac{U_3}{U_1}+O\left(\left(\frac{u_2}{U_1},\frac{u_3}{U_1}\right)^3\right)\right] \qquad (29)$$

$$a_{1m}=a_{1m}(\alpha_1,\theta_1) \; .$$

All second-order terms cancel out. Thus, when $a_{12}\cdot a_{13}\neq 0$, by first and second approximation, we have:

$$U_2=U_3=0 \quad \longleftrightarrow \quad \bar{e}_1=\bar{e}_2=:\bar{e}_{1/2} \qquad (30)$$

Thus, the orientation of the X-wire will be varied until $\bar{e}_1=\bar{e}_2$ for all rotation angles θ. Then, the x_1-axis is the main flow direction and $U_2=U_3=0$. Or more accurately: U_2/U_1 and U_3/U_1 are then at least on the order of the 3rd order terms, that is, two orders of magnitude smaller than the lowest occurring terms.

One must keep in mind that the criterion (30) was derived for a placement of the x_1-axis from a series expansion and thus applies only for small, perhaps for medium, turbulence intensity. No one can say how far this condition is reliable; it can be viewed as a calibration of the hot wire.

4.1 The Second Approximation

After the alignment of the X-wire into the mean flow direction, one can use the series expansion (28) with $U_2=U_3=0$ and terms up to second order. This seems reasonable since quantities of second order, e.g. $\overline{u_1u_2}/u_1^2$ are to be computed. Since the two signals of the X-wire are available simultaneously, the time-averaged quadratic quantities $\overline{e_{1/2}^2}$, $\overline{e_{1/2}^2}$, $\overline{e_1e_2}$ are available to calculate the correlations $\overline{u_1u_m}$ and the speed U_1. From (28) follows for one X-wire position, the system of equations: /39

$$\begin{pmatrix} a_{11}^2 & 0 & a_{11}a_{22}-a_{12}^2 & a_{11}a_{33}-a_{31}^2 & 0 & 2(a_{11}a_{23}-a_{12}a_{31}) & 0 \\ a_{11}^2 & a_{11}^2 & a_{11}a_{22} & a_{11}a_{33} & 2a_{11}a_{12} & 2a_{11}a_{23} & 2a_{11}a_{31} \\ a_{11}^2 & a_{11}^2 & a_{11}a_{22} & a_{11}a_{33} & -2a_{11}a_{12} & 2a_{11}a_{23} & -2a_{11}a_{31} \\ a_{11}^2 & a_{11}^2 & a_{11}a_{22}-2a_{12}^2 & a_{11}a_{33}-2a_{31}^2 & 0 & 2(a_{11}a_{23}-2a_{12}a_{31}) & 0 \end{pmatrix} \cdot \qquad (31)$$

$$\begin{pmatrix} U_1^2 \\ \overline{u_1'^2} \\ \overline{u_2'^2} \\ \overline{u_3'^2} \\ \overline{u_1'u_2'} \\ \overline{u_2'u_3'} \\ \overline{u_3'u_1'} \end{pmatrix} = a_{11} \begin{pmatrix} \overline{e_{1/2}}^2 \\ \overline{e_1^2} \\ \overline{e_2^2} \\ \overline{e_1 e_2} \end{pmatrix} \quad ; \quad a_{1m} = a_{1m}(\alpha_1, \theta_1) \; .$$

The second and third equation of the system are precise, whereas in the first and fourth equation, terms from third order can be neglected.

By transformation of this system of equations, we obtain

$$\begin{bmatrix} a_{11}^2 & 0 & a_{11}a_{22} - a_{12}^2 & a_{11}a_{33} - a_{31}^2 & 0 & 2(a_{11}a_{23} - a_{12}a_{31}) & 0 \\ 0 & a_{11}^2 & 0 & 0 & 0 & 0 & 0 \\ 0 & 0 & 0 & 0 & a_{11}a_{12} & 0 & a_{11}a_{31} \\ 0 & 0 & a_{12}^2 & a_{31}^2 & 0 & 2a_{12}a_{31} & 0 \end{bmatrix} \cdot \begin{pmatrix} U_1^2 \\ \overline{u_1'^2} \\ \overline{u_2'^2} \\ \overline{u_3'^2} \\ \overline{u_1'u_2'} \\ \overline{u_2'u_3'} \\ \overline{u_3'u_1'} \end{pmatrix} = \tag{32}$$

$$= a_{11} \cdot \begin{pmatrix} \overline{e_{1/2}}^2 \\ \frac{1}{4}\overline{e_1^2} + \frac{1}{4}\overline{e_2^2} + \frac{1}{2}\overline{e_1 e_2} + \overline{e_{1/2}}^2 \\ \frac{1}{4}\overline{e_1^2} - \frac{1}{4}\overline{e_2^2} \\ \frac{1}{4}\overline{e_1^2} + \frac{1}{4}\overline{e_2^2} - \frac{1}{2}\overline{e_1 e_2} \end{pmatrix} = a_{11} \cdot \begin{pmatrix} \overline{e_{1/2}}^2 \\ \frac{1}{4}\overline{(e_2' + e_1')^2} \\ \frac{1}{4}\overline{(e_1'^2 - e_2'^2)} \\ \frac{1}{4}\overline{(e_2' - e_1')^2} \end{pmatrix}$$

/40

with $e_i' = e_i - \overline{e_i}$.

For resolution of velocities, two suitable positions of an X-wire probe would suffice. The usual practice dictates selection of four orientations, and to be sure, the angles $\theta = 0, \pi; \frac{\pi}{2}, -\frac{\pi}{2}; \frac{\pi}{4} - \frac{3\pi}{4}; -\frac{\pi}{4}; \frac{3\pi}{4}$ since the resolution is simpler and nearly all correlations can be obtained from the measured values of one x-wire position. α is held constant at $\frac{\pi}{4}$ and the corresponding hot-wire signals are again designated as $e_1, e_2, e_3, e_4, e_5, e_6, e_7, e_8$

Thus one obtains a non-homogeneous linear system of equations with seven unknowns and 16 equations. Not all equations are needed for the solution. Equations with the signals e_1 to e_4 are preferred, so we obtain:

$$\overline{u_1'^2} = \frac{2}{1+k^2}\frac{\overline{(e_2'+e_1')^2}}{4} = \frac{2}{1+k^2}\frac{\overline{(e_4'+e_3')^2}}{4} = \frac{2}{1+k^2}\frac{\overline{(e_6'+e_5')^2}}{4} = \frac{2}{1+k^2}\frac{\overline{(e_8'+e_7')^2}}{4}, \tag{33.1}$$

$$\overline{u_2'^2} = \frac{2}{1+k^2}\cdot\left(\frac{1+k^2}{1-k^2}\right)^2\cdot\frac{\overline{(e_2'-e_1')^2}}{4}, \tag{33.2}$$

$$\overline{u_3'^2} = \frac{2}{1+k^2}\left(\frac{1+k^2}{1-k^2}\right)^2\cdot\frac{\overline{(e_4'-e_3')^2}}{4}, \tag{33.3}$$

$$\overline{u_1'u_2'} = \frac{2}{1+k^2}\,\frac{1+k^2}{1-k^2}\,\frac{\overline{(e_2'^2-e_1'^2)}}{4}, \tag{33.4}$$

$$\overline{u_2'u_3'} = \frac{2}{1+k^2}\left(\frac{1+k^2}{1-k^2}\right)^2\frac{\overline{(e_6'-e_5')^2}-\overline{(e_8'-e_7')^2}}{8}, \tag{33.5}$$

$$\overline{u_3'u_4'} = \frac{2}{1+k^2}\,\frac{1+k^2}{1-k^2}\,\frac{\overline{(e_4'^2-e_3'^2)}}{4}, \tag{33.6}$$

$$\left(\frac{1+k^2}{2}\right)^2U_1^2 + k^2\overline{u_2'^2} + \frac{1+k^2}{2}\overline{u_3'^2} = \frac{1+k^2}{2}\overline{e_{1/2}}^2, \tag{33.7}$$

$$\left(\frac{1+k^2}{2}\right)^2U_1^2 + \frac{1+k^2}{2}\overline{u_2'^2} + k^2\overline{u_3'^2} = \frac{1+k^2}{2}\overline{e_{3/4}}^2, \tag{33.8}$$

$$\left(\frac{1+k^2}{2}\right)^2U_1^2 + \frac{1+3k^2}{4}(\overline{u_2'^2}+\overline{u_3'^2}) + \frac{k^2-1}{2}\overline{u_2'u_3'} = \frac{1+k^2}{2}\overline{e_{5/6}}^2, \tag{33.9}$$

$$\left(\frac{1+k^2}{2}\right)^2U_1^2 + \frac{1+3k^2}{4}(\overline{u_2'^2}+\overline{u_3'^2}) - \frac{k^2-1}{2}\overline{u_2'u_3'} = \frac{1+k^2}{2}\overline{e_{7/8}}^2. \tag{33.10}$$

/41

From equations (33.9) and (33.10), we have:

$$\overline{u_2'u_3'} = \frac{1+k^2}{2(1-k^2)}\left(\overline{e_{7/8}}^2 - \overline{e_{5/6}}^2\right), \tag{33.11}$$

which is an alternative to equation (33.5) with which one can make do with the determination of average values $\overline{e_{7/8}}$ and $\overline{e_{5/6}}$. Another possibility to calculate $\overline{u_2'u_3'}$ is provided by eq. (6.2) with $U_2=U_3=0$:

$$\overline{u_2'u_3'} = \frac{1}{1-k^2}\left(\frac{\overline{e_8^2}+\overline{e_7^2}}{2} - \frac{\overline{e_6^2}+\overline{e_5^2}}{2}\right),$$

and this formula is exactly correct. Equations (6.1) and (6.3) show that (33.4) and (33.6) are actually not approximations, but precise solutions.

From eq. (33.7) to (33.10) we also find that in general, the average values $\overline{e_{1/2}}$, $\overline{e_{3/4}}$, $\overline{e_{5/6}}$, $\overline{e_{7/8}}$ are not all the same, and this can be confirmed by experiment. Deviations from the average values are related to the anisotropy of the turbulence. According to (33.7)-(33.9), $\overline{u_2'^2}-\overline{u_3'^2} = \frac{1+k^2}{1+k^2}(\overline{e_{3/4}}^2 - \overline{e_{1/2}}^2) = \frac{1+k^2}{1-k^2}(\overline{e_{5/6}}^2 + \overline{e_{7/8}}^2 - \overline{2e_{1/2}}^2)$. Apparently, $\overline{e_{3/4}}^2 = \overline{e_{1/2}}^2$ if and only if $\overline{u_2'^2} = \overline{u_3'^2}$; at the same time $\overline{e_{1/2}}^2 = \overline{e_{3/4}}^2 = \frac{1}{2}(\overline{e_{5/6}}^2 + \overline{e_{7/8}}^2)$ However, $\overline{e_{7/8}}^2 = \overline{e_{5/6}}^2$ is equivalent to $\overline{u_2'u_3'} = 0$.

Since all averages $\overline{e_i}$ are measured, one can define anisotropy factors:

$$\lambda := \overline{e_{3/4}}/\overline{e_{1/2}}, \quad \mu := \overline{e_{5/6}}/\overline{e_{1/2}}, \quad \nu := \overline{e_{7/8}}/\overline{e_{1/2}} \tag{34}$$

and from (17.7), (17.8), (17.2) we obtain:

$$U_1^2 = \frac{2}{1+k^2}\overline{e_{1/2}}^2\cdot F^{-2} = \frac{2}{1+k^2}\overline{e_{3/4}}^2\cdot\frac{1}{\lambda^2}\cdot F^{-2} = \frac{2}{1+k^2}\overline{e_{5/6}}^2\cdot\frac{1}{\mu^2}\cdot F^{-2} = \frac{2}{1+k^2}\overline{e_{7/8}}^2\cdot\frac{1}{\nu^2}\cdot F^{-2} \tag{35}$$

with the abbreviation:

$$F := \left[1 + (\lambda^2 - 1)\frac{1+k^2}{1-k^2} - 2\frac{1+3k^2}{(1-k^2)^2}\frac{\overline{(e_2' - e_1')^2}}{4\,\overline{e_{1/2}}^2} \right]^{-1/2} \qquad (36)$$ /42

For the local turbulence intensities and the normed Reynolds shear stresses, there follows:

$$\frac{\overline{u_1'^2}}{U_1^2} = \frac{\overline{(e_2' + e_1')^2}}{4\,\overline{e_{1/2}}^2} \cdot F^2 \,, \qquad (37.1)$$

$$\frac{\overline{u_2'^2}}{U_1^2} = \left(\frac{1+k^2}{1-k^2}\right)^2 \cdot \frac{\overline{(e_2' - e_1')^2}}{4\,\overline{e_{1/2}}^2} \cdot F^2 \,, \qquad (37.2)$$

$$\frac{\overline{u_3'^2}}{U_1^2} = \left(\frac{1+k^2}{1-k^2}\right)^2 \cdot \frac{\overline{(e_4' - e_3')^2}}{4\,\overline{e_{3/4}}^2} \cdot \lambda^2 \cdot F^2 \,, \qquad (37.3)$$

$$\frac{\overline{u_1' u_2'}}{U_1^2} = \frac{1+k^2}{1-k^2} \cdot \frac{\overline{(e_2'^2 - e_1'^2)}}{4\,\overline{e_{1/2}}^2} \cdot F^2 \,, \qquad (37.4)$$

$$\frac{\overline{u_2' u_3'}}{U_1^2} = \left(\frac{1+k^2}{1-k^2}\right)^2 \cdot \left[\mu^2 \frac{\overline{(e_6' - e_5')^2}}{8\,\overline{e_{5/6}}^2} - \nu^2 \frac{\overline{(e_8' - e_7')^2}}{8\,\overline{e_{7/8}}^2} \right] \cdot F^2 \qquad (37.5)$$

$$= \left(\frac{1+k^2}{1-k^2}\right)^2 \cdot \frac{1-k^2}{4} (\nu^2 - \mu^2) \cdot F^2 \,,$$

$$\frac{\overline{u_3' u_4'}}{U_1^2} = \frac{1+k^2}{1-k^2} \cdot \frac{\overline{(e_4'^2 - e_3'^2)}}{4\,\overline{e_{3/4}}^2} \cdot \lambda^2 \cdot F^2 \qquad (37.6)$$

4.2 The First Approximation

In the first approximation, only the linear terms in eq. (28) are taken into account and all higher ones are neglected.

$$e = \sqrt{a_{11}}\, U_1 \cdot \left[1 + \frac{u_1'}{U_1} + \frac{a_{12}}{a_{11}} \cdot \frac{u_2'}{U_1} + \frac{a_{31}}{a_{11}} \cdot \frac{u_3'}{U_1} + \ldots\ldots \right] \qquad (38)$$

With the same hot-wire orientations as above, one obtians a linear system of equationsin U_1, u_i', which can be solved by these variables and which then gives the desired time averages. We have:

$$\frac{\overline{u_1'^2}}{U_1^2} = \frac{\overline{(e_2' + e_1')^2}}{4\,\overline{e_{1/2}}^2} = \frac{\overline{(e_4' + e_3')^2}}{4\,\overline{e_{3/4}}^2} \qquad (39.1)$$

$$\frac{\overline{u_2'^2}}{U_1^2} = \left(\frac{1+k^2}{1-k^2}\right)^2 \cdot \frac{\overline{(e_2' - e_1')^2}}{4\,\overline{e_{1/2}}^2} \,, \qquad (39.2)$$ /43

$$\frac{\overline{u_3'^2}}{U_1^2} = \left(\frac{1+k^2}{1-k^2}\right)^2 \cdot \frac{\overline{(e_4' - e_3')^2}}{4\,\overline{e_{3/4}}^2} \,, \qquad (39.3)$$

$$\frac{\overline{u_1' u_2'}}{U_1^2} = \frac{1+k^2}{1-k^2} \cdot \frac{\overline{(e_2'^2 - e_1'^2)}}{4\,\overline{e_{1/2}}^2} \,, \qquad (39.4)$$

$$\frac{\overline{u_2' u_3'}}{U_1^2} = \left(\frac{1+k^2}{1-k^2}\right)^2 \cdot \left[\frac{\overline{(e_6' - e_5')^2}}{8\,\overline{e_{5/6}}^2} - \frac{\overline{(e_8' - e_7')^2}}{8\,\overline{e_{7/8}}^2} \right] \,, \qquad (39.5)$$

$$\frac{\overline{u_3' u_4'}}{U_1^2} = \frac{1+k^2}{1-k^2} \frac{\overline{(e_4'^2 - e_3'^2)}}{4\,\overline{e_{3/4}}^2}, \tag{39.6}$$

$$U_1^2 = \frac{2}{1+k^2} \cdot \overline{e_i}^2, \qquad i = 1, \ldots, 8. \tag{39.7}$$

The same result is obtained if we proceed from (38) and form $\overline{e_{1/2}}^2$, $\overline{e_1^2}$, $\overline{e_2^2}$, $\overline{e_1 e_2}$. There results an equation system analogous to (31)

$$\begin{pmatrix} a_{11}^2 & 0 & 0 & 0 & 0 & 0 & 0 \\ a_{11}^2 & a_{11}^2 & a_{12}^2 & a_{31}^2 & 2a_{11}a_{12} & 2a_{12}a_{31} & 2a_{11}a_{31} \\ a_{11}^2 & a_{11}^2 & a_{12}^2 & a_{31}^2 & -2a_{11}a_{12} & 2a_{12}a_{31} & -2a_{11}a_{31} \\ a_{11}^2 & a_{11}^2 & -a_{12}^2 & -a_{31}^2 & 0 & -2a_{12}a_{31} & 0 \end{pmatrix} \cdot \begin{pmatrix} U_1^2 \\ \overline{u_1'^2} \\ \overline{u_2'^2} \\ \overline{u_3'^2} \\ \overline{u_1' u_2'} \\ \overline{u_2' u_3'} \\ \overline{u_3' u_1'} \end{pmatrix} = \tag{40}$$

$$= a_{11} \cdot \begin{pmatrix} \overline{e_{1/2}}^2 \\ \overline{e_1^2} \\ \overline{e_2^2} \\ \overline{e_1 e_2} \end{pmatrix}$$

But a comparison with (31) shows that the relations between the speed fluctuations and the hot-wire signals are apparently wrong for weak turbulence. By transformation we obtain the system of equations analogous to (32): /44

$$\begin{pmatrix} a_{11}^2 & 0 & 0 & 0 & 0 & 0 & 0 \\ 0 & a_{11}^2 & 0 & 0 & 0 & 0 & 0 \\ 0 & 0 & 0 & 0 & 2a_{11}a_{12} & 0 & 2a_{11}a_{31} \\ 0 & 0 & a_{12}^2 & a_{31}^2 & 0 & 2a_{12}a_{31} & 0 \end{pmatrix} \cdot \begin{pmatrix} U_1^2 \\ \overline{u_1'^2} \\ \overline{u_2'^2} \\ \overline{u_3'^2} \\ \overline{u_1' u_2'} \\ \overline{u_2' u_3'} \\ \overline{u_3' u_1'} \end{pmatrix} =$$

$$= a_{11} \cdot \begin{pmatrix} \overline{e_{1/2}}^2 \\ \frac{1}{4}\overline{e_1^2} + \frac{1}{4}\overline{e_2^2} + \frac{1}{2}\overline{e_1 e_2} - \overline{e_{1/2}}^2 \\ \frac{1}{2}\overline{e_1^2} - \frac{1}{2}\overline{e_2^2} \\ \frac{1}{4}\overline{e_1^2} + \frac{1}{4}\overline{e_2^2} - \frac{1}{2}\overline{e_1 e_2} \end{pmatrix} = a_{11} \cdot \begin{pmatrix} \overline{e_{1/2}}^2 \\ \frac{1}{4}\overline{(e_2' + e_1')^2} \\ \frac{1}{2}\overline{(e_1'^2 - e_2'^2)} \\ \frac{1}{4}\overline{(e_2' - e_1')^2} \end{pmatrix}$$

Now the first and second approximations differ only by that equation containing the average speed U_1, whereas the other equations containing only the fluctuation quantities $e_{1/2}'$, u_1', are identical. Thus, via a wrong interim result, we have come to a partly correct end-result. But this is not mere chance: If we proceed

from a series expansion (28) from

$$e = \sqrt{a_{11}}\, U_1 \cdot [\, 1 + \xi + \tfrac{1}{2}(\eta^2 - \xi^2) + O((\xi,\eta)^3)\,],$$

then a linear approximation follows:

$$e = \sqrt{a_{11}}\, U_1\, [\, 1 + \xi\,],$$

$$\bar{e} = \sqrt{a_{11}}\, U_1\, [\, 1 + \bar{\xi}\,],$$

$$e' = e - \bar{e} = \sqrt{a_{11}}\, U_1 \cdot \xi',$$

$$\overline{e'^2} = (\sqrt{a_{11}}\, U_1)^2 \cdot \overline{\xi'^2},$$

in quadradic approximation: /45

$$e = \sqrt{a_{11}}\, U_1\, [\, 1 + \xi + \tfrac{1}{2}(\eta^2 - \xi^2)\,],$$

$$\bar{e} = \sqrt{a_{11}}\, U_1\, [\, 1 + \bar{\xi} + \tfrac{1}{2}(\overline{\eta^2} - \overline{\xi^2})\,],$$

$$e' = \sqrt{a_{11}}\, U_1\, [\, \xi' + \tfrac{1}{2}(\eta^2 - \overline{\eta^2} - \xi^2 + \overline{\xi^2})\,],$$

$$\overline{e'^2} = (\sqrt{a_{11}}\, U_1)^2 \cdot \overline{\xi'^2}.$$

Apparently, the relations between the quadratic fluctuation quantities $\overline{e'^2}$ and $\overline{\xi'^2}$ are the same in both approximations, but not e. This means that according to the first approximation, e should be independent of θ, whereas this does not apply for the second approximation.

Equations (39.1) to (39.7) with k=0 give relations which apply for low turbulence and slight tangential cooling; these have long been known. For greater turbulence and inclusion of tangential cooling, this first and the second approximation give the following corrections:

/46

-The "k-correction", expressed by the prefactors $[(1+k^2)/(1-k^2)]^2$, $(1+k^2)/(1-k^2)$ in (37). This correction is also provided by the first approximation and is easy to see since the coordinate 1 is assigned the factor 1, and the coordinates 2 and 3 are assigned the factor $(1+k^2)/(1-k^2)$. This correction was already given by Champagne and Sleicher [24] for some turbulence quantities (eq. 39.2 and 39.4), if we take into account the identity

$$\left(\frac{1+k^2}{1-k^2}\right)^2 = \frac{1+k^2}{1-3k^2+4k^4}$$

valid for small k.

-The "turbulence intensity correction", specified by the term

$$\left[\, 1 - 2\,\frac{1+3k^2}{(1-k^2)^2}\,\frac{\overline{(e_2' - e_1')^2}}{4\,\overline{e_{1/2}}^2}\,\right]^{-1}$$

This correction has been given by other authors [25, 26, 27]. For turbulence levels up to 0.5, it amounts to about 50%.

-The "anisotropy correction" which is specified by the values for the anisotropy coefficients λ, μ, ν. This correction is not provided

by the linear approximation. It means that the linear approximation is permitted only for the isotropic turbulence ($\lambda=\mu=\nu=1$).

Figures 7-9 show the correction factors F^2 and $\lambda^2 F^2$ as well as the corrected average speed U_1 for various values of the turbulence parameter. For simplicity, the quantities are presented as functions of $\varepsilon_{1/2} = [(\overline{e_2^2}-\overline{e_1^2})^2/4\ \overline{e_{1/2}}^2]^{1/2}$ for fixed parameter values of k and λ, although the anisotropy coefficient λ surely depends on the turbulence intensity. For $\lambda=1$ the values $\lambda^2F^2=F^2$ coincide. According to the relations at a plate boundary layer, where $\overline{u_1'^2} > \overline{u_3'^2} > \overline{u_2'^2}$ applies, when x_2 is the coordinate perpendicular to the plate, the corrections are denoted only for the case $\lambda^2\leq 1$, since in every case the axes x_1, x_2 can be selected so that we have $\lambda^2\leq 1$. Estimations from measurements show that the factor λ generally is almost equal to 1; about $0.95<\lambda<1$ /47
From eq. (37.2) follows: $0 \leq \varepsilon_{1/2} \leq 1/\sqrt{6}$ $(0\leq k\leq 0.2)$
when $0 \leq \sqrt{\overline{u_2'^2}/U_1^2} \leq 0.5$

and we shall limit the discussion to this very region.

It turns out--and this can be shown analytically--that the correction factors F^2, λ^2F^2 rise continuously with k and $\varepsilon_{1/2}$, but they fall continuously with λ. The influence of the tangential cooling factor k is small for small turbulence intensity (small $\varepsilon_{1/2}$) and weak anisotropy ($\lambda\approx 1$), but grows rapidly with both quantities. The influence of turbulence intensity on the correction factors is similar in all cases; the curves rise continuously with $\varepsilon_{1/2}$ and are convex to the bottom. For an anisotropic turbulence, we have $F^2>\lambda^2F^2$. The anisotropy of the turbulence has a strong influence on the correction factors. In particular, λ has a great effect on F^2.

5. Analysis of the Quadratic Signals /48

The attempt to use the quadratic signals e^2 alone for the hot wire analysis would eliminate the square root expansion since this apparently leads to a systemmatic error in the analysis. Rodi [18] found that one can calculate the values $U_1^2+\overline{u_1'^2}$, $\overline{u_2'^2}$, $\overline{u_3'^2}$, $\overline{u_1'u_2'}$ from the quadratic signals of three suitable hot-wire directions, if we presume $U_2=U_3=0$; but it is not possible to compute the average speed U_1. In order to determine this, Rodi refers back to the series expansion. He supposes that in the case of strong turbulence, this method is still better than the conventional one, since the series expansion is used only at this point.

Another attempt to avoid the series expansion comes from Acrivellis [28] to [31]. He proceeds from the time averages $\overline{e^2}$, $\overline{e'^2}=\overline{e^2}-\overline{e}^2$ of differently-oriented hot wires and derives equations for the turbulence quantities $\overline{u_l'u_m'}$ $(l,m=1,2,3)$, which are supposed to be valid for any level of turbulence. This unrestricted validity must be doubted since in the course of the analysis, no sign problem occurs; and as we know from section 3.2.1.1, this is unavoidable for larger

turbulences. Actually, Acrivlellis gives a functional relation between the fluctuation signal $\overline{e'^2}$ and the turbulence quantity $\overline{u_l' u_m'}$ (eq. (21) in [28]), which is not derived and which leads to a linear relation $\bar{e} \sim u$ (eq. (24) in [28]), regardless of the turbulence intensity. From other investigations, it follows that such an exact linear relation does not exist (Bartenwerfer [32]). Thus, of the results of Acrivlellis only one is exact and was used in the derivation of eq. (21) or (24)--the other results are approximations for low turbulence intensity. In a later work [21], Acrivlellis also stopped using such a linear relation, in this case he did not find any exact solution for all sought quantities u_1, $\overline{u_l' u_m'}$ for X-wire probes.

So if an exact analysis with a two-wire probe is not possible, then there are yet several possible approximations in the case of low turbulence. A very close approximation is to proceed from the averages $\overline{e_1^2}^2$, $\overline{e_2^2}^2$, $\overline{e_1^4}$, $\overline{e_2^4}$, $\overline{e_1^2 e_2^2}$ of an X-wire probe, instead of the usual $\overline{e_1}^2$, $\overline{e_2}^2$, $\overline{e_1^2}$, $\overline{e_2^2}$, $\overline{e_1 e_2}$. We thus avoid a square root expansion, but in order to get solvable equations, we must neglect terms greater than 2nd order in the fluctuations in the second approximation in the terms $\overline{e_1^2 e_2^2}$. If $u_2 = u_3 = 0$ again, or if the criterion (30) approximately exists, then one obtains the following system of equations analogous to eq. (31): /49

$$\begin{pmatrix}
a_{11}^2 & 2a_{11}^2 & 2a_{11}a_{22} & 2a_{11}a_{33} & 4a_{11}a_{12} & 4a_{11}a_{23} & 4a_{11}a_{31} \\
a_{21}^2 & 2a_{21}^2 & 2a_{21}a_{23} & 2a_{21}a_{33} & -4a_{21}a_{12} & 4a_{21}a_{23} & -4a_{21}a_{31} \\
a_{31}^2 & 6a_{31}^2 & 2a_{31}a_{22}+4a_{32}^2 & 2a_{31}a_{33}+4a_{13}^2 & 12a_{31}a_{12} & 8a_{12}a_{13}+4a_{31}a_{23} & 12a_{11}a_{31} \\
a_{21}^2 & 6a_{21}^2 & 2a_{21}a_{22}+4a_{22}^2 & 2a_{21}a_{33}+4a_{13}^2 & -12a_{21}a_{12} & 8a_{12}a_{13}+4a_{21}a_{23} & -12a_{21}a_{31} \\
a_{11}^2 & 6a_{11}^2 & 2a_{11}a_{12}-4a_{12}^2 & 2a_{11}a_{33}-4a_{13}^2 & 0 & -8a_{12}a_{13}+4a_{11}a_{23} & 0
\end{pmatrix}$$

$$\cdot \begin{pmatrix} U_1^4 \\ \overline{u_1'^2}\cdot U_1^2 \\ \overline{u_2'^2}\cdot U_1^2 \\ \overline{u_3'^2}\cdot U_1^2 \\ \overline{u_1' u_2'}\cdot U_1^2 \\ \overline{u_2' u_3'}\cdot U_1^2 \\ \overline{u_3' u_1'}\cdot U_1^2 \end{pmatrix} = \begin{pmatrix} \overline{e_1^2}^2 \\ \overline{e_2^2}^2 \\ \overline{e_1^4} \\ \overline{e_2^4} \\ \overline{e_1^2 e_2^2} \end{pmatrix} \qquad (42)$$

This system of equations is derived in more detail in Appendix D; the other transformations and computation steps are presented there also. As the final result, we obtain:

$$\frac{\overline{u_1'^2}}{U_1^2} = \frac{1}{4}\cdot\left[\frac{\overline{(c_2'+c_1')^2} - \overline{d_{1/2}}^2}{4\,\overline{c_{1/2}}^2}\right]\cdot F_q^2 \,, \qquad (43.1)$$

$$\frac{\overline{u_2'^2}}{U_1^2} = \left(\frac{1+k^2}{1-k^2}\right)^2\cdot\frac{1}{4}\cdot\left[\frac{\overline{(c_2'-c_1')^2} + \overline{d_{1/2}}^2}{4\,\overline{c_{1/2}}^2}\right]\cdot F_q^2 \,, \qquad (43.2)$$

$$\frac{\overline{u_3'^2}}{U_1^2} = \left(\frac{1+k^2}{1-k^2}\right)^2\cdot\frac{1}{4}\cdot\left[\frac{\overline{(c_4'-c_3')^2} + \overline{d_{3/4}}^2}{4\,\overline{c_{3/4}}^2}\right]\cdot \lambda_q\cdot F_q^2 \,, \qquad (43.3)$$

$$\frac{\overline{u_1' u_2'}}{U_1^2} = \frac{1+k^2}{1-k^2}\cdot\frac{1}{4}\cdot\left[\frac{\overline{(c_2'^2-c_1'^2)}}{4\,\overline{c_{1/2}}^2}\right]\cdot F_q^2 \,, \qquad (43.4)$$

$$\frac{\overline{u_2' u_3'}}{U_1^2} = \left(\frac{1+k^2}{1-k^2}\right)^2\cdot\frac{1}{4}\cdot\left[\mu_q^2\,\frac{\overline{(c_6'-c_5')^2} + \overline{d_{5/6}}^2}{8\,\overline{c_{5/6}}^2} - \nu_q^2\,\frac{\overline{(c_8'-c_7')^2} + \overline{d_{7/8}}^2}{8\,\overline{c_{7/8}}^2}\right]\cdot F_q^2 \,, \qquad (43.5)$$ /50

$$\frac{\overline{u_i' u_q'}}{U_1^2} = \frac{1+k^2}{1-k^2} \cdot \frac{1}{4} \left[\frac{(\overline{c_4'^2} - \overline{c_3'^2})}{4\,\overline{c_{3/4}}^2} \right] \cdot \lambda_q^2 \cdot F_q^2 \quad , \tag{43.6}$$

$$U_1^4 = \frac{4}{(1+k^2)^2} \cdot \overline{c_{1/2}}^2 \cdot F_q^{-2} = \frac{4}{(1+k^2)^2}\,\overline{c_{3/4}}^2 \cdot \frac{1}{\lambda_q^2} \cdot F_q^{-2} = \tag{43.7}$$

$$= \frac{4}{(1+k^2)^2} \cdot \overline{c_{6/6}}^2 \cdot \frac{1}{\mu_q^2} \cdot F_q^{-2} = \frac{4}{(1+k^2)^2}\,\overline{c_{7/8}}^2 \cdot \frac{1}{\nu_q} \cdot F_q^{-2} \quad ,$$

with

$$\begin{aligned} c &:= e^2 \quad , \\ \overline{c_{ij}}^2 &:= \tfrac{1}{2}(\overline{c_i}^2 + \overline{c_j}^2) \quad , \quad \overline{d_{ij}} = \overline{c_i} - \overline{c_j} \quad , \\ \lambda_q^2 &:= \overline{c_{3/4}}^2 / \overline{c_{1/2}}^2 \quad , \\ \mu_q^2 &:= \overline{c_{6/6}}^2 / \overline{c_{1/2}}^2 \quad , \\ \nu_q^2 &:= \overline{c_{7/8}}^2 / \overline{c_{1/2}}^2 \quad , \end{aligned} \tag{43.8}$$

$$F_q^{-2} := \left[1 + \frac{2}{1-k^2}(\lambda_q^2 - 1) - \frac{1}{2} \frac{\overline{(c_2' + c_1')^2} - \overline{d_{1/2}}^2}{4\,\overline{c_{1/2}}^2} - \right. \tag{43.9}$$

$$\left. - \frac{(3+k^2)(1+k^2)}{2(1-k^2)} \cdot \frac{\overline{(c_2' - c_1')^2} + \overline{d_{1/2}}^2}{4\,\overline{c_{1/2}}^2} \right] .$$

If we compare equations (43.1) to (43.9) with equations (37.1) to (37.6), (34) and (36), then a strong formal similarity is found. But regarding the quadratic signals, note that for turbulent signals, $\overline{c}_1 \neq \overline{c}_2$ etc. applies, thus the appearance of these differences in formulas (43.1), (43.2), (43.3), (43.5).

Also, in this analysis there is a linear approximation. This results formally from the second approximation, by setting $F_q = 1$ and $\overline{d}_{i/j} = 0$. The approximation $F_q = 1$, but possibly $\overline{d}_{i/j} \neq 0$ is called quasi-linear.

Measurements with X-wires in turbulent flows could show whether the results computed with the quadratic signals differ significantly from the conventional approximations (sec. 4.1 and 4.3). In sec. 6 these approximations will be included in the numeric testing of conventional analysis formulas. /51

6. Numeric Check of Some Approximations /52

The formulas named in sections 4 and 5 fail when the turbulence intensity is high, since in the derivation "sufficiently" low turbulence was presumed. In the measurement, the question is more real: How large are the errors in computed turbulence quantities $\overline{u_l u_m}/U$ in the various approximations? By experiments it is not possible to answer this question since no exact analysis is known (e.g. as per sec. 3) which is also reliable in practice. Through

a principally different measurement method, e.g. Laser-Doppler anemometry, an experimental comparison would be possible; this will only be generally accepted as a check of the one measurement method if we know which method is more reliable and accurate, especially for high turbulence intensity. There is still no agreement on this.

One can suppose that the accuracy of the series expansion by small fluctuation quantities is more a mathematic than a physical problem and that the used formulas can be tested with simple functions. These functions do not have to describe real, stochastic turbulence signals, they only have to describe correctly the turbulence intensities in the three coordinate directions and the correlations between the components, including perhaps the bulging factor $\Gamma=\overline{u'^4}/\overline{u'^2}^2$ which plays an important role in other correction formulas (Vagt [27]). If these assumptions are correct and if the functions are also to be easily integrable, the possibility arises of checking formulas used for turbulence quantities by means of computer.

For the periodic step function:

$$g(t',s,\sigma)=\begin{cases}\sqrt{1/s-1/\sigma}\,, & 0\le t'\le s\,,\\ -(1/\sigma)/\sqrt{1/s-1/\sigma}\,, & s\le t'\le\sigma\,,\\ 0\,, & \sigma\le t'\le 1\,,\end{cases}\qquad(44)$$

continued periodically on the whole t'-axis, /53
with $0<s<\sigma<1$

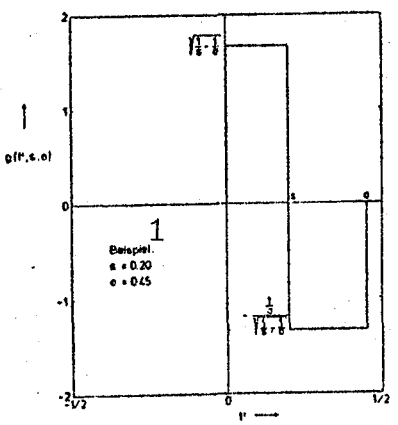

Key: 1-example

we have (see Appendix E)

$$\bullet\quad \overline{g} = \int_0^1 dt'\, g = 0 \quad ,$$

$$\bullet\quad \overline{g^2} = 1 \quad ,$$

$$\bullet\quad \Gamma = \overline{g^4} / \overline{g^2}^2 = \frac{\sigma}{s(\sigma - s)} - \frac{3}{\sigma} \quad ,$$

$$\bullet\quad \overline{g(t',s,\sigma)\, g(t'-\tau,s,\sigma)} = \begin{cases} 1 - \frac{|\tau|}{\sigma}\left(\frac{\sigma}{s} + \frac{1/\sigma}{1/s - 1/\sigma}\right), & 0 \le |\tau| \le s \\ -\frac{|\tau|}{\sigma} \cdot \frac{1/\sigma}{1/s - 1/\sigma}, & s \le |\tau| \le \sigma - s \\ -1 + |\tau|/\sigma, & \sigma - s \le |\tau| \le \sigma \\ 0, & \sigma \le |\tau| \le 1/2 \end{cases}$$

periodically continued for other r,
if $2s \le \sigma \le \frac{1}{2}$.

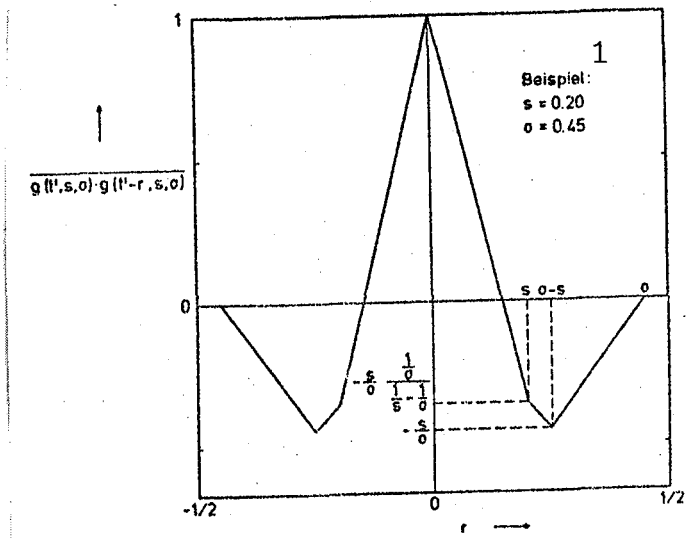

Key: 1-example

/54

For the imagined speed fluctuations, we now set:

$$\frac{u_1'}{U} = A_1 \cdot g\left(\frac{t}{T} - \tau_1, s, \sigma\right) \quad , \quad 1 = 1,2,3 \quad ;$$
$$U_1 = U \, , \; U_2 = U_3 = 0 \, ; \; 2s \le \sigma \le \tfrac{1}{2} \; ; \; T \text{ random} \qquad (45)$$

In order to use only meaningful parameters A_1, τ_1, s, σ, known experimental results can be used; here, the works by Elsenaar and Boelsma [27], Charnay [28], Dechow [29], and unpublished measurement results of Lehmann [30], in order to estimate the value-range of the following turbulence quantities:

$$C_1 := \frac{\overline{u_1'^2}}{U_1^2} \quad , \quad C_2 := \frac{\overline{u_2'^2}}{\overline{u_1'^2}} \quad , \quad C_3 := \frac{\overline{u_3'^2}}{\overline{u_1'^2}} \quad ;$$
$$C_{1m} := \frac{\overline{u_1' u_m'}}{\sqrt{\overline{u_1'^2}} \cdot \sqrt{\overline{u_m'^2}}} \quad , \quad 1 \neq m \quad . \qquad (46)$$

Although the named papers pertain to entirely different test arrangements; they were measured in regions of different turbulence intensity and anisotropy, and with hot-wire technology [33-35] or

with Laser-Doppler anemometry (LDA) [36]--figures 10 to 16 show examples--the following uniform range of parameters results:

-isotropic turbulence

$$C_2 = C_3 = 1, \quad C_{1m} = 0 \ (1{*}m) \ ; \tag{47.1}$$

/55

-two-dimensional boundary layer

$$\left.\begin{aligned} &0.3 \le C_2 \le C_3 \le 0.6 \ , \\ &|C_{12}| = 0.3\text{-}0.4 \ , \\ &C_{13} \approx C_{23} \approx 0.0 \ ; \end{aligned}\right. \tag{47.2}$$

-three-dimensional boundary layer

$$\left.\begin{aligned} &0.4 \le C_2 \le C_3 \le 1.1 \ , \\ &|C_{1m}| = 0.0\text{-}0.3 \ , \\ &|C_{23}| \le |C_{13}| \le |C_{12}| \ \text{(with exceptions)} \end{aligned}\right. \tag{47.3}$$

The x_2-axis was always the direction perpendicular to the two-dimensional boundary layer. For the turbulence intensity C_1 we have:

- $0.001 \le C_1 \le 0.05$ for the hot-wire measurements (turbulence 3-24%)
- $0.1 \le C_1 \le 1.2$ for the LDA measurements at the round, free-jet (turbulence 30-110%)

Accordingly, the following parameters are selected for the numeric test:

-isotropic turbulence

$$\left.\begin{aligned} &0 \le A_1^2 \le 0.25 \ , \\ &A_2^2/A_1^2 = A_3^2/A_1^2 = 1 \ , \\ &r_1 = 1/3 \ , \ r_2 = 0 \ , \ r_3 = r_1 + 1/3 \ , \\ &\sigma = 1/8 \ , \ s = 1/6 \ \text{bzw.} \ 0.0665 \ , \end{aligned}\right\} \quad \left.\begin{aligned} &C_2 = C_3 = 1 \ , \\ &C_{12} = C_{23} = C_{31} = 0 \ , \\ &\Gamma = 3 \ \text{bzw.} \ 10 \ . \end{aligned}\right. \tag{48.1}$$

-two-dimensional boundary layer

$$\left.\begin{aligned} &0 \le A_1^2 \le 0.25 \ , \\ &A_2^2/A_1^2 = A_3^2/A_1^2 = 0.5 \ , \\ &r_1 = (1 - 0.4)/(1/s + 9/(1s-3)) \ , \\ &\sigma = 1/3 \ , \ s = 1/6 \ \text{bzw.} \ 0.0655 \ , \\ &\text{sign } A_1 \cdot \text{sign } A_2 = -1 \ , \end{aligned}\right\} \quad \left.\begin{aligned} &C_2 = C_3 = 0.5 \ , \\ &C_{12} = -0.4 \ , \\ &C_{13} = C_{23} = 0 \ , \\ &\Gamma = 3 \ \text{bzw.} \ 10 \end{aligned}\right. \tag{48.2}$$

-three-dimensional boundary layer

/56

$$
\left.\begin{array}{l}
0 \le A_1^2 \le 0.25\,, \\
A_2^2/A_1^2 = 0.5\,,\ A_3^2/A_1^2 = 0.7\,, \\
r_1 = \tfrac{2}{3}(1+C)\,s,\ r_2 = 0,\ r_3 = 2r_1\,, \\
\qquad\qquad \text{mit } C = 0.1,\ 0.3\,, \\
\sigma = 2s = 1/3\,,
\end{array}\right\}
\qquad
\left.\begin{array}{l}
C_2 = 0.5\,, \\
C_3 = 0.7\,, \\
C_{12} = C_{13} = -C\,, \\
C_{23} = \tfrac{1}{3}(2C-1)\,, \\
\Gamma = 3\,.
\end{array}\right\}
\qquad (48.3)
$$

Details of the numeric calculation can be found in the programs in Appendix F.

Before presenting the results, three problem areas have to be mentioned. The procedure in the numeric test differs from the measurement with an X-wire probe since the x_1-axis of the former can be set as the main flow direction $(U_2=U_3=0)$. With increasing turbulence intensity, differences $\tilde{e}_1-\tilde{e}_2$, $\tilde{e}_3-\tilde{e}_4$ result which point up the limitations of the method. The measurement begins--as explained above--with the search for the main flow direction, but the criterion for this: $\tilde{e}_1=\tilde{e}_2$, $\tilde{e}_3=\tilde{e}_4$ is valid only for low turbulence intensity. For greater turbulence, in this manner we do not find the sought flow-line specific coordinate system, rather one with average speed components $U_2, U_3 \neq 0$. The turbulence quantities are thus not only inaccurately measured with increasing turbulence intensity due to the series expansion by the fluctuation quantities, but in addition they are described in a "wrong" coordinate system. These two sources of error are thus two sides of the same coin, namely the approximation nature of the series expansion.

/57

The step functions used for the test can indeed simulate the turbulence intensity and the correlations of the speed components, but the slope $\Sigma=\overline{g^3}/(\overline{g^2})^{3/2}$ depends greatly on the selection of parameters s,σ (see appendix E). For the used values $(s,\sigma) = (1/6,\ 1/3)$ or $(0.0655,\ 1/3)$ it follows $(\Gamma,\Sigma) = (3,0)$ or $(10,2.6)$. Whereas for the low bulge factor $\Gamma=3$ the slope Σ actually disappears, as expected, for the high bulging factor $\Gamma=10$ one obtains a large slope for the test functions of 2.6. Now in the series expansions the factors for terms of higher order are small compared to 1, but appear to be less suitable for such signal analyses, which presume a neglect of uneven powers of the fluctuation quantities (e.g. Vagt [27]).

Finally, one could doubt whether the used test functions lead to representative error estimations. The supposition also arises that the errors in the turbulence quantities are overestimated, since in the specified profile of speed, only the extreme values are taken, in addition to the averages. The probability distributions of the speed components are discrete with only three possible values, thus they are not normal distributions. We shall later compare our results with those of Tutu and Chevray [16] and Bradbury [17], where normal-distributed speed fluctuations were presumed.

The results of the numeric test are presented in figures 14-24 as follows: In constant conditions

$$\frac{\overline{u_2'^2}}{\overline{u_1'^2}}\ ,\quad \frac{\overline{u_3'^2}}{\overline{u_1'^2}}\ ,\quad \frac{\overline{u_1' u_m'}}{\sqrt{\overline{u_1'^2}\cdot\sqrt{\overline{u_m'^2}}}}$$

various turbulence quantities $\overline{u_1' u_m'}/U^2$ are plotted as a function of the turbulence intensity in the direction of the x_1-axis, $\overline{u_1'^2}/U^2$. This turbulence intensity varies from 0 to 0.25 or from 0 to 0.05. (Greater turbulence intensities than 0.25 were only computed for testing, and it was found that in these cases, the computed results lead to entirely wrong results). The quadratic quantity $\overline{u_1'^2}/U^2$ is plotted as the abscissa, since quadratic quantities $\overline{u_1' u_m'}/U^2$ are to be determined. In the described procedure, the exact quantities $\overline{u_1' u_m'}/U^2$ are linear functions of the intensity $\overline{u_1'^2}/U^2$ and are represented in the figure as lines, e.g. /58

$$\frac{\overline{u_1' u_2'}}{U^2} = \frac{\overline{u_1' u_2'}}{\sqrt{\overline{u_1'^2}\cdot\sqrt{\overline{u_2'^2}}}}\cdot\frac{\sqrt{\overline{u_2'^2}}}{\sqrt{\overline{u_1'^2}}}\cdot\frac{\overline{u_1'^2}}{U^2} \sim \frac{\overline{u_1'^2}}{U^2}$$

The error in the various approximations shows up as a deviation from these lines. As relative error, we define

$$\Delta_{lm} = \left[\left(\frac{\overline{u_l' u_m'}}{U^2}\right)_{\text{approx.}} - \left(\frac{\overline{u_l' u_m'}}{U^2}\right)_{\text{exact}}\right] \Big/ \left(\frac{\overline{u_l' u_m'}}{U^2}\right)_{\text{exact}}$$

which can be positive or negative. As a second, non-linear abscissa, the turbulence degree $\sqrt{\overline{u_1'^2}/U^2}$ is used, it extends from the interval 0 to 50% or 0 to 22% respectively. Now we shall discuss individual results.

Figure 14 shows the relative fluctuations $\overline{u_l'^2}/U^2$ $(l=1,2,3)$ as a function of increasing turbulence intensity $0 \le \overline{u_1'^2}/U^2 \le 0.25$ for isotropic turbulence, as provided by the analysis of the "normal" signal e in first, second and specifically fourth approximation. The tangential cooling is neglected here and in the following figures (k=0); the bulging factor is set as $\Gamma=3$. (The influence of these two factors will be discussed later). For this parameter selection results the linear approximation (solid curve) in the whole region $0 \le (\overline{u_1'^2}/U^2) \le 0.25$ as a good approximation just for this quantity $\overline{u_1'^2}/U^2$, but gives too small values throughout. The second approximation (long dashes) gives too large values throughout and deviates in the entire interval more greatly from the actual value than the first approximation. The special, fourth approximation of Vagt [26] (short dashes) proves to be best here; even at a max. turbulence intensity of 0.5 it gives a value too small only by ca. 1.3%. The relative errors of the first, second and fourth approximation at $(\overline{u_1'^2}/U^2)=0.15$ are -4.5%, +25.5% and -0.0%. The turbulence intensities $\overline{u_2'^2}/U^2$ and $\overline{u_3'^2}/U^2$ prove to be equal in the approximations, as must be the case for isotropic turbulence. The accuracy of the approximations shows a somewhat different trend than for $\overline{u_1'^2}/U^2$: Of course, the first and fourth approximations again give too small values, and the second gives too large values, but the second approximation differs from the actual value by less than the first one and proves to be the better one here. The relative errors at $(\overline{u_1'^2}/U^2)=0.15$ are -21.1%, +3.3% and -1.1%. /59

Figure 15 shows the relative fluctuations $\overline{u_l'^2}/U^2$ (l=1,2,3) for the same parameter, but this time determined in first or second approximation from the "quadratic" signals e^2. Apparently, in this case the analysis of the quadratic signals leads to much greater errors than the analysis of the normal signals e. Of course, the second approx. proves to be more accurate than the first in the entire range, but for turbulence intensities >0.05 it deviates considerably from the true values. The rel. errors at $(\overline{u_1'^2}/U^2)=0.15$ amount to -57.8% or -18.9% for $\overline{u_1'^2}/U^2$ and -51.1% or -25.6% for $\overline{u_{2/3}'^2}/U^2$. It will be shown whether the analysis of quadratic signals generally lead to greater errors than the analysis of normal signals.

In fig. 16 the rel. fluctuations $\overline{u_l'^2}/U^2$ (l=1,1,2) are shown again; they are obtained from the normal signals and plotted for a small range $0\leq(\overline{u_1'^2}/U^2)\leq 0.05$ of turbulence intensity (compared to fig. 14), thus for turbulence levels 0 to 22.4%. It turns out that in this region, the turbulence intensity $\overline{u_1'^2}/U^2$ can be defined practically without error by the first or fourth approximation, but the turbulence intensities $\overline{u_{2/3}'^2}/U^2$ are defined with equal accuracy by the second approximation. Figure 17 shows the same quantities as fig. 16, but they are computed here by the quadratic signals. The second approximation proves to be useful for this region of small to moderate turbulence, but stays clearly behind the analysis of normal signals.

Figure 18 shows the same quantities as fig. 14, but now for the case of non-isotropic turbulence. The selection of parameters $\overline{u_2'^2}/\overline{u_1'^2}=0.3$, $\overline{u_3'^2}/\overline{u_1'^2}=0.5$, $\overline{u_1'u_2'}/(\sqrt{\overline{u_1'^2}}\cdot\sqrt{\overline{u_2'^2}})=-0.4$, $\overline{u_2'u_3'}/(\sqrt{\overline{u_2'^2}}\cdot\sqrt{\overline{u_3'^2}})=\overline{u_1'u_3'}/(\sqrt{\overline{u_1'^2}}\cdot\sqrt{\overline{u_2'^2}})=0$ should simulate a two-dimensional boundary layer. In comparison to fig. 14, all approximations of the "normal" analysis for turbulence intensities $0\leq\overline{u_1'^2}/U^2\leq 0.10$ prove to be just about as good as in the case of isotropic turbulence. Above $\overline{u_1'^2}/U^2=0.10$ to 0.15, in all approximations a clear bending off from the exact linear profile occurs, which even leads to negative gradients for $\overline{u_{2/3}'^2}/U^2$, but to very large errors for all turbulence quantities. For $0\leq\overline{u_1'^2}/U^2$ the second and fourth approximations are more accurate than the first, however, not to the same extent as for isotropic turbulence. Figure 19 again shows the turbulence intensities $\overline{u_l'^2}/U^2$ (l=1,2,3) computed with the linear and second approximation of the quadratic signals. Whereas the first approx. proves to be definitely inaccurate, the second one lies surprisingly close to the true values in contrast to the case of isotropic turbulence. A plausible explanation cannot be given for this. /60

Figure 20 shows computed approximation values for the sole shear stress quantity $\overline{u_1'u_2'}/U^2$, which does not disappear in the two-dimensional boundary layer. In the upper part of the figure we see that the normal signal leads to good approximation values, as long as $\overline{u_1'^2}/U^2<0.10$. As in fig. 18 for the turbulence intensities $\overline{u_l'^2}/U^2$, for values above $(\overline{u_1'^2}/U^2)=0.10$ to 0.15 there results a clear bending of the approx. curves from the exact lines. The analysis of the quadratic signals--middle part of the figure--only gives good results here for the first approximation. The lower part of fig. 18

shows that the striking deterioration of various approximations above $\overline{u_1'^2}/U^2 \geq 0.15$ is related to the approximation character of the calibration criterion for finding the average flow direction; see section 4. In contrast to measurements, here we have set $U_2=U_3=0$. From a certain turbulence intensity, a difference of $\tilde{e}_1-\tilde{e}_2 \neq 0$ results. Thus it can be concluded that above this certain value of turbulence intensity, the specification of the flow-related coordinate system $(U_1=U>0,\ U_2=U_3=0)$ is problematic. /61

From eq. (6.1) we can derive the relation between $\overline{u_1'u_2'}/U^2$ and the difference of averages $\tilde{e}_1-\tilde{e}_2$: For $U_2=U_3=0$ it follows form (6.1):

$$\overline{u_1'u_2'} = \frac{1}{2}\left(\overline{e_2^2}-\overline{e_1^2}\right) = \frac{1}{2}\left(\overline{e_2'^2}-\overline{e_1'^2}\right) + \frac{1}{2}\left(\bar{e}_2^2-\bar{e}_1^2\right)$$

and again:

$$\overline{u_1'u_2'} = \frac{2}{1-k^2}\left(\frac{\bar{e}_1+\bar{e}_2}{2}\right)^2\left[\frac{\overline{e_2'^2}-\overline{e_1'^2}}{4\left(\frac{\bar{e}_1+\bar{e}_2}{2}\right)^2} - \frac{\bar{e}_1-\bar{e}_2}{\bar{e}_1+\bar{e}_2}\right] =$$

$$= \frac{2}{1-k^2}\left(\frac{\bar{e}_1+\bar{e}_2}{2}\right)^2\left[\left(\frac{\overline{u_1'u_2'}}{U^2}\right)_{1.\,\mathrm{app.}} - \frac{\bar{e}_1-\bar{e}_2}{\bar{e}_1+\bar{e}_2}\right]$$

If we divide by the average speed U, we have:

$$\left(\frac{\overline{u_1'u_2'}}{U^2}\right)_{\mathrm{exact}} = F^2\cdot\left[\left(\frac{u_1'u_2'}{U^2}\right)_{1.\,\mathrm{app.}} - \frac{\bar{e}_1-\bar{e}_2}{\bar{e}_1+\bar{e}_2}\right] =$$

$$= \left(\frac{u_1'u_2'}{U^2}\right)_{2.\,\mathrm{app.}} - F^2\,\frac{\bar{e}_1-\bar{e}_2}{\bar{e}_1+\bar{e}_2}\ ,$$

(F from eq. (36)).

So if $\tilde{e}_1>\tilde{e}_2$, then the 2nd approx. gives too large values, for $\tilde{e}_1<\tilde{e}_2$ too small. Figure 20 confirms this and also the quantitative relation if we note that here $\overline{u_1'u_2'}<0$.

In the case of a three-dimensional boundary layer, all correlations $\overline{u_1'u_m'}$ $(1\neq m)$ are different from zero. In the following figures the parameters $\overline{u_2'^2}/\overline{u_1'^2}=0.5$, $\overline{u_3'^2}/\overline{u_1'^2}=0.7$, $\overline{u_1'u_2'}/\sqrt{\overline{u_1'^2}\cdot\overline{u_2'^2}}=\overline{u_1'u_3'}/\sqrt{\overline{u_1'^2}\cdot\overline{u_3'^2}}=-0.3$ and $\overline{u_2'u_3'}/\sqrt{\overline{u_2'^2}\cdot\overline{u_3'^2}}=-0.13$ were selected. Since the analysis of the quadratic signals leads to worse results than the analysis of normal signals almost everywhere, only results of the latter are shown. Figure 21 gives the turbulence intensities $\overline{u_1'^2}/U^2$ and $\overline{u_2'^2}/U^2$ in first to fourth approximations. The various approximations do not differ significantly here. The curves are similar to the case of 2-dim. boundary layer (see fig. 18), especially the same bending of the curves from the exact linear run in the range of turbulence intensity$(\overline{u_1'^2}/U^2)\approx 0.10$–$0.15$ is found. The errors above 0.15 are about the same magnitude and below 0.10, they are slightly larger than for the 2-dim. boundary layer. The same thing applies for the shear stress quantity $\overline{u_1'u_2'}/U^2$, fig. 22, upper section. The approximations differ only a little from each other, but exhibit very large errors above $\overline{u_1'^2}/U^2 > 0.10$. Above $\overline{u_1'^2}/U^2=0.175$ all approximations for this parameter selection give a wrong sign. For all turbulence intensities, the error in $\overline{u_1'u_2'}/U^2$ is greater than for the 2-dim. boundary layer. The lower part of fig. 22 shows $\overline{u_1'u_3'}/U^2$ and the first approximation gives improbably accurate values, even for extremely high turbulence intensity of 0.25 ($\hat{=}$ 50% turbulence level). /62

But this result cannot be generalized, since it is a result of the special selection of parameters. The profile of $\overline{u_2'u_3'}/U^2$ over the turbulence intensity $\overline{u_1'^2}/U^2$, fig. 23 top, is again "normal": For turbulence intensities below 0.10 good approximations, above 0.10 large errors increasing quickly with the turbulence intensity. The lower part of the figure again shows $(\tilde{e}_1-\tilde{e}_2)/(\tilde{e}_1+\tilde{e}_2)$, representative for the other differences $(\tilde{e}_i-\tilde{e}_{i+1})/(\tilde{e}_i+\tilde{e}_{i+1})$, $i=3,5,7,$ whose profile is quite similar. As in the case of a two-dimensional boundary layer, we see a sudden rise in these differences in the same region $\overline{u_1'^2}/U^2 \approx 0.10\text{-}0.15$ in which the frequent bending of the graph (mentioned above) of different approximations from the exact profile occurs.

If we summarize previous results, then we find:

-All examined analyses of hot-wire signals based on series expansion by small fluctuations, lead to systematic errors in all turbulence quantities $\overline{u_l'u_m'}/U^2$ $(l,m=1,2,3)$ for a high turbulence intensity

-The analysis of the "squared" signals usually leads to worse results than the analysis of "normal" signals and can thus be discarded.

The systematic error is linked with the approximation character of the criterion for finding the direction of the average speed and to specify a "flow-line specific" coordinate system.

-The turbulence intensities $\overline{u_l'^2}/U^2$ $(l=1,2,3)$ are as a rule computed with a smaller error than the shear stress terms $\overline{u_l'u_m'}/U^2$ $(l\neq m)$, if these are different from zero. But this was already expected, since the latter terms are generally almost an order of magnitude smaller than the former. /63

-The different approximations are loaded with errors of comparable magnitude for high turbulence. In particular, it is not true that the higher approximation is generally the better one.

-One can distinguish three regions of ascending turbulence intensity (naturally somewhat arbitrarily within the limits) in which the approximations are good, useable and useless:

Region	$\overline{u_1'^2}/U^2$	$\sqrt{\overline{u_1'^2}/U^2}$ [%]	$\lvert\Delta_{11}\rvert$ [%]	$\lvert\Delta_{lm}\rvert l\neq m$ [%]
I	0-0.05	0-22	0-30	0-100
II	0.05-0.10	22-32	0-50	0-über 100
III	> 0.10	> 32	0-über 100	100

Key: über=more than

-For regions II and III, or regions of high and very high turbulence intensity, the deviations of approximation values from the actual values can become very great and depend on the turbulence structure without any discernable trend. In region I, the devia-

tions increase slowly with the turbulence intensity by a minimum quadratic amount.

Since in many cases of turbulent flows, the turbulence intensity is less than 20% and since in this range the systematic error increases by the series expansion by the small fluctuation quantities in a monotonous manner with the turbulence intensity, then by consideration of as many results as possible we could check whether the interaction of turbulence structure and tangential cooling affect the error in a discernable manner. For this purpose, in tables 1 to 3 the errors Δ_{1m} in the turbulence intensity $\overline{u_1'^2}/U^2=0.05$ (turbulence degree 22.4%) are presented for a large number of parameter values of $k, \Gamma, \overline{u_2'^2}/\overline{u_1'^2}$, $\overline{u_3'^2}/\overline{u_1'^2}$ and $\overline{u_1'u_m'}/(\sqrt{\overline{u_1'^2}}\sqrt{\overline{u_m'^2}})$. As an example fig. 24 also shows the influence of tangential cooling and of the bulging (convexity) factor Γ on $\overline{u_1'^2}/U^2$ for region I. In this example, the influence of tangential cooling is low, but that of the bulging factor is great. /64

Tables 1 to 3 point up trends, but no invariant rules. In general, the studied systematic error increases with increasing anisotropy of the turbulence, and also with increasing bulging factor Γ. The tangential cooling changes the error only a little, but it can be larger or smaller. The result presented above that the turbulence intensities are determined more accurately than the shear stress terms is also confirmed. If the latter disappear, then the approximations give the value zero, even at high turbulence. But for finite values, the error can apparently be up to 95%, and the bulging factor does not have to be large. In the example with this large error (table 3, 3rd and 4th line), a 3-dimensional boundary layer is simulated with

$$\overline{u_1'u_2'}/(\sqrt{\overline{u_1'^2}}\sqrt{\overline{u_2'^2}}) = -0.10 ,$$

$$\overline{u_1'u_3'}/(\sqrt{\overline{u_1'^2}}\sqrt{\overline{u_3'^2}}) = -0.10 ,$$

$$\overline{u_2'u_3'}/(\sqrt{\overline{u_2'^2}}\sqrt{\overline{u_3'^2}}) = 0.27 .$$

The large errors occur in the quantities $\overline{u_1'u_2'}/U^2$ and $\overline{u_1'u_3'}/U^2$, which are determined one order of magnitude too small. At even greater turbulence intensity, a wrong sign even occurs and even greater errors.

For small bulging factors ($\Gamma \gtrsim 3$) in the case of isotropic turbulence at the point $\overline{u_1'^2}/U^2=0.05$, the maximum error of turbulence intensities $\overline{u_1'^2}/U^2$ for the first, second and fourth approximations is 12, 10 and 6%; for very high bulging factor ($\Gamma=10$) 20%, 31% and 15%. For anisotropic turbulence (two- and three-dimensional boundary layer) the corresponding max. errors are 14%, 16% and 14% ($\Gamma=3$) or 32%, 29% and 31% ($\Gamma=10$). (The large errors Δ_{33} given in the table for the fourth approximation were not taken into account because they arise from the incorrect assumption $\overline{u_2'^2}=\overline{u_1'^2}$). For the 2-D boundary layer, the max. error $|\Delta_{12}|\approx 8\%$ at low Γ and 61% at large Γ. In the 3-D boundary layer finally, the named max. error of around $|\Delta_{12}|\approx 96\%$ occurs even for small bulging (convexity) factor. /65

As a final result we find:

-For turbulence intensities between 0 and 20%, the turbulence quantities $\overline{u_l' u_m'}/U^2$ are determined with an error which depends on the turbulence structure with no discernable trend. Thus no method can be given for correcting this error. For the shear stress term, this error can become so large that its determination at turbulence intensities above 20% must be placed in question.

Tutu and Chevray [16] showed in 1975 that in the determination of the average speed U and of the turbulent fluctuations $\overline{u_1'^2}, \overline{u_2'^2}, \overline{u_1' u_2'}$ in 2-D boundary or shear layers via X-wire probes in high turbulence, very large errors can occur. These errors, it became clear, are based not only on the termination of the Taylor series expansion by the small fluctuations, but also on the following rectification effect of the X-wire probe: When neglecting the tangential cooling (k=0) and the speed component u_3, the following expression from (21) applies for the orthogonal X-wire:

$$e_{1/2}^2 = \frac{1}{2}(u_1 \pm u_2)^2$$

or

$$e_{1/2} = \frac{1}{\sqrt{2}} |u_1 \pm u_2| .$$

But in the signal analysis, if we proceed from the relation

$$e_{1/2} = \frac{1}{\sqrt{2}} (u_1 \pm u_2)$$

which proceeds from the linear approximation, then we presume that due to $e_{1/2} \geq 0$ we also have:

$$-\frac{\pi}{4} \leq \arctan(u_2/u_1) \leq \frac{\pi}{4} .$$

This condition is not fulfilled in higher turbulence.

Now Tutu and Chevray calculated the errors in /66

$$U = U_1, \quad \overline{u_1'^2}, \quad \overline{u_2'^2}, \quad \overline{u_1' u_2'}$$

assuming normal-distributed probability distributions of the speed components as functions of $\overline{u_1'^2}/U^2$ for different parameters $\overline{u_2'^2}/\overline{u_1'^2}$, $\overline{u_3'^2}/\overline{u_1'^2}$, k and presented them in a table (table 1 in [16]). By using these values, one can set up the following comparison table:

		k = 0, C_{12} = 0.4, $C_2 = C_3$ = 0.64					
$\frac{\overline{u_1'^2}}{U^2}$	$\sqrt{\frac{\overline{u_1'^2}}{U^2}}$ [%]	Δ_{11} [%]		Δ_{22} [%]		Δ_{12} [%]	
		a nach [16]	Autor, 1.Näh.	a nach [16]	Autor, 1.Näh.	a nach [16]	Autor, 1.Näh.
0.01	10	-1.8	-0.5	-2.6	-1.0	-2.6	-0.96
0.04	20	-7.6	-2.4	-10.7	-4.8	-11.5	-4.3
0.09	30	-18.8	-4.7	-24.8	-8.8	-29.5	-8.8
0.16	40	-32.9	-33.7	-41.2	-42.5	-49.3	-29.9
0.25	50	-46.1	-57.6	-55.0	-63.0	-64.2	-48.1

Key: a-from [16], 1st approx.

Among these parameters the errors are apparently comparable. A precise agreement cannot be expected, since in both investigations it was found that the errors depend a great deal on the turbulence structure. Even the fast increase in errors for turbulence degrees of 20-30% shows agreement.

A corresponding error estimation (to the one of Tutu and Chevray) was conducted by Bradbury [17] for the one-wire probe. He also proceeded from normal-distributed fluctuations, but plots

$$\bar{U}_{exact}/\bar{U}_{measured} \quad \text{and} \quad \overline{u_1'^2}_{exact} / \overline{u_1'^2}_{measured}$$

as a function of /67

$$\overline{u_1'^2}_{measured}/\bar{U}_{measured}$$ for various parameters

$$\overline{u_2'^2}_{exact}/\overline{u_1'^2}_{exact}.$$

The following comparison results:

$\left(\frac{\overline{u_1'^2}}{U^2}\right)_{exakt}$ [%] a	$\left(\frac{\sqrt{\overline{u_1'^2}}}{U}\right)_{exakt}$ [%] a	$\left(\frac{\overline{u_1'^2}}{U}\right)_{Messung}$ [%] b	c Δ_{11} nach[17]	[%] Autor
0.010	10.0	10	0	0
0.042	20.6	20	-5.5	-0.5
0.107	32.7	30	-16.1	-2.4
0.247	49.7	40	-35.2	-6.8
1.030	101.5	50	-75.7	--
		(≤52)	k = 0	
			$\sqrt{\overline{u_1'^2}} = \sqrt{\overline{u_2'^2}} = \sqrt{\overline{u_3'^2}}$	
0.010	10.0	10	0	-0.5
0.040	20.0	20	0	-2.0
0.094	30.6	30	-4.1	-4.7
0.185	43.0	40	-13.6	-35.0
0.380	61.7	50	-34.2	--
		(≤0.60)	k = 0	
			$\sqrt{\overline{u_1'^2}} = 2\cdot\sqrt{\overline{u_2'^2}} = 2\sqrt{\overline{u_3'^2}}$	

Key: a-exact; b-measured; c-from

In this comparison too, it turns out that the errors are of the same magnitude, even though one-wire probes are compared with two-wire probes; the errors stay within a reasonable range only below a turbulence degree of 30-40%, that is, they stay below 40%.

The error estimations of Tutu and Chevray and of Bradbury relate only to the isotropic turbulence or to the two-dimensional boundary layer. For these cases, errors resulted in the present investigation which are on average smaller than in the case of the 3-D boundary layer and which are otherwise of the same magnitude as in [16, 17]. This result supports the contention that representative errors are estimated here. /68

7. The "Undirected" X-Wire /69

It is naturally troublesome, but generally unavoidable, to search for the main flow direction for each measured point, to compute the turbulence quantities with respect to a flow-line related coordinate system, and finally to transform it into a fixed coordinate system. If the main flow direction changes only a little, e.g. in a round free-jet, in which it is everywhere nearly parallel to the jet axis, the analysis of sec. 4 can be generalized to a fixed coordinate system.

Now when the main flow direction is nearly constant, then the x_1-axis can be fixed (in the round free-jet, e.g. as jet axis) so that:

$$U_1 \gg |U_2|, |U_3|$$

and for sufficiently low turbulence:

$$U_1 \gg |u_1'|, |u_2'|, |u_3'|$$

Thus, one can proceed again from the expansion (28), but now an alignment in the local main flow direction can be omitted.

As in section 4, there are again approximations of varying order depending on how far the series expansion is carried. Since the first approximation has proven to be good for low turbulence, as a rule the first approximation will also suffice here when $|U_2/U_1|$ and $|U_3/U_1|$ are sufficiently small. At $U_3=0$ the values

$$|U_2/U_1| = 0.1\ ,\ 0.2\ ,\ 0.3$$

correspond to the deviations at 5.7°, 11.3°, 16.7° of the main flow direction from the x_1-axis. For greater angles, the second expansion should be taken into consideration; this is presented in appendix G.

In close approximation, for an X-wire lying symmetric to the x_1-axis, we have: /70

$$e_{112} = \sqrt{a_{11}}\, U_1 \cdot \left[1 + \frac{u_1'}{U_1} \pm \frac{a_{12}}{a_{11}} \left(\frac{U_2}{U_1} + \frac{u_2'}{U_1} \right) \pm \frac{a_{13}}{a_{11}} \left(\frac{U_3}{U_1} + \frac{u_3'}{U_1} \right) \right]$$

For an orthogonal X-wire in the usual positions $\alpha=\pi/4$; $\theta=0,\pi$; $\pi/2, -\pi/2$; $\pi/4, -3\pi/4$; $-\pi/4, 3\pi/4$ with the signals e_1 to e_8, it follows:

$$e_{1/2} = \sqrt{\frac{1+k^2}{2}}\left[(U_1+u_1') \mp \frac{1-k^2}{1+k^2}(U_2+u_2') \right],$$

$$e_{3/4} = \sqrt{\frac{1+k^2}{2}}\left[(U_1+u_1') \mp \frac{1-k^2}{1+k^2}(U_3+u_3') \right],$$

$$e_{5/6} = \sqrt{\frac{1+k^2}{2}}\left[(U_1+u_1') \mp \frac{1-k^2}{(1+k^2)\sqrt{2}}(U_2+u_2') \mp \frac{1-k^2}{(1+k^2)\sqrt{2}}(U_3+u_3') \right],$$

$$e_{7/8} = \sqrt{\frac{1+k^2}{2}}\left[(U_1+u_1') \mp \frac{1-k^2}{(1+k^2)\sqrt{2}}(U_2+u_2') \pm \frac{1-k^2}{(1+k^2)\sqrt{2}}(U_3+u_3') \right].$$

From this we obtain:

$$\overline{u_1'^2} = \frac{2}{1+k^2}\cdot\frac{\overline{(e_2'+e_1')^2}}{4}, \tag{49.1}$$

$$\overline{u_2'^2} = \frac{2}{1+k^2}\cdot\left(\frac{1+k^2}{1-k^2}\right)^2\cdot\frac{\overline{(e_3'-e_1')^2}}{4}, \tag{49.2}$$

$$\overline{u_3'^2} = \frac{2}{1+k^2}\cdot\left(\frac{1+k^2}{1-k^2}\right)^2\cdot\frac{\overline{(e_4'-e_3')^2}}{4}, \tag{49.3}$$

$$\overline{u_1'u_2'} = \frac{2}{1+k^2}\left(\frac{1+k^2}{1-k^2}\right)\cdot\frac{\overline{(e_2'^2-e_1'^2)}}{4}, \tag{49.4}$$

$$\overline{u_2'u_3'} = \frac{2}{1+k^2}\left(\frac{1+k^2}{1-k^2}\right)^2\cdot\left[\frac{\overline{(e_6'-e_5')^2}}{8} - \frac{\overline{(e_8'-e_7')^2}}{8}\right], \tag{49.5}$$

$$\overline{u_3'u_1'} = \frac{2}{1+k^2}\left(\frac{1+k^2}{1-k^2}\right)\frac{\overline{(e_4'^2-e_3'^2)}}{4}, \tag{49.6}$$

$$U_1 = \sqrt{\frac{2}{1+k^2}}\cdot\frac{\bar{e}_2+\bar{e}_1}{2}, \tag{49.7}$$

$$U_2 = \sqrt{\frac{2}{1+k^2}}\cdot\frac{1+k^2}{1-k^2}\cdot\frac{\bar{e}_2-\bar{e}_1}{2}, \tag{49.8}$$

$$U_3 = \sqrt{\frac{2}{1+k^2}}\cdot\frac{1+k^2}{1-k^2}\cdot\frac{\bar{e}_4-\bar{e}_3}{2}. \tag{49.9}$$

The equations (49.1) to (49.6) are identical with (33.1) to (33.6); so in the signal evaluation of the fluctuations, nothing is changed. The components of the middle flow are given by (49.7) to (49.9), where necessarily the following expression must apply:

$$|\bar{e}_2-\bar{e}_1|/|\bar{e}_2+\bar{e}_1|,\ |\bar{e}_4-\bar{e}_3|/|\bar{e}_4+\bar{e}_3| \ll 1$$

Proceeding from equations (6.1) to (6.4) and the linearized equations above, by neglecting the fluctuations, the error in the velocity components U_1, U_2, U_3 can be accurately determined due to the linearization. We have: /71

$$\left(\frac{U_{2/3}}{U_1}\right)_{lin.} = \frac{1}{x^2}\left(\frac{U_{2/3}}{U_1}\right)_{exact},$$

$$U_{1,lin.} = x\cdot U_{1,exact},$$

with

$$x^2 = \frac{1}{2}\left\{\left[1+\frac{3}{2}\zeta^2\right] + \sqrt{\left[1+\frac{3}{2}\zeta^2\right]^2 + 25\zeta^2}\right\},$$

$$\zeta^2 = \left(\frac{U_2}{U_1}\right)^2_{exact} + \left(\frac{U_3}{U_1}\right)^2_{exact} \quad \text{for } k=0.$$

For the example $U_3/U_1 = 0$, $U_2/U_1 = 0.1, 0.2, 0.3$ we obtain the following number values:

U_2/U_1	angle deviation	$\frac{1}{x^2}$	x
0.1	5.7°	0.980	1.001
0.2	11.3°	0.927	1.039
0.3	16.7°	0.852	1.083

The large component U_1 is thus determined as too large in the linear approximation, the small components U_2,U_3 are too small and have about twice the deviation as the component U_1. For turbulent flows, these errors can be even greater.

Practically speaking, it is also of interest to know how much the turbulence quantities $\overline{u_l' u_m'}$ in this coordinate system differ from the corresponding correlations $\overline{v_l' v_m'}$ in the arbitrary flow-line related coordinate system ($V_2=V_3=0$). The question is usually how far can a transformation of measured quantities be omitted; up to what deviation of coordinate systems is this possible, or at what ratios U_2/U_1, U_3/U_1. This question will be answered in the following section.

8. Transformation of Fluctuation Quantities

/72

Two ortho-normal, right-hand-oriented base vector systems (coordinate systems) $\hat{\underline{x}}_l$ and $\hat{\underline{y}}_l$ ($l=1,2,3$) can be converted one into the other by rotation:

$$\hat{\underline{x}}_l = \sum_{m=1}^{3} A_{ml}\, \hat{\underline{y}}_m \quad , \tag{50.1}$$

$$\det(A_{ml}) = +1 \quad , \tag{50.2}$$

$$\sum_{m=1}^{3} A_{ml} A_{mn} = \delta_{ln} \quad . \tag{50.3}$$

The matrix elements A_{kl} of matrix A are the scalar products of the corresponding base vectors, or the cosine of the enclosed angle:

$$\cos(\hat{x}_l, \hat{y}_k) = \hat{x}_l \cdot \hat{y}_k = \sum_m A_{ml}\, \hat{y}_m \cdot \hat{y}_k = \sum_m A_{ml}\, \delta_{mk} = A_{kl} \quad .$$

A velocity vector $\underline{u}$ will have the components u_l or v_l with respect to these bases:

$$\underline{u} = \sum_{l=1}^{3} u_l\, \hat{x}_l = \sum_{l=1}^{3} v_l\, \hat{y}_l \quad .$$

We then have:

$$v_l = \underline{u} \cdot \hat{y}_l = \sum_{m=1}^{3} u_m\, \hat{x}_m \cdot \hat{y}_l = \sum_{m=1}^{3} A_{lm}\, u_m$$

or

$$\begin{pmatrix} v_1 \\ v_2 \\ v_3 \end{pmatrix} = \begin{pmatrix} A_{11} & A_{12} & A_{13} \\ A_{21} & A_{22} & A_{23} \\ A_{31} & A_{32} & A_{33} \end{pmatrix} \cdot \begin{pmatrix} u_1 \\ u_2 \\ u_3 \end{pmatrix}$$

or briefly:

$$\underline{v} = \underline{\underline{A}} \cdot \underline{u} \quad . \tag{51}$$

Since $\underline{\underline{A}}$ is a linear, time-independent operator, the same relation applies both for the average velocity components U_1, V_1 as for the fluctuations u_1', v_1':

$$\underline{U} = \underline{\underline{A}} \cdot \underline{V} \tag{51.1}$$

$$\underline{u}' = \underline{\underline{A}} \cdot \underline{v}' \tag{51.2}$$

Consequently, we have:

$$\overline{V_K V_1} = \sum_{m=1}^{3} \sum_{n=1}^{3} A_{km} A_{1n} \overline{u_m u_n} , \tag{52.1}$$

$$V_K V_1 = \sum_{m=1}^{3} \sum_{n=1}^{3} A_{km} A_{1n} U_m U_n , \tag{52.2}$$

$$\overline{v_k' v_1'} = \sum_{m=1}^{3} \sum_{n=1}^{3} A_{km} A_{1n} \overline{u_m' u_n'} . \tag{52.3}$$

Three examples: /73

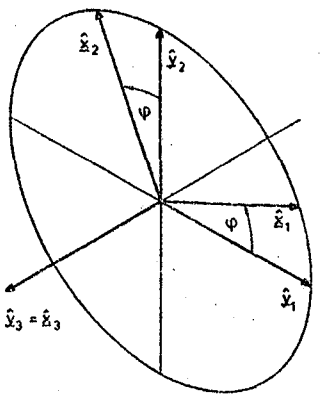

$$\begin{pmatrix} \hat{x}_1 \\ \hat{x}_2 \\ \hat{x}_3 \end{pmatrix} = \begin{pmatrix} \cos\varphi & \sin\varphi & 0 \\ -\sin\varphi & \cos\varphi & 0 \\ 0 & 0 & 1 \end{pmatrix} \cdot \begin{pmatrix} \hat{y}_1 \\ \hat{y}_2 \\ \hat{y}_3 \end{pmatrix} ,$$

thus

$$\underline{\underline{A}} = \begin{pmatrix} \cos\varphi & -\sin\varphi & 0 \\ \sin\varphi & \cos\varphi & 0 \\ 0 & 0 & 1 \end{pmatrix}$$

$$\begin{pmatrix} \overline{v_1^2} \\ \overline{v_2^2} \\ \overline{v_3^2} \\ \overline{v_1 v_2} \\ \overline{v_2 v_3} \\ \overline{v_3 v_1} \end{pmatrix} = \underbrace{\begin{pmatrix} \cos^2\varphi & \sin^2\varphi & 0 & -\sin 2\varphi & 0 & 0 \\ \sin^2\varphi & \cos^2\varphi & 0 & \sin 2\varphi & 0 & 0 \\ 0 & 0 & 1 & 0 & 0 & 0 \\ \frac{1}{2}\sin 2\varphi & -\frac{1}{2}\sin 2\varphi & 0 & \cos 2\varphi & 0 & 0 \\ 0 & 0 & 0 & 0 & \cos\varphi & \sin\varphi \\ 0 & 0 & 0 & 0 & -\sin\varphi & \cos\varphi \end{pmatrix}}_{= : \underline{\underline{B}} \quad , \quad \det(\underline{\underline{B}}) = 1} \cdot \begin{pmatrix} \overline{u_1^2} \\ \overline{u_2^2} \\ \overline{u_3^2} \\ \overline{u_1 u_2} \\ \overline{u_2 u_3} \\ \overline{u_3 u_1} \end{pmatrix} \tag{53}$$

By means of eq. (53) we now also find how much the turbulence quantities $\overline{v_l' v_m'}$ differ from the $\overline{u_l' u_m'}$ for small angles φ, or when the transformation can still be omitted.

Equation (53) is of interest only in a non-isotropic case. Let us consider the 2D boundary layer, and take only the shear stresses:

$$\overline{v_1' v_2'} = \cos 2\varphi \cdot \overline{u_1' u_2'} + \frac{1}{2} \cdot \sin 2\varphi \cdot (\overline{u_1'^2} - \overline{u_2'^2}),$$

$$\frac{\overline{v_1' v_2'}}{\overline{u_1' u_2'}} = \cos 2\varphi + \frac{1}{2} \sin 2\varphi \cdot \left(\sqrt{\frac{\overline{u_1'^2}}{\overline{u_2'^2}}} - \sqrt{\frac{\overline{u_2'^2}}{\overline{u_1'^2}}} \right) \cdot \frac{\sqrt{\overline{u_1'^2}}\sqrt{\overline{u_2'^2}}}{\overline{u_1' u_2'}}$$

/74

With the values gained from experience:

$$\sqrt{\overline{u_2'^2} / \overline{u_1'^2}} \approx 0.7 ,$$

$$\frac{\overline{u_1' u_2'}}{\sqrt{\overline{u_1'^2}}\sqrt{\overline{u_2'^2}}} \approx 0.5$$

there follows:

$$\frac{\overline{v_1' v_2'}}{\overline{u_1' u_2'}} - 1 = \cos 2\varphi + \frac{1}{2} \sin 2\varphi \cdot 1.4 - 1$$

Examples:

$\frac{U_2}{U_1}$	φ	$\frac{\overline{v_1' v_2'}}{u_1' u_2'} - 1$
0.01	0.57°	-0.014
0.03	1.72°	-0.044
0.05	2.86°	-0.075
0.1	5.7°	-0.158
0.2	11.3°	-0.346
0.3	16.7°	-0.550

Apparently, we will only be able to omit the transformation for very small angles φ, since a difference of 4.4% shows up even for an angle of 1.7°, and it increases more than linearly for larger angles. And it must not be forgotten that due to the linearization, the angle φ is underestimated (see sec. 7).

/75

-For the orthogonal probe from fig. 3, we have:

$$\begin{pmatrix} \hat{x}_1' \\ \hat{x}_2' \\ \hat{x}_3' \end{pmatrix} = \begin{pmatrix} 1/\sqrt{3} & 0 & 2/\sqrt{6} \\ 1/\sqrt{3} & -1/\sqrt{2} & -1/\sqrt{6} \\ 1/\sqrt{3} & 1/\sqrt{2} & -1/\sqrt{6} \end{pmatrix} \cdot \begin{pmatrix} \hat{y}_1 \\ \hat{y}_2 \\ \hat{y}_3 \end{pmatrix} ,$$

Thus:

$$\underline{\underline{A}} = \begin{pmatrix} 1/\sqrt{3} & 1/\sqrt{3} & 1/\sqrt{3} \\ 0 & -1/\sqrt{2} & 1/\sqrt{2} \\ 2/\sqrt{6} & -1/\sqrt{6} & -1/\sqrt{6} \end{pmatrix} ,$$

where $\hat{\underline{x}}_1$ (1=1,2,3) is the orthogonal coordinate system given by the hot-wire directions, whereas $\hat{\underline{y}}_1$ is the coordinate system defined by the probe axis and two directions orthogonal to it (as indicated in fig. 3). Thus we have:

$$\begin{pmatrix} \overline{v_1^2} \\ \overline{v_2^2} \\ \overline{v_3^2} \\ \overline{v_1 v_2} \\ \overline{v_2 v_3} \\ \overline{v_3 v_1} \end{pmatrix} = \begin{pmatrix} \frac{1}{3} & 0 & 0 & 0 & 0 & 0 \\ 0 & \frac{1}{2} & 0 & 0 & 0 & 0 \\ 0 & 0 & \frac{1}{6} & 0 & 0 & 0 \\ 0 & 0 & 0 & \frac{1}{\sqrt{6}} & 0 & 0 \\ 0 & 0 & 0 & 0 & \frac{1}{\sqrt{12}} & 0 \\ 0 & 0 & 0 & 0 & 0 & \frac{1}{\sqrt{18}} \end{pmatrix} \cdot \begin{pmatrix} 1 & 1 & 1 & 2 & 2 & 2 \\ 0 & 1 & 1 & 0 & -2 & 0 \\ 4 & 1 & 1 & -4 & 2 & -4 \\ 0 & -1 & 1 & -1 & 0 & 1 \\ 0 & 1 & -1 & -2 & 0 & 2 \\ 2 & -1 & -1 & 1 & -2 & 1 \end{pmatrix} \cdot \begin{pmatrix} \overline{u_1^2} \\ \overline{u_2^2} \\ \overline{u_3^2} \\ \overline{u_1 u_2} \\ \overline{u_2 u_3} \\ \overline{u_3 u_1} \end{pmatrix} . \qquad (54.1)$$

-For the probe design as per fig. 4, we have

$$\begin{pmatrix} \hat{x}_1 \\ \hat{x}_2 \\ \hat{x}_3 \end{pmatrix} = \begin{pmatrix} 1/\sqrt{3} & -2/\sqrt{6} & 0 \\ 1/\sqrt{3} & 1/\sqrt{6} & -1/\sqrt{2} \\ 1/\sqrt{3} & 1/\sqrt{6} & 1/\sqrt{2} \end{pmatrix} \cdot \begin{pmatrix} \hat{y}_1 \\ \hat{y}_2 \\ \hat{y}_3 \end{pmatrix} ,$$

$$\underline{\underline{A}} = \begin{pmatrix} 1/\sqrt{3} & 1/\sqrt{3} & 1/\sqrt{3} \\ -2/\sqrt{6} & 1/\sqrt{6} & 1/\sqrt{6} \\ 0 & -1/\sqrt{2} & 1/\sqrt{2} \end{pmatrix}$$

and

/76

$$\begin{pmatrix} v_1^2 \\ v_2^2 \\ v_3^2 \\ v_1 v_2 \\ v_2 v_3 \\ v_3 v_1 \end{pmatrix} = \begin{pmatrix} \frac{1}{3} & 0 & 0 & 0 & 0 & 0 \\ 0 & \frac{1}{6} & 0 & 0 & 0 & 0 \\ 0 & 0 & \frac{1}{2} & 0 & 0 & 0 \\ 0 & 0 & 0 & \frac{1}{\sqrt{18}} & 0 & 0 \\ 0 & 0 & 0 & 0 & \frac{1}{\sqrt{12}} & 0 \\ 0 & 0 & 0 & 0 & 0 & \frac{1}{\sqrt{6}} \end{pmatrix} \cdot \begin{pmatrix} 1 & 1 & 1 & 2 & 2 & 2 \\ 4 & 1 & 1 & -4 & 2 & -4 \\ 0 & 1 & 1 & 0 & -2 & 0 \\ -2 & 1 & 1 & -1 & 2 & -1 \\ 0 & -1 & 1 & 2 & 0 & -2 \\ 0 & -1 & 1 & -1 & 0 & 1 \end{pmatrix} \cdot \begin{pmatrix} \overline{u_1^2} \\ \overline{u_2^2} \\ \overline{u_3^2} \\ \overline{u_1 u_2} \\ \overline{u_2 u_3} \\ \overline{u_3 u_1} \end{pmatrix} . \qquad (54.2)$$

Theoretically, the transformation of the fluctuation quantities is quite simple, but practically the following problems come up:

-Even if only one fluctuation $\overline{v_l v_m}$ is to be computed, in general the entire set $\overline{u_l u_m}$ must be known.

-Due to the linear transformation, the error in $\overline{v_l v_m}$ increases, since the measuring errors of the individual, included $\overline{u_l u_m}$ are additive.

/77

9. Correlations of Frequency Components

The frequency spectrum of the speed fluctuations of a turbulent flow is broad; in addition, it can contain discrete frequency components, e.g. for periodic, external disturbances or in rotating flow machines. Thus we will be interested not only in the correlations $\overline{u_l' u_m'}$ of the fluctuations themselves, but also in the correlations $\overline{u_{l\omega}' u_{m\omega}'}$ of individual frequency components. As long as linear relations prevail between the speed fluctuations and certain hot-wire signals--e.g. in the exact analysis (sec. 3) or in the 1st approxi-

mation (sec. 4.2)--the equations derived there apply equally for individual frequency components since eq. (14) or (38) can be Fourier-transformed entirely. But note that for the 3-wire probe, the signals e_j are not to be filtered, but the signals $\tilde{e}_j$!

For the second approximation it was found that the equations (33.1) to (33.6) result for the fluctuation quantities $\overline{u_l' u_m'}$ and from the linear expansion (38), but not equations (33.7) to (33.10), which contain the average speed U_1. Consequently, the equations (37.1) to (37.6) of the second approximation also apply for frequency components if the unfiltered fluctuation quantities are used for the average values and for the correction factors.

/78

10. The One-Wire Probe

A simple, single hot-wire is used for speed measurements more frequently than an X-wire, e.g. when we only want the average speed U and the turbulence intensity $\overline{u_1'^2}/U^2$ or when we only want a qualitative picture of the flow. But what can be said about the accuracy of these measurements?

The main direction of flow is found by the criterion (30), but not in a manner so that the probe rotates continually and the signal must be symmetric to the angle $\alpha=\frac{\pi}{2}$. Next, the main direction of flow is chosen as x_1-axis ($U=U_1$) and the probe is used in the position $\alpha=\frac{\pi}{2}$:

$$e^2 = (U+u_1')^2 + [1+(k^2-1)\cos^2\theta]\cdot u_2'^2 + \\ + [1+(k^2-1)\sin^2\theta]\, u_3'^2 + (k^2-1)\cos\theta\sin\theta\; u_2' u_3' \quad . \tag{55}$$

Although in this case we have only four variables for which to solve-- $(U+u_1')^2$, $u_2'^2$, $u_3'^2$, $u_2'u_3'$ --this solution is not possible no matter how many values θ we use. We obtian only one exact equation:

$$\overline{e^2(\theta)} - \overline{e^2(-\theta)} = 2(k^2-1)\cos\theta\sin\theta\;\overline{u_2' u_3'} \quad \text{(for any } \theta) \tag{56}$$

This quantity is of interest in measurements with one-wire probes in rare cases only. To compute the other quantities U, $\overline{u_1'^2}$, approximations are needed agian. A consistent series expansion out to the second order (as in sec. 4.1) gives:

$$\overline{u_1'^2} = \overline{e_1'^2} = \overline{e_2'^2} \quad , \tag{57.1}$$

$$U^2 + k^2\overline{u_2'^2} + \overline{u_3'^2} = \overline{e_1}^2 \quad , \tag{57.2}$$

$$U^2 + \overline{u_2'^2} + k^2\overline{u_3'^2} = \overline{e_2}^2 \quad ; \tag{57.3}$$

with

$$e_1 = e(\theta=0) = \overline{e}_1 + e_1' \quad ,$$
$$e_2 = e(\theta=\tfrac{\pi}{2}) = \overline{e}_2 + e_2' \quad .$$

The equations are not sufficient for computing U, $\overline{u_2'^2}$ and $\overline{u_3'^2}$. From (57.2) and (57.3) we know only:

$$\overline{u_2'^2} - \overline{u_3'^2} = \frac{1}{1-k^2}(\bar{e}_2^2 - \bar{e}_1^2).$$

In order to determine the average velocity U, we set: /79

$$\overline{u_{2/3}'^2} = C_{2/3} \cdot \overline{u_1'^2} \tag{59}$$

with values gained from experience $C_{2/3}$ of 0.5 (boundary layer) to 1.0 (isotropic turbulence). Then we have:

$$U^2 = \bar{e}_2^2 \cdot [\,1 - (C_2 + k^2 C_3)\,\overline{e_2'^2}/\bar{e}_2^2\,] = \tag{60}$$
$$= \bar{e}_1^2 \cdot [\,1 - (C_3 + k^2 C_2)\,\overline{e_1'^2}/\bar{e}_1^2\,]$$

and

$$\frac{\overline{u_1'^2}}{U^2} = \frac{\overline{e_2'^2}}{\bar{e}_2^2} \cdot \frac{1}{1-(C_2+k^2C_3)\,\overline{e_2'^2}/\bar{e}_2^2} = \tag{61}$$
$$= \frac{\overline{e_1'^2}}{\bar{e}_1^2} \cdot \frac{1}{1-(C_3+k^2C_2)\,\overline{e_1'^2}/\bar{e}_1^2}\,.$$

A linear approximation gives:

$$U^2 = \bar{e}_1^2 = \bar{e}_2^2 \tag{62}$$

and

$$\frac{\overline{u_1'^2}}{U^2} = \frac{\overline{e_1'^2}}{\bar{e}_1^2} = \frac{\overline{e_2'^2}}{\bar{e}_2^2}\,. \tag{63}$$

According to the results of section 6 for the X-wire probe, it should be expected that even for the one-wire probe, the second approximation will not give much more accurate values than the first approx. and that the deviations of these approx. values from the actual ones will lie on the same order of magnitude.

11. Slowly Rotating Hot-Wire Probe /80

Instead of a one-wire probe set into different positions in sequence, it can also be rotated about its axis so that the hot wire is always at the same place. The rotation should be slow enough that during the time averaging of the signal, the orientation of the wire can be viewed as constant.

From eq. (4) it follows:

$$\begin{aligned}\overline{e^2} &= \sum_{l,m} a_{lm}(\alpha,\theta)\,\overline{u_l u_m} = \\ &= \{[1+(k^2-1)\cos^2\alpha]\,\overline{u_1^2} + [1+\tfrac{1}{2}(k^2-1)\sin^2\alpha]\cdot[\overline{u_2^2}+\overline{u_3^2}]\} + \\ &+ \{[2(k^2-1)\cos\alpha\cdot\sin\alpha]\,\overline{u_1u_2}\}\cdot\cos\theta + \\ &+ \{[2(k^2-1)\cos\alpha\cdot\sin\alpha]\,\overline{u_1u_3}\}\cdot\sin\theta + \\ &+ \{[\tfrac{1}{2}(k^2-1)\sin^2\alpha]\cdot[\overline{u_2^2}-\overline{u_3^2}]\}\cdot\cos 2\theta + \\ &+ \{[(k^2-1)\sin^2\alpha]\,\overline{u_2u_3}\}\cdot\sin 2\theta\,;\end{aligned} \tag{64}$$

specifically for:

$\alpha = \pi/2$ (normal hot-wire probe)

$$\overline{e^2} = \overline{u_1^2} + \frac{1+k^2}{2}\overline{u_2^2} + \frac{1+k^2}{2}\overline{u_3^2} + \frac{k^2-1}{2}(\overline{u_2^2} - \overline{u_3^2})\cos 2\theta + (k^2-1)\overline{u_2 u_3}\cdot \sin 2\theta;$$

$\alpha = \pi/4$ (slant-wire probe)

$$\overline{e^2} = \frac{1+k^2}{2}\overline{u_1^2} + \frac{3+k^2}{4}\overline{u_2^2} + \frac{3+k^2}{4}\overline{u_3^2} +$$

$$+ (k^2-1)\overline{u_1 u_2}\cdot\cos\theta + (k^2-1)\overline{u_1 u_3}\cdot\sin\theta +$$

$$+ \frac{k^2-1}{4}(\overline{u_2^2} - \overline{u_3^2})\cdot\cos 2\theta + \frac{k^2-1}{2}\overline{u_2 u_3}\cdot\sin 2\theta.$$

Through an analysis of the functional dependence $\overline{e^2}(\theta)$, at most the correlations $\overline{u_1u_2}$, $\overline{u_1u_3}$, $\overline{u_2u_3}$ can be determined, and the difference $\overline{u_2^2} - \overline{u_3^2}$ and a linear combination of $\overline{u_1^2}$, but not the individual terms $\overline{u_1^2}$, $\overline{u_2^2}$, $\overline{u_3^2}$ separately. This result thus corresponds exactly to the result of section 3, equations (6.1) to (6.4). /81

Let us consider the case of low turbulence intensity and presume that the main direction of flow is known, thus:

$$U_2 = U_3 = 0 \quad \text{and} \quad |u_2'| \ll U_1$$

Now we can distinguish two essentially different cases, namely that the rotation axis (= probe axis) is aligned parallel or perpendicular to the main flow.

If the rotation axis is parallel to the main flow direction, then from equations (31) or (40), we have the following expression both for the second and first approximation:

$$a_{11}\overline{e'^2} = a_{11}(\overline{e^2} - \bar{e}^2) =$$

$$= a_{11}^2\overline{u_1'^2} + a_{12}^2\overline{u_2'^2} + a_{13}^2\overline{u_3'^2} +$$

$$+ 2a_{11}a_{12}\overline{u_1'u_2'} + 2a_{11}a_{13}\overline{u_1'u_3'} +$$

$$+ 2a_{12}a_{13}\overline{u_2'u_3'} = \qquad (65)$$

$$= [1 + (k^2-1)\cos^2\alpha]^2\overline{u_1'^2} + [(k^2-1)\cos\alpha\sin\alpha]^2\overline{u_2'^2}\cdot\cos^2\theta +$$

$$+ [(k^2-1)\cos\alpha\cdot\sin\alpha]^2\overline{u_3'^2}\cdot\sin^2\theta +$$

$$+ 2[1+(k^2-1)\cos^2\alpha][(k^2-1)\cos\alpha\sin\alpha]\cdot\overline{u_1'u_2'}\cdot\cos\theta +$$

$$+ 2[1+(k^2-1)\cos^2\alpha]\cdot[(k^2-1)\cos\alpha\sin\alpha]\overline{u_1'u_3'}\cdot\sin\theta +$$

$$+ 2[(k^2-1)\cos\alpha\sin\alpha]^2\overline{u_2'u_3'}\cdot\cos\theta\cdot\sin\theta =$$

/82

$$= w_1 + w_2 \cdot \cos^2\theta + w_3 \cdot \sin^2\theta +$$
$$+ w_4 \cdot \cos\theta + w_5 \sin\theta + w_6 \cos\theta \cdot \sin\theta =$$
$$= \left(w_1 + \tfrac{1}{2} w_2 + \tfrac{1}{2} w_3\right) + w_4 \cos\theta + w_5 \cdot \sin\theta +$$
$$+ \tfrac{1}{2} w_6 \cdot \sin 2\theta + \tfrac{1}{2} (w_2 - w_3) \cos 2\theta ;$$

with the abbreviations:

$$w_1 = \left[1 + (k^2-1)\cos^2\alpha\right]^2 \cdot \overline{u_1'^2} , \qquad (66.1)$$

$$w_2 = \left[(k^2-1)\cos\alpha \sin\alpha\right]^2 \cdot \overline{u_2'^2} , \qquad (66.2)$$

$$w_3 = \left[(k^2-1)\cos\alpha \sin\alpha\right]^2 \cdot \overline{u_3'^2} , \qquad (66.3)$$

$$w_4 = 2\left[1 + (k^2-1)\cos^2\alpha\right]\cdot\left[(k^2-1)\cos\alpha \sin\alpha\right] \overline{u_1' u_2'} , \qquad (66.4)$$

$$w_5 = 2\left[1 + (k^2-1)\cos^2\alpha\right]\cdot\left[(k^2-1)\cos\alpha \sin\alpha\right] \cdot \overline{u_1' u_3'} , \qquad (66.5)$$

$$w_6 = 2\left[(k^2-1)\cos\alpha \cdot \sin\alpha\right]^2 \overline{u_2' u_3'} . \qquad (66.6)$$

$a_{11}\,\overline{e'^2}$ is thus a periodic function of θ with a finite Fourier expansion:

$$a_{11}\,\overline{e'^2}(\theta) = \alpha_0 + \sum_{\nu=1}^{2} (\alpha_\nu \cos\nu\theta + \beta_\nu \cdot \sin\nu\theta) .$$

A very careful determination of the Fourier coefficients α_ν, β_ν gives the values:

$$w_1 + \tfrac{1}{2}(w_2+w_3) = \alpha_0$$
$$w_2 - w_3 = 2\,\alpha_2$$
$$w_4 = \alpha_1$$
$$w_5 = \beta_1$$
$$w_6 = 2\,\beta_2$$

A normal one-wire probe ($\alpha=\pi/2$) would only permit determination of $\overline{u_1'^2}$; a slant-wire probe will give in principle

/83

-the correlations $\overline{u_1' u_2'}$, $\overline{u_1' u_3'}$, $\overline{u_2' u_3'}$,

-the difference $\overline{u_2'^2} - \overline{u_3'^2}$,

-the linear combination $\left[1 + (k^2-1)\cos^2\alpha\right]^2 \overline{u_1'^2} + \tfrac{1}{2}\left[(k^2-1)\cos\alpha \sin\alpha\right]^2 \cdot \left(\overline{u_2'^2} + \overline{u_3'^2}\right)$

but not the individual turbulence quantities $\overline{u_1'^2}$, $\overline{u_2'^2}$, $\overline{u_3'^2}$. Thus the result resembles the general case, equation (64), quite closely.

Things look better if in the case of low turbulence intensity the rotation axis stands perpendicular, or nearly so, to the main flow direction. In order to retain θ as rotation angle (for α =const), the polar angles ϑ, α are now selected with respect to the x_2-axis (= rotation axis) and $|u_1'|$, $|u_2+u_2'|$, $|u_3+u_3'| \ll u_1$ are presumed. In linear approximation, we obtain:

$$e = \sqrt{a_{22}}\, u_1 \cdot \left[1 + \frac{u_1'}{u_1} + \frac{a_{22}}{a_{22}} \cdot \frac{u_2+u_2'}{u_1} + \frac{a_{21}}{a_{22}} \frac{u_3+u_3'}{u_1}\right] , \qquad (67)$$

ORIGINAL PAGE IS
OF POOR QUALITY

and a_{22} may not be small. If we choose for instance, $\alpha=\pi/4$, then $a_{22} \geq 1/2$ for all θ.

For the average signal, after brief intermediate steps, we have:

$$\sqrt{a_{22}}\,\bar{e} = \left[1+\frac{k^2-1}{2}\sin^2\alpha\right]\cdot U_1 + \left[(k^2-1)\cos\sin\alpha\right] U_3 \cos\theta + \left[\frac{k^2-1}{2}\sin^2\alpha\right]\cdot U_1 \cos 2\theta + \left[\frac{k^2-1}{2}\sin^2\alpha\right] U_2 \sin 2\theta \,. \tag{68}$$

From this, U_1, U_2, U_3 can be determined and the prerequisite $|U_2|, |U_3| \ll U_1$ must be confirmed.

For the fluctuation quantities, from (67) we have:

$$a_{22}\,\overline{e'^2} = a_{22}^2\,\overline{u_1'^2} + a_{23}^2\,\overline{u_2'^2} + a_{12}^2\,\overline{u_3'^2} + 2\,a_{22}\,a_{23}\,\overline{u_1' u_2'} + 2\,a_{22}\,a_{12}\,\overline{u_1' u_3'} + 2\,a_{23}\,a_{13}\,\overline{u_2' u_3'} \,. \tag{69}$$

After lengthy calculation it turns out that $a_{22}\,\overline{e'^2}$ as a function of θ now has a Fourier expansion: /84

$$a_{22}\,\overline{e'^2} = \alpha_0 + \sum_{\nu=1}^{4} (\alpha_\nu \cos\nu\theta + \beta_\nu \cdot \sin\nu\theta)$$

with the coefficients:

$$\alpha_0 = \left[1+(k^2-1)\sin^2\alpha + \tfrac{3}{8}(k^2-1)^2\sin^4\alpha\right]\overline{u_1'^2} + \left[\tfrac{1}{8}(k^2-1)^2\sin^4\alpha\right]\overline{u_2'^2} + \left[\tfrac{1}{8}(k^2-1)^2\sin^2 2\alpha\right]\overline{u_3'^2} \,, \tag{70.1}$$

$$\alpha_1 = \left[\sin 2\alpha\left((k^2-1)+\tfrac{3}{4}(k^2-1)^2\sin^2\alpha\right)\right]\overline{u_1' u_3'} \,, \tag{70.2}$$

$$\beta_1 = \left[\tfrac{1}{2}(k^2-1)^2\sin^3\alpha\cos\alpha\right]\cdot\overline{u_2' u_3'} \,, \tag{70.3}$$

$$\alpha_2 = \left[(k^2-1)\sin^2\alpha\left(1+\frac{k^2-1}{2}\sin^2\alpha\right)\right]\overline{u_1'^2} + \left[\tfrac{1}{8}(k^2-1)^2\sin^2 2\alpha\right]\overline{u_3'^2} \,, \tag{70.4}$$

$$\beta_2 = \left[(k^2-1)\sin^2\alpha\left(1+\frac{k^2-1}{2}\sin^2\alpha\right)\right]\overline{u_1' u_2'} \,, \tag{70.5}$$

$$\alpha_3 = \left[\tfrac{1}{4}(k^2-1)^2\sin^2\alpha\cdot\sin 2\alpha\right]\cdot\overline{u_1' u_3'} \,, \tag{70.6}$$

$$\beta_3 = \left[\tfrac{1}{4}(k^2-1)^2\sin^2\alpha\cdot\sin 2\alpha\right]\cdot\overline{u_2' u_3'} \,, \tag{70.7}$$

$$\alpha_4 = \left[\tfrac{1}{8}(k^2-1)^2\sin^4\alpha\right]\cdot\left(\overline{u_1'^2} - \overline{u_2'^2}\right) \,, \tag{70.8}$$

$$\beta_4 = \left[\tfrac{1}{4}(k^2-1)^2\sin^4\alpha\right]\overline{u_1' u_2'} \,. \tag{70.9}$$

The quantities $\overline{u_1' u_2'}$, $\overline{u_1' u_3'}$ and $\overline{u_2' u_3'}$ result from eq. (70.5) or (70.9), (70.2) or (70.6), (70.3) or (70.7) directly, when $0 < \alpha < \pi/2$. . The equations (70.1, 70.4 and 70.8) give a linear system of equations. in which $\overline{u_1'^2}$, $\overline{u_2'^2}$, $\overline{u_3'^2}$ are always solvable for $k \ll 1$ and $0 < \alpha < \pi/2$.

De Grande and Kool [37] came to the same result for the case of a non-linearized, slanting one-wire probe and small fluctuations.

When $\alpha = \pi/2$, or for a normal probe, from equations (70.1) to (70.9) only the quantities $\overline{u_1' u_2'}$ (from (70.5) or (70.9)) and $\overline{u_1'^2}$, $\overline{u_2'^2}$ can be determined. This result too, was found earlier for a non-linear probe and small fluctuations, by Fujita and Kovasznay [38]. /85

In addition, it became clear here that even for slowly rotating probes, a precise signal analysis is not possible, rather a series expansion by the small fluctuation quantities is unavoidable. Thus large errors result with this method too, for large turbulence intensity.

12. Summary

/86

The measurement of flow speeds and in turbulent flows, of the speed fluctuations by means of hot-wire probes and anemometers, is a widely used and indespensible technology, although today various contactless (probe-free) laser measuring methods are available. In the determination of speed fluctuations and correlations of various speed components, the hot-wire measuring techniques with multi-wire probes are by no means inferior to the laser methods, but they are less complicated.

Through decades of development, the hot-wire anemometry has been constantly improved and its useage expanded. But like all measuring techniques, it has its limitations which have to be known for a realistic error estimation in measured values. Besides possible errors due to the electronic control of the anemometer and due to interactions between the probe and the flow, the usual methods of signal analysis for one- and two-wire probes contain a systematic error, since the functional relation between the hot wire signals and the components of the velocity are approximated by a series expansion by the velocity fluctuations. Naturally it must be assumed that the components of the velocity fluctuations are small compared to the average velocity. This error is as a rule even greater, the higher the level of turbulence. Above a certain turbulence level, the use of conventional hot-wire anemometers is no longer meaningful--regardless of other possible errors which can also increase with the turbulence intensity.

A precise consideration of linearized hot-wire signals leads to the conclusion that hot-wire probes with at least three independent hot wires will permit an accurate signal analysis in the sense that the time history profile of the speed can be determined by direction and magnitude from the time history of the hot-wire signals. From three orthogonal components $u_l(t)$, $l=1,2,3$, for example, both the components of average speed and random averages of the fluctuations can be determined, including the turbulence intensities $\overline{u_l'^2}$, $l = 1, 2, 3$, and the correlations $\overline{u_l' u_m'}$, $l \neq m$. The direction vectors determining the hot-wire orientations need not span the 3-dimensional space, but can simply point to 3 different directions in a plane.

/87

For the obvious case of three perpendicular hot-wires, the analytic relation between the signals and the corresponding orthogonal speed components--a quadratic form in the speed components--is very simple, but due to the high level of symmetry of such an arrangement, information is lost. Since the quadratic form is diagonal in this case, we obtain only the square of the speed components $u_l^2(t)$, $l=1,2,3$ and in case the sign of the speed component changes over time, the particular, correct sign must be found by other means, e.g. by other hot-wires. If occurring sign changes are not taken into account, then too high averages and too small turbulence intensities are measured.

For the other extreme case of an asymmetric three-wire probe, the resolution of the quadratic shape into the speed components is unique (except for one sign), but it is not analytically possible, so that one then has to rely on numeric methods. For the case of a "smooth" 3-wire probe, i.e. when the direction vectors of the three wires lie in a plane, different examples can be found for which the resolution of the square shape is simple and the symmetry of the probe is less than for the orthogonal probe. Depending on the type of turbulent flow, it may be useful to set this plane perpendicular to the main flow direction or at a specified acute angle.

The directions of the hot-wires does not specify their positions, so that even different wire arrangements are possible. In sections 3.2.1 and 3.2.2 examples are presented. Experiments will have to show which probe design is suitable for which flow, since interactions between the wires and reactions of prongs and shaft on the wire flow cannot be described theoretically. /88

In two-dimensional flows in which a speed component can be neglected (not only its fluctuations), e.g. in the wake of axial-symmetric or 2-dimensional bodies, the two remaining speed components can be accurately determined from the signals of conventional X-wire probes. Again, to avoid ambiguity it is useful not to have the probe at max. symmetry. One can use either non-orthogonal X-wire probes or the flat, conventional orthogonal X-wire probes screwed slightly out of the speed plane. In this manner, speeds and their fluctuations can be measured in regions in which instantaneous reactions and extremely high local turbulence intensities occur.

As long as hot-wire anemometers with three-wire probes are not adequately tested and reliable, in the future turbulent flows will continue to be measured with standard orthogonal X-wire probes, even in high levels of turbulence. The different conventional analyses of such hot-wire signals are formally very similar. First, an orthogonal coordinate system is defined by means of the X-wire probe, such that $U_2=U_3=0$. (This "flow-line related" coordinate system will generally be different at each point of the flow field). Next, from the hot-wire signals, the average speed $U=U_1$ and the turbulence quantities $\overline{u_l' u_m'}$ are determined. In both steps, the functional relationships between the signals and the speed components are approximated by power-series expansions by the presumed-small components U_2/U_1, U_3/U_1 and the small fluctuation quantities u_1'/U_1. As time averages we get in the first case a criterion for the position of the "flow-line related" coordinate system and in the second case, with sufficiently numerous, sequentially set orientations of the probe, an equation system which can be solved for the desired average fluctuation quantities $\overline{u_l' u_m'}$ and the average speed U, if we neglect enough higher terms. The condition to specify the average flow direction is thus recognized as an approximation, and it can apparently lead to a wrong calibration of the system in higher turbulence. Depending on the order to which the series expansion is carried, one obtains various approximations in the determination of U and $\overline{u_l' u_m'}$, of which the first (linear) and the /89

second are best-known. In suitable systematic notation, the series expansion can easily be taken to the fourth order in order to derive special, higher approximations.

Instead of beginning from the average values $\overline{e_1^2}$, $\overline{e_1^2}$, $\overline{e_2^2}$, $\overline{e_2^2}$ and $\overline{e_1 e_2}$ of the X-wire, one can also use the quadratic signals $\overline{e_1^2}^2$, $\overline{e_1^4}$, $\overline{e_2^2}^2$, $\overline{e_2^4}$, $\overline{e_1^2 e_2^2}$ but neglect higher terms. This approximation and the conventional approximations of first and second order, as well as a special fourth approximation of Vagt, are subjected to a numeric test since an experimental check of the various end-formulas is not possible. No better measurement method is available for this. As a great simplification, in a computer program, stochastic speed fluctuations of a turbulent flow are replaced by periodic fluctuations describable by step functions which are then easy to integrate, whereby the turbulence intensity $\overline{u_1^2}/U^2$ varies and through suitable parameters, the quantities $\overline{u_2^2}/\overline{u_1^2}$, $\overline{u_3^2}/\overline{u_1^2}$ and $\overline{u_1 u_m}/(\sqrt{\overline{u_1^2}}\sqrt{\overline{u_m^2}})$, $1 \neq m$, can be assigned to different, fixed values. Even the convexity factor $\overline{u_1^4}/\overline{u_1^2}^2$ can assume different values.

The test leads to the following results: All studied analyses lead to a systematic error in all turbulence quantities $\overline{u_1 u_m}/U^2$ at high turbulence levels. This error is as a rule, greater in the analysis of quadratic signals than in the analysis of standard signals, so that the former can be discarded. The error is linked with the approximation character of the criterion for finding the direction of the average speed. The turbulence intensities $\overline{u_1^2}/U^2$ are as a rule, computed with a greater accuracy than the shear stress terms $\overline{u_1 u_m}/U^2$, $1 \neq m$, if these are different from zero. The different approximations are affected with errors of comparable size for large turbulence. In particular, it is not true that the higher approximation is generally the better one. For the limited range of turbulence intensity of 0-0.05 (turbulence degree 0-22%), the max. error in the determination of turbulence intensities $\overline{u_1^2}/U^2$ is about 30%, whereas the error in the shear stress terms can be up to 100%. The deviations from the exact values depend on the turbulence structure without any discernable trend. Thus, no method can be given for correcting this error. However, from the calculations the maximum error can be found for each turbulence intensity. /90

For minor deviations in the main direction of flow from the direction of the probe axis of an X-wire probe, the usual analysis of the hot-wire signals can be slightly modified and gives--with various-order approximations--the direction of the average flow and the turbulence quantities. For larger deviations, alignment of the probe is required so that when measuring a flow field, all measured quantities have to be transformed if they are to be related to a fixed coordinate system. These transformations can be given in a generalized form.

Besides the average values $\overline{u_1 u_m}$ of the speed fluctuations, we are naturally also interested in the corresponding averages of

individual frequency components, or the spectral intensity densities $\overline{u_{1\omega}^{\prime 2}}$ and the cross-spectra $\overline{u_{1\omega}^{\prime} u_{m\omega}^{\prime}}$, $1 \neq m$. As long as linear relations exist between the speed fluctuations and certain hot-wire signals, e.g. in the precise analysis via 3-wire probes or in the first approximation of conventional hot-wire anemometers with X-wire probes, the equations derived there apply equally for individual frequency components. Also, the equations of the second approximation remain valid for frequency components and the unfiltered signals are to be used only for the correction factors. /91

Instead of X-wire probes, one-wire probes rotating slowly about the probe axis can be used if the main flow direction is known approximately. For the signal analysis however, low turbulence intensity must again be presumed, since a series expansion by the fluctuation quantities is unavoidable. The max. information, namely all quantities $\overline{u_l' u_m'}$ $(l,m = 1,2,3)$ is provided by a probe with slant-set hot-wire whose axis lies exactly or approximately perpendicular to the main flow direction. With this method too, an error is expected in the turbulence quantities at higher turbulence levels due to the series expansion; this error is of the same magnitude as for the X-wire probes.

REFERENCES

/92

1. Bradshaw, P., An Introduction to Turbulence and its Measurement, Oxford, Pergamon Press, 1971.

2. Strickert, H., Hitzdraht- und Hitzfilmanemometrie [Hot-Wire and Hot Film Anemometry], Berlin, State Pub. Technik, 1974.

3. Comte-Bellot, C., "Hot-Wire Anemometry," Annual Rev. Fluid Mech. 8, 209-231 (1976).

4. Helland, K.N. and C.W. van Atta, "Response of Constant-Current and Constant-Temperature Anemometers to Artificial Turbulence," Phys. Fluids 19, 1109-1117 (1976).

5. Hinze, J.O., Turbulence, New York, McGraw Hill, 1959.

6. Webster, C.A.G., "A Note on the Sensitivity to Yaw of a Hot-Wire Anemometer," J. Fluid Mech. 13, 307-312 (1962).

7. Corrsin, S., "Turbulence: Experimental Methods," in: Handbuch der Physik [Handbook of Physics], ed. S. Flügge, Vol. VIII/2, Berlin, Springer Verlag, 1963, pp. 524-590.

8. Champagne, F.H., C.A. Sleicher, and O.H. Wehrmann, "Turbulence Measurements with Inclined Hot-Wires," J. Fluid Mech. 28, 153-175 (1967).

9. Davies, P.O.A.L. and H.H. Bruun, "The Performance of a Yawed Hot-Wire," ISVR Memorandum No. 284 (1969).

10. Friehe, C.A. and W.H. Schwarz, "Deviations from the Cosine Law for Yawed Cylindrical Anemometer Sensors," J. Applied Mech., Trans. ASME 35, 566-662 (1968). /93

11. Simmons, L.F.G. and A. Bailey, Phil. Mag. 3, 81-96 (1927) cited in: J.M. Burgers, "Hot Wire Measurements," in: Handbuch der Experimentalphysik [Handbook of Experimental Physics], ed. Wien-Harms, Vol. IV, Part I, Leipzig, 1931, p. 657.

12. Freymuth, P., "A Bibliography of Thermal Anemometry," TSI (Thermo Systems Instruments) Inc. Report, St. Paul, Minn., 1978.

13. Vagt, J.O., "Hot-Wire Probes in Low-Speed Flow," Prog. Aerospace Sci. 18, 271-323 (1978).

14. Bechert, O., "An Acoustic-Flow Method for Dynamic Calibration of Hot-Wire Anemometers," Proc. of the 7th Int. Congr. Acoustics, ICA, Budapest, 1971, pp. 389-392.

15. Bremhorst, K. and D.B. Gilmore, "Comparison of Dynamic and Static Hot-Wire Anemometer Calibrations for Velocity Perturbation Measurements," J. Phys. E., Scient. Instrum. 9, 1097-1100 (1976).

16. Tutu, N.K. and R. Chevray, Cross-Wire Anemometry in High Intensity Turbulence," J. Fluid Mech. 71, 785-800 (1975).

17. Bradbury, L.J.S., "Measurements with a Pulsed-Wire and a Hot-Wire Anemometer in the Highly Turbulent Wake of a Normal Flat Plate," J. Fluid Mech. 77, 473-497 (1976).

18. Rodi, W., "A New Method of Analysing Hot-Wire Signals in Highly Turbulent Flow and Its Evaluation in a Round Jet," DISA Inform. 17, 8-18 (1975). /94

19. Gaulier, C., "Measurements of Air Velocity by Means of a Triple Hot-Wire Probe," DISA Inform. 21, 16-20 (1977).

20. Moffat, R.I., S. Yavuzkurt, and M.E. Crawford," Real Time Measurements of Turbulence Quantities with a Triple Hot-Wire System," in: Proceedings of the Dynamics Flow Conference 1978 on Dynamic Measurements in Unsteady Flows, Sept. 1978, Marseille (France) and Baltimore (USA), pp. 1013-1035.

21. Acrivlellis, M., Auswertung von Hitzdrahtmessungen mehrdimensionaler Strömung beliebiger Turbulenzintensität [Evaluation of Hot-Wire Measurements of Multidimensional Flows of Variable Turbulence Intensity], Strömungsmechanik und Strömungsmaschinen (Mitt. d. Inst. für Strömungslehre und Strömungsmaschinen Universität Karlsruhe (TH) 25, 1-59 (1978).

22. Fabris, G., "Probe and Method for Simultaneous Measurements of 'True' Instantaneous Temperature and Three Velocity Components in Turbulent Flow," Rev. Sci. Instrum. 49, 654-664 (1978).

23. Bartenwerfer, M., Bemerkungen zur Analyse von Hitzdrahtsignalen stark turbulenter Strömungen [Comments on the Analysis of Hot-Wire Signals in Highly Turbulent Flows], DLR-FB (Deutsche Luft- und Raumfahrt Forschungsbericht) 76-41, 1976.

24. Champagne, F.H. and C.A. Sleicher, "Turbulence Measurements with Inclined Hot-Wires. Part 2: Hot-Wire Response Equations," J. Fluid Mech. 28, 177-182 (1967).

25. Guitton, D.E., Correction of Hot-Wire Data for High-Intensity Turbulence, Longitudinal Cooling and Probe Interference, McGill University, Mech. Eng. Dept. Rep. No. 68-6, 1968. /95

26. Heskestad, G., "Hot-Wire Measurements in a Plane Turbulent Jet," Journ. Applied Mech., 721-729 (1965).

27. Vagt, J.D., "Hot-Wire Measurement Technique in a Highly Turbulent Flow and the Calculation of Intensities," International Centre for Heat and Mass Transfer, Intern. Seminar on Heat and Mass Transfer in Flows with Separated Regions and Measurement Techniques, Herceg-Novi, Yugoslavia, 1969.

28. Acrivlellis, M., "Hot-Wire Measurements in Flows of Low and High Turbulence Intensity," DISA Inform. 22, 15-20 (1977).

29. Acrivlellis, M., "Finding the Spatial Flow Field by Means of Hot-Wire Anemometry," DISA Inform. 22, 21-28 (1977).

30. Acrivlellis, M., "An Improved Method for Determining the Flow Field of Multidimensional Flows of Any Turbulence Intensity," DISA Inform. 23, 11-16 (1978).

31. Acrivlellis, M., "Flow Field Dependence on Hot-Wire Probe Cooling Law and Probe Adjustment," DISA Inform. 23, 17-23 (1978).

32. Bartenwerfer, M., "Remarks on Hot-Wire Anemometry Using 'Squared Signals' (Letter to the Editor)," DISA Inform. 24, 4, 40 (1979).

33. Elsenaar, A. and S.H. Boelsma, Measurements of the Reynolds Shear Stress Tensor in a Three-Dimensional Turbulent Boundary Layer Under Infinite Swept Wing Conditions, NLR-TR 74 095 U, 1974. /96

34. Charnay, G., Characteristique d'une couche limité turbulente evoluant en présence d'un ecoulement exterieur turbulent [Characteristic of a turbulent boundary layer developing in the presence of an external turbulent flow], Dissertation, University of Lyon, 1974.

35. Dechow, R., Mittlere Geschwindigkeit und Reynoldsscher Spannungstensor in der drei-dimensionalen turbulenten Wandgrenzschicht vor einem stehenden Zylinder [Average Speed and Reynolds Shear-Stress Tensor in the Three-Dimensional Turbulent Wall Boundary Layer in Front of a Standing Cylinder], Dissertation, TH Karlsruhe, 1977; appeared in Strömungsmechanik und Strömungsmaschinen (Mitt. des Instituts für Strömungslehre und Stromungsmaschinen Universität Karlsruhe (TH) 21, 1-78 (1977).

36. Lehmann, B., "Laser-Doppler Anemometry," Presented to Course No. 4377/06.184 at the Tech. Academy of Esslingen, Feb. 11-12, 1980.

37. De Grande, G. and P. Kool, "An Improved Experimental Method to Determine the Complete Reynolds Stress Tensor with a Single Rotating Slanting Hot Wire," J. Phys. E., Sci. Instrum. 14, 196-201 (1981).

38. Fujita, H. and L.S.G. Kovasznay, "Measurements of Reynolds Stress by a Single Rotating Hot Wire Anemometer," Rev. Sci. Instrum. 39, 1351-1355 (1968).

14. Tables

/97

Table 1: ERRORS Δ_{lm} AT $\overline{u_1'^2}/U^2 = 0.05$ AND ISOTROPIC TURBULENCE

k s σ	Γ C_2 C_3	sign(A_1) sign(A_2) sign(A_3)	C_{12} C_{13} C_{23}	approx.	Δ_{11} %	Δ_{22} %	Δ_{33} %	Δ_{12} %	Δ_{13} %	Δ_{23} %
0.0	3	-1	0	1.	-0.8	-8.8	-8.8	-	-	-
0.1667	1	-1	0	2.	+9.2	+0.4	+0.4	-	-	-
0.3333	1	-1	0	4.	±0.0	±0.0	±0.0	-	-	-
0.2	3	-1	0	1.	-2.4	-11.4	-11.4	-	-	-
0.1667	1	-1	0	2.	+7.4	-2.4	-2.4	-	-	-
0.3333	1	-1	0	4.	-0.8	-5.6	-5.6	-	-	-
0.0	10	-1	0	1.	+18.8	-7.8	-7.8	-	-	-
0.0655	1	-1	0	2.	+30.8	+1.4	+1.4	-	-	-
0.3333	1	-1	0	4.	-7.0	+0.8	+0.8	-	-	-
0.2	10	-1	0	1.	+15.8	-19.2	-19.2	-	-	-
0.0655	1	-1	0	2.	+26.4	-11.8	-11.8	-	-	-
0.3333	1	-1	0	4.	+2.8	-14.4	-14.4	-	-	-
0.0	3	+1	0	1.	-0.8	-9.6	-9.6	-	-	-
0.1667	1	+1	0	2.	+9.2	+0.4	+0.4	-	-	-
0.3333	1	+1	0	4.	±0.0	-0.2	-0.2	-	-	-
0.2	3	+1	0	1.	-2.4	-11.4	-11.4	-	-	-
0.1667	1	+1	0	2.	+7.4	-2.4	-2.4	-	-	-
0.3333	1	+1	0	4.	-0.8	-5.6	-5.6	-	-	-
0.0	10	+1	0	1.	+18.8	-7.8	-7.8	-	-	-
0.0655	1	+1	0	2.	+30.8	+1.4	+1.4	-	-	-
0.3333	1	+1	0	4.	-7.0	+0.8	+0.8	-	-	-
0.2	10	+1	0	1.	+15.8	-19.2	-19.2	-	-	-
0.0655	1	+1	0	2.	+26.4	-11.8	-11.8	-	-	-
0.3333	1	+1	0	4.	+2.8	-14.4	-14.4	-	-	-

/98

Table 2: ERRORS Δ_{lm} AT $\overline{u_1'^2}/U^2 = 0.05$ AND 2-DIMENSIONAL BOUNDARY LAYER

k s σ	Γ C_2 C_3	sign(A_1) sign(A_2) sign(A_3)	C_{12} C_{13} C_{23}	approx.	Δ_{11} %	Δ_{22} %	Δ_{33} %	Δ_{12} %	Δ_{13} %	Δ_{23} %
0.0	3	+1	-0.4	1.	-2.4	-4.7	-3.6	+5.4	-	-
0.1667	0.3	-1	0	2.	+1.8	-0.7	-0.4	+0.9	-	-
0.3333	0.5	+1	0	4.	-0.4	-2.0		+2.7	-	-
0.2	3	+1	-0.4	1.	-4.0	-6.0	-4.8	+5.5	-	-
0.1667	0.3	-1	0	2.	+0.2	-2.0	-2.0	+1.8	-	-
0.3333	0.5	+1	0	4.	-2.2	-4.7		+3.6	-	-
0.0	10	+1	-0.4	1.	+4.0	-4.7	-2.8	+7.3	-	-
0.0655	0.3	-1	0	2.	+9.0	±0.0	±0.0	±0.0	-	-
0.3333	0.5	+1	0	4.	+3.2	-1.3		+1.8	-	-
0.2	10	+1	-0.4	1.	+3.2	-7.3	-7.6	+0.9	-	-
0.0655	0.3	-1	0	2.	+8.0	-2.7	-4.8	-3.6	-	-
0.3333	0.5	+1	0	4.	+3.0	-5.3		-0.9	-	-
0	3	-1	-0.4	1.	-2.4	-4.7	-2.8	+5.5	-	-
0.1667	0.3	+1	0	2.	+2.2	±0.0	±0.0	+0.9	-	-
0.3333	0.5	-1	0	4.	-0.4	-2.0		+2.7	-	-
0.2	3	-1	-0.4	1.	-3.0	-5.3	-4.4	+6.4	-	-
0.1667	0.3	+1	0	2.	+1.6	-1.3	-1.2	+1.8	-	-
0.3333	0.5	-1	0	4.	-1.2	-4.0		+4.5	-	-
0	10	-1	-0.4	1.	-13.0	-30.0	-4.0	+58.2	-	-
0.0655	0.3	+1	0	2.	-9.6	-27.3	-1.6	+56.4	-	-
0.3333	0.5	-1	0	4.	-13.2	-28.7		+57.2	-	-
0.2	10	-1	-0.4	1.	-13.8	-31.3	-8.8	+60.9	-	-
0.0655	0.3	+1	0	2.	-10.6	-28.7	-6.4	+59.1	-	-
0.3333	0.5	-1	0	4.	-13.6	-30.7		+60.5	-	-

Table 3: ERROR Δ_{1m} AT $\overline{u_1'^2}/u^2$ AND 3-DIMENSIONAL BOUNDARY LAYER /99

k s σ	Γ C_2 C_3	sign(A_1) sign(A_2) sign(A_3)	C_{12} C_{13} C_{23}	approx.	Δ_{11} %	Δ_{22} %	Δ_{33} %	Δ_{12} %	Δ_{13} %	Δ_{23} %
0.0	3	+1	-0.30	1.	+10.6	-8.8	-8.6	+20.7	-6.4	+1.3
0.1667	0.5	+1	-0.30	2.	+15.8	-4.8	-4.0	+17.0	-12.0	+1.8
0.3333	0.7	+1	-0.13	4.	+13.4	-4.8		+17.0	-	-
0.2	3	+1	-0.30	1.	+7.0	-11.2	-9.7	+23.6	-4.8	+7.6
0.1667	0.5	+1	-0.30	2.	+12.2	-6.8	-5.4	+19.8	-9.6	+7.4
0.3333	0.7	+1	-0.13	4.	+9.6	-8.4		+20.8	-	-
0.0	3	+1	-0.10	1.	+5.4	-12.4	-11.1	+96.3	-67.8	+1.4
0.1667	0.5	+1	-0.10	2.	+10.4	-8.0	-6.9	+96.2	-75.4	+2.2
0.3333	0.7	+1	-0.27	4.	+8.0	-8.4		+96.2	-	-
0.2	3	+1	-0.10	1.	+2.4	-14.0	-12.3	+95.3	-62.7	+7.6
0.1667	0.5	+1	-0.10	2.	+7.4	-10.0	-8.0	+95.1	-70.3	+7.7
0.3333	0.7	+1	-0.27	4.	+4.8	-11.6		+95.1	-	-

15. Figures /101

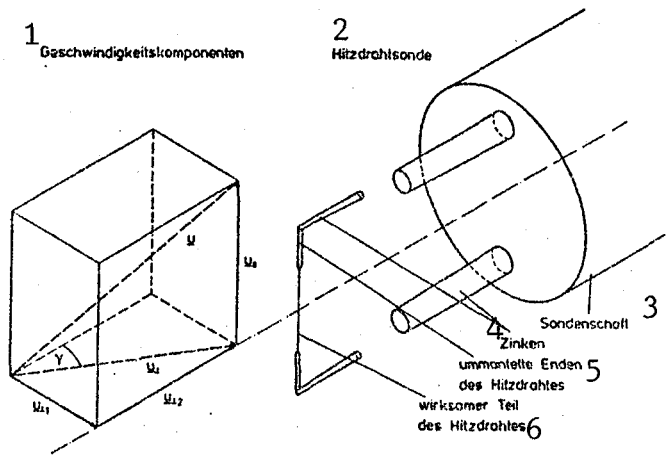

Figure 1: Normal One-wire Probe with Speed Components and Instantaneous Setting Angle

Key: 1-speed components 2-hot-wire probe 3-probe shaft 4-prongs 5-mantled ends of the hot-wire 6-effective part of the hot wire

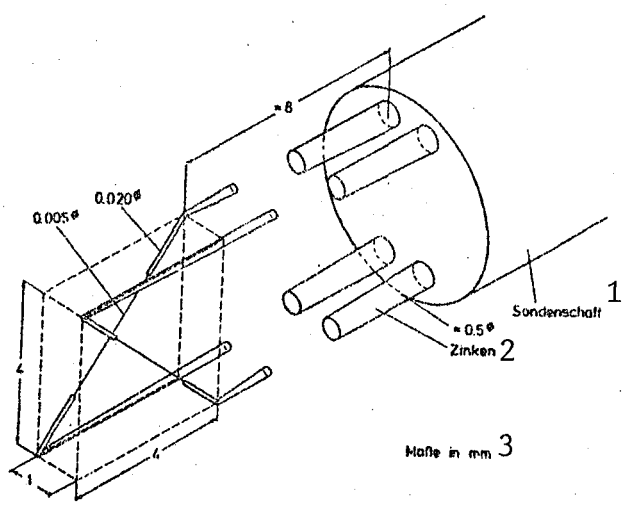

Fig. 2: X-Wire Probe with normal Prong Leads and Typical Dimensions.

Key: 1-probe shaft 2-prongs 3-dimensions in mm

/102

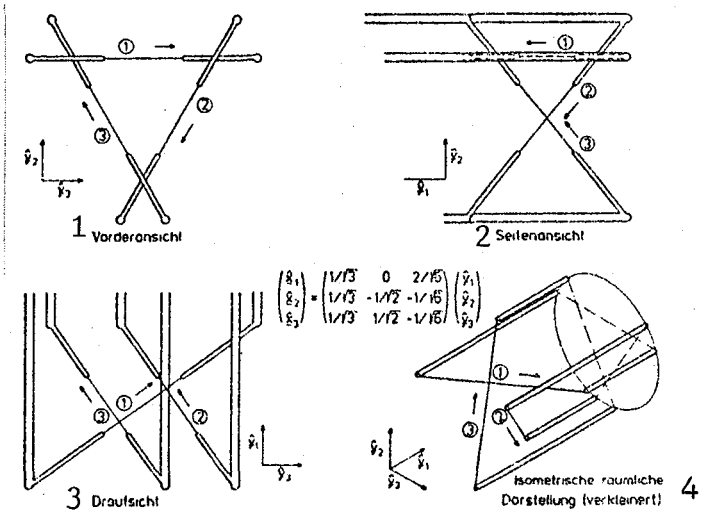

Fig. 3: Orthogonal Three-Wire Probe ("Triangular Probe")

Key: 1-front view 2-side view 3-top view 4-isometric spatial illustration (reduced)

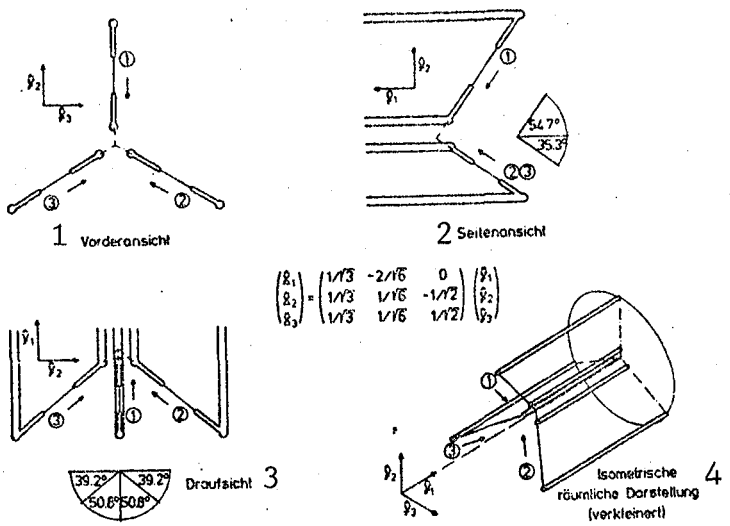

Fig. 4: Orthogonal Three-Wire Probe ("Tripod").

Key: 1-front view 2-side view 3-top view 4-isometric spatial illustration (reduced)

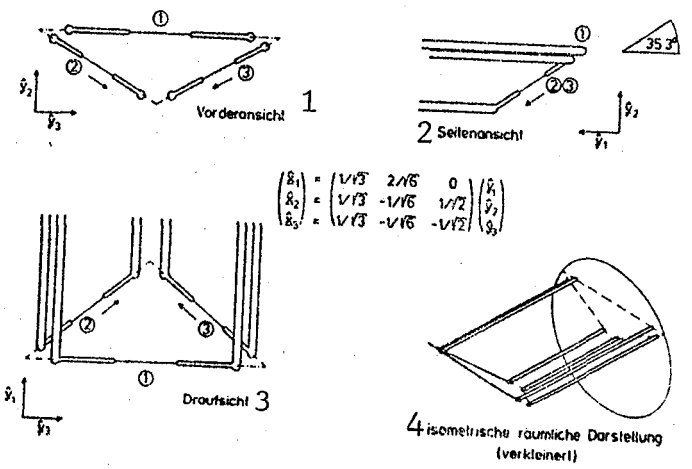

Fig. 5: Plane Three-Wire Probe ("Right angle triangular probe") Application 1

Key: 1-front view 2-side view 3-top view 4-isometric, spatial illustration (reduced)

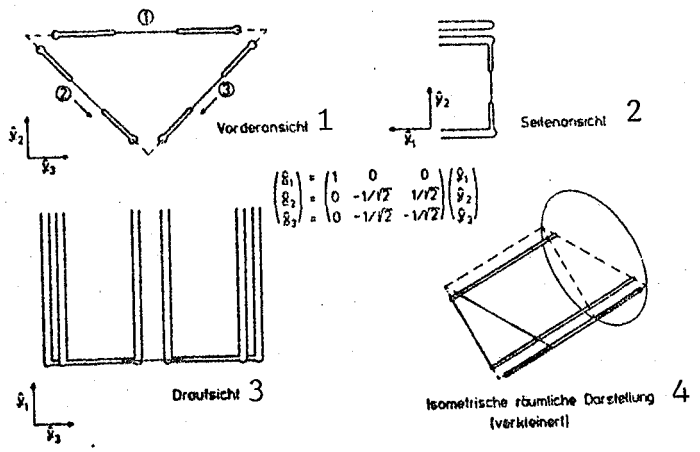

Fig. 6: Plane Three-Wire Probe ("Right angle triangular Probe") Application 2

Key: 1-front view 2-side view 3-top view 4-isometric, spatial illustration (reduced)

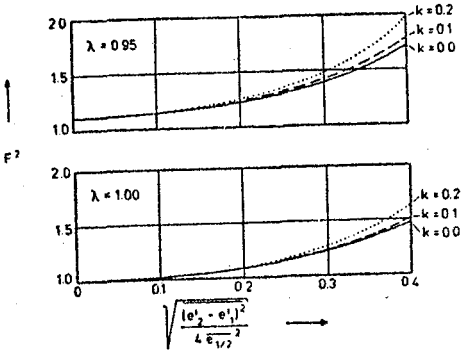

Fig. 7: Correction Factor F^2 for Various Turbulence Intensities and Anisotropy Factors

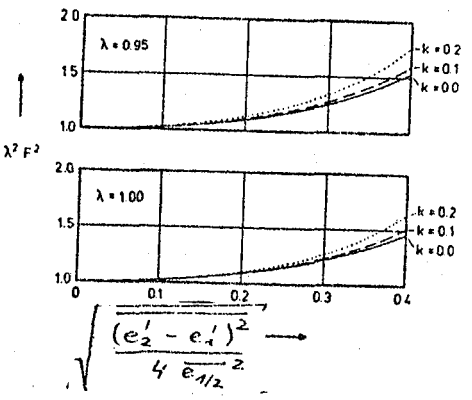

Fig. 8: Correction Factor $\lambda^2 F^2$ for Various Turbulence Intensities and Anisotropy Factors

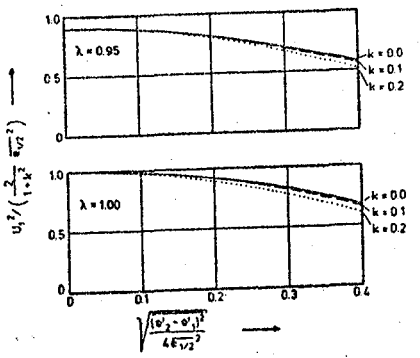

Fig. 9: The Corrected, Average Speed

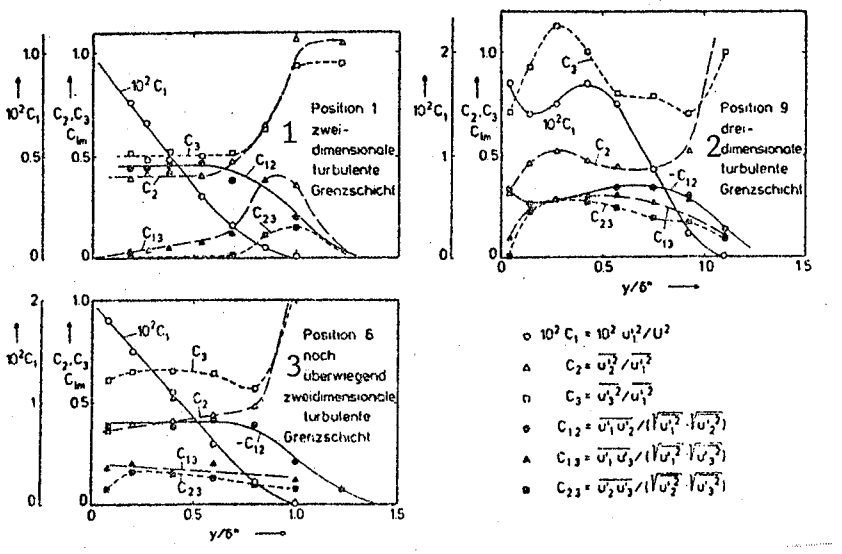

Fig. 10: Turbulence Quantities in an Airplane Wing Boundary Layer, Hot wire measurements by Elsenaar and Boelsma [33]; y= local coordinate perpendicular to the surface
δ^* = boundary layer density

Key: 1-two-dimensional turbulent boundary layer 2-three-dimensional turbulent boundary layer 3-still predominantly two-dimensional turbulent boundary layer

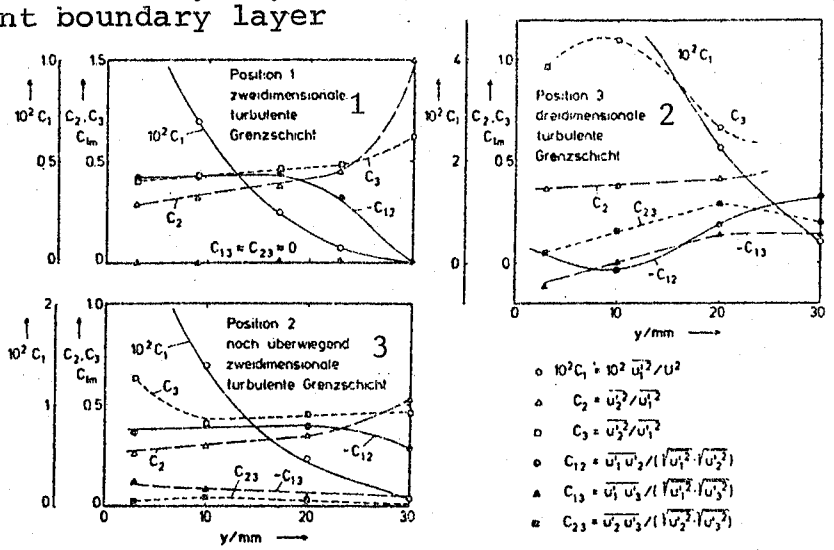

Fig. 11: Turbulence Quantities in a Boundary Layer in Front of a Cylinder Standing on a Flat Plate, Hot-wire measurements by Dechow [35]; (y = local coordiante perpendicular to the plate).

Key: 1-two-dimensional turbulent boundary layer 2-three-dimensional turbulent boundary layer 3-still predominately two-dimensional boundary layer

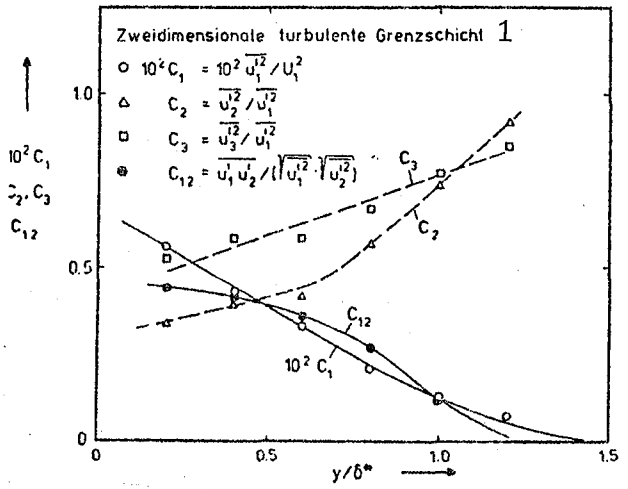

Fig. 12: Turbulence Quantities in a Boundary Layer Generated by a Trip Wire on a Flat Plate, Hot wire Measurements by Charnay [34]; (y = local coord. perpendicular to the plate δ^* = boundary layer thickness)

Key: 1-two-dimensional turbulent boundary layer

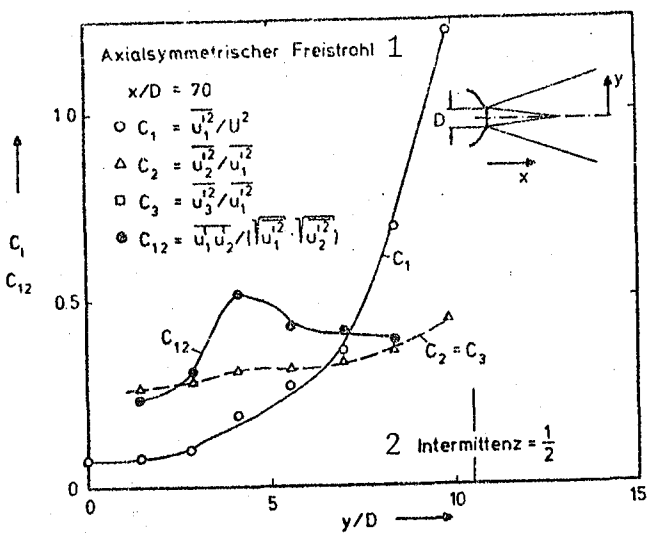

Fig. 13: Turbulence Quantities in a Shear Layer of a Fully Expanded Axial-symmetric Free Jet, LDA Measurements by Lehmann [36]

Key: 1-axial-symmetric free jet 2-intermittence

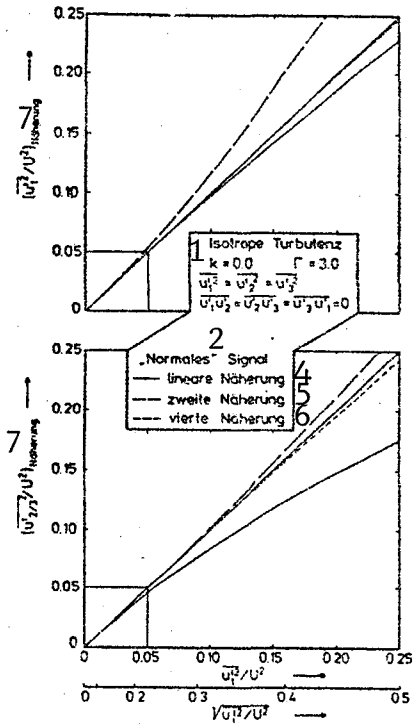

Fig. 14: Relative Speed Fluctuations $\overline{u_l^2}/U^2$ (l=1,2,3) for Isotropic Turbulence; analysis of "normal" signals: $0 \leq \overline{u_1^2}/U^2 \leq 0.25$

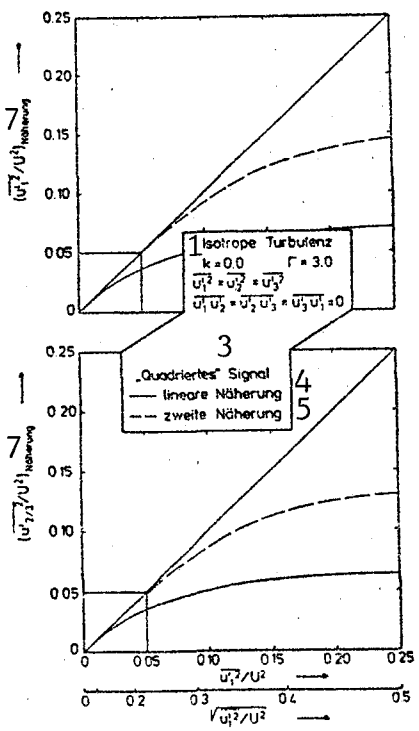

Fig. 15: Relative Speed Fluctuations $\overline{u_l^2}/U^2$ (l=1,2,3) for Isotropic Turbulence; analysis of "squared" signals: $0 \leq \overline{u_1^2}/U^2 \leq 0.25$

Key: 1-isotropic turbulence 2-"normal" signal 3-"squared" signal 4-linear approximation 5-second approx. 6-fourth approx. 7-approximation

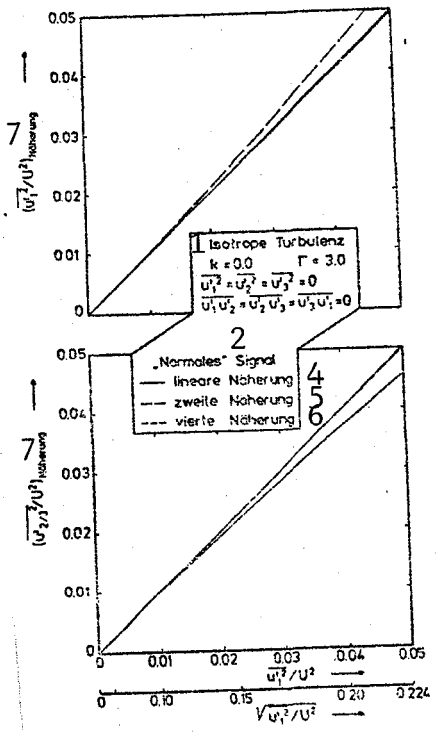

Fig. 16: Relative Speed Fluctuations $\overline{u_1'^2}/U^2$ (1=1,2,3) for Isotropic Turbulence; analysis of "normal" signals; $0 \leq \overline{u_1'^2}/U^2 \leq 0.05$

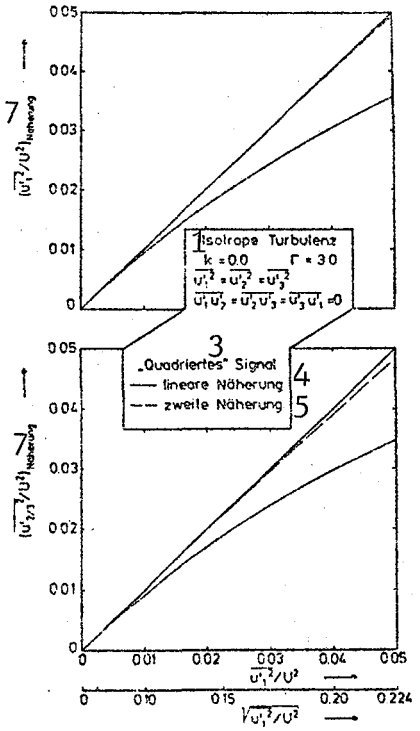

Fig. 17: Relative Speed Fluctuations $\overline{u_1'^2}/U^2$ (1=1,2,3) for Isotropic Turbulence; analysis of "squared" signals; $0 \leq \overline{u_1'^2}/U^2 \leq 0.05$

Key: 1-isotropic turbulence 2-"normal" signal 3-"squared" signal 4-linear approx. 5-second approx. 6-fourth approx. 7-approximation

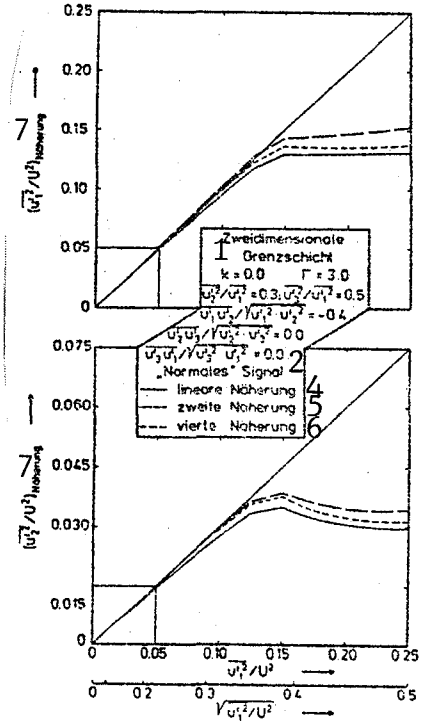

ORIGINAL PAGE IS
OF POOR QUALITY

Fig. 18: Relative Speed Fluctuations $\overline{u_1^{1^2}}/U^2$ (1=1,2) for two-dimensional Boundary Layer; analysis of "normal" signals; $0 \leq \overline{u_1^{1^2}}/U^2 \leq 0.25$

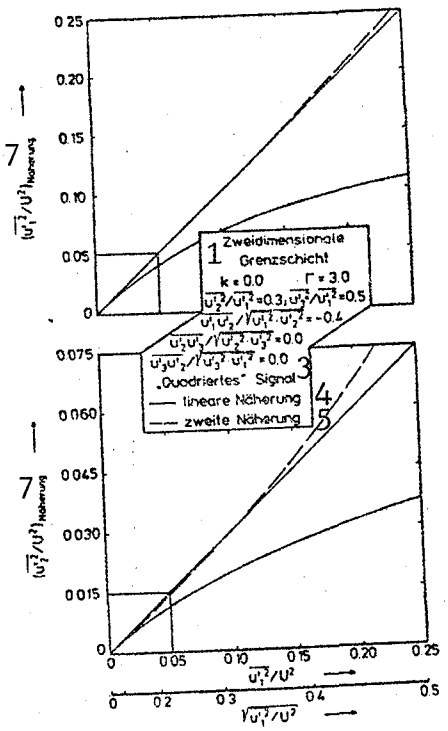

Fig. 19: Relative Speed Fluctuations $\overline{u_1^{1^2}}/U^2$ (1=1,2) for two-dimensional Boundary Layer; analysis of "normal" signals: $0 \leq \overline{u_1^{1^2}}/U^2 \leq 0.25$

Key: 1-two-dimensional boundary layer 2-"normal" signal
3-"squared" signal 4-linear approx. 5-second approx.
6-fourth approx. 7-approximation

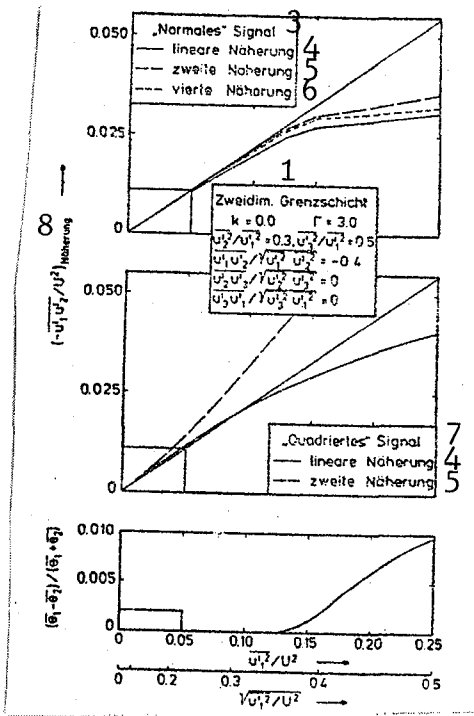

Fig. 20: Relative Speed Correlation $\overline{u_1 u_2}/U^2$ and Rel. Difference $(\bar{e}_1-\bar{e}_2)/(\bar{e}_1+\bar{e}_2)$ for 2D boundary layer; analysis of "normal" and "squared" signals; $0 \le \overline{u_1^2}/U^2 \le 0.25$

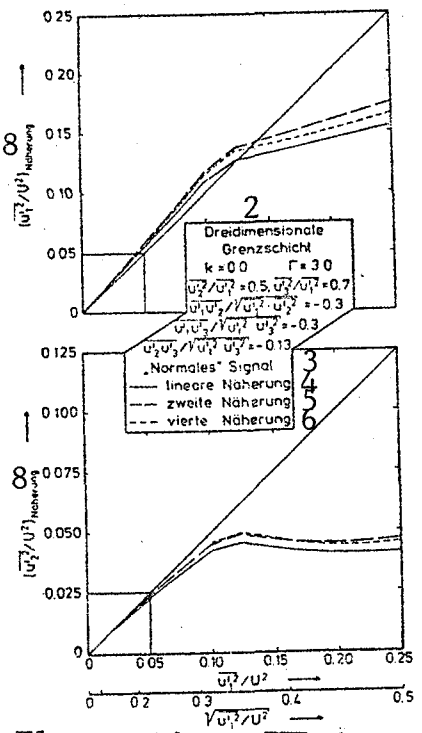

Fig. 21: Relative Speed Fluctuations $\overline{u_i^2}/U^2$ $(i=1,2)$ for 3D Boundary Layer; analysis of "normal" signals; $0 \le \overline{u_1^2}/U^2 \le 0.25$

Key: 1-two-diminsional boundary layer 2-three-dim. boundary layer 3-"normal" signal 4-linear approx. 5-second approx. 6-fourth approx. 7-"squared" signal 8-approximation

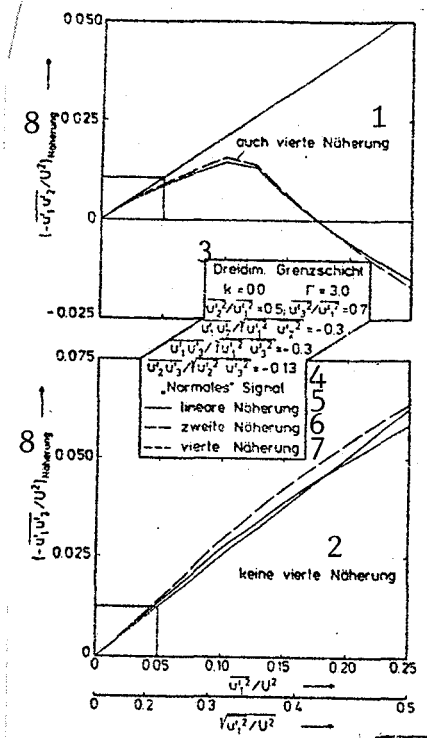

Fig. 22: Relative Speed Correlations $-\overline{u_1' u_2'}/U^2$ and $-\overline{u_1' u_3'}/U^2$ for 3D Boundary Layer; analysis of "normal" signals;

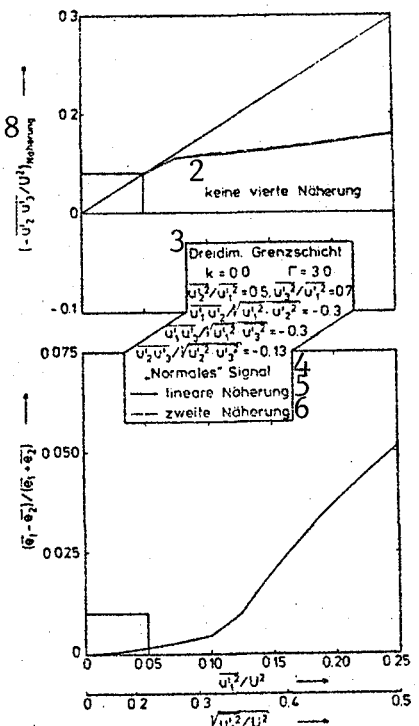

Fig. 23: Relative Speed Correlations $-\overline{u_2' u_3'}/U^2$ and relative difference $(\vec{e}_1 - \vec{e}_2)$ $(\vec{e}_1 + \vec{e}_2)$ for 3D boundary layer; analysis of "normal" signals; $0 \leq \overline{u'^2}/U^2 \leq 0.25$

Key: 1-also 4th approx. 2-no fourth approx. 3-Three-D boundary layer 4-"normal" signal 5-linear approx. 6-second approx. 7-fourth approx. 8-approximation

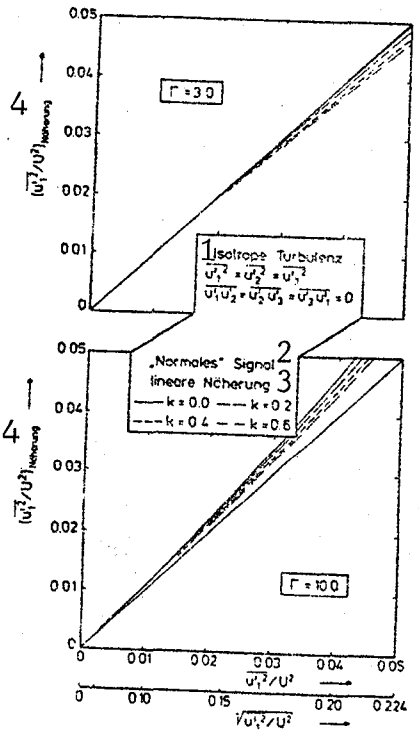

Fig. 24: Relative Speed Fluctuations $\overline{u_1'^2}/U^2$ for Various Tangential Cooling Factors k and various Convexity Factors Γ; analysis of "normal" signals: $0 \leq \overline{u_1'^2}/U^2 \leq 0.05$

Key: 1-isotropic turbulence 2-"normal" signal 3-linear approximation 4-approximation

Appendix A: Linear Equation Systems, Matrix Multiplication, Derivation of Equations (5.1) to (5.4) /114

A linear system of equations:

$$\sum_{k=1}^{K} a_{ik} x_k = b_i \quad , \quad i = 1, \ldots, I \quad ,$$

is abbreviated as

$$\underline{\underline{A}} \circ \underline{x} = \underline{b}$$

Here, $\underline{\underline{A}}$ represents the matrix $(a_{ik})_{k=1,K}^{i=1,I}$, $\underline{x}$ represents the matrix $(x_k)_{k=1,K}$, $\underline{b}$ represents the matrix $(b_i)_{i=1,I}$.

Written explicitly, with K=3, I=4 for example:

$$\begin{pmatrix} a_{11} & a_{12} & a_{13} \\ a_{21} & a_{22} & a_{23} \\ a_{31} & a_{32} & a_{33} \\ a_{41} & a_{42} & a_{43} \end{pmatrix} \circ \begin{pmatrix} x_1 \\ x_2 \\ x_3 \end{pmatrix} = \begin{pmatrix} b_1 \\ b_2 \\ b_3 \\ b_4 \end{pmatrix}$$

The $\circ$ multiplication is thus performed so that the individual rows of $\underline{\underline{A}}$ are multiplied with column $\underline{x}$ like vectors handled as scalars. In this notation, linear equation systems are easy to handle since the rows can be multiplied by any scalars ($\neq 0$) and added.

The equation system (5) is written for the orientations $\alpha = \pi/4;\ \theta = 0, \pi;\ \pi/2, -\pi/2;\ \pi/4, -3\pi/4;\ -\pi/4, 3\pi/4$ as follows:

$$
\begin{bmatrix}
\frac{1+k^2}{2} & \frac{1+k^2}{2} & 1 & -\frac{1-k^2}{1} & 0 & 0 \\
\frac{1+k^2}{2} & \frac{1+k^2}{2} & 1 & \frac{1-k^2}{1} & 0 & 0 \\
\frac{1+k^2}{2} & 1 & \frac{1+k^2}{2} & 0 & 0 & -\frac{1-k^2}{1} \\
\frac{1+k^2}{2} & 1 & \frac{1+k^2}{2} & 0 & 0 & \frac{1-k^2}{1} \\
\frac{1+k^2}{2} & \frac{3+k^2}{4} & \frac{3+k^2}{4} & -\frac{1-k^2}{\sqrt{2}} & -\frac{1-k^2}{2} & -\frac{1-k^2}{\sqrt{2}} \\
\frac{1+k^2}{2} & \frac{3+k^2}{4} & \frac{3+k^2}{4} & \frac{1-k^2}{\sqrt{2}} & -\frac{1-k^2}{2} & \frac{1-k^2}{\sqrt{2}} \\
\frac{1+k^2}{2} & \frac{3+k^2}{4} & \frac{3+k^2}{4} & -\frac{1-k^2}{\sqrt{2}} & \frac{1-k^2}{2} & \frac{1-k^2}{\sqrt{2}} \\
\frac{1+k^2}{2} & \frac{3+k^2}{4} & \frac{3+k^2}{4} & \frac{1-k^2}{\sqrt{2}} & \frac{1-k^2}{2} & -\frac{1-k^2}{\sqrt{2}}
\end{bmatrix}
\circ
\begin{bmatrix}
(U_1+u_1')^2 \\
(U_2+u_2')^2 \\
(U_3+u_3')^2 \\
(U_1+u_1')(U_2+U_2') \\
(U_2+u_2')(U_3+u_3') \\
(U_3+u_3')(U_1+u_1')
\end{bmatrix}
=
\begin{bmatrix}
e_1^2 \\ e_2^2 \\ e_3^2 \\ e_4^2 \\ e_5^2 \\ e_6^2 \\ e_7^2 \\ e_8^2
\end{bmatrix}
$$

From this follows:

$$
\begin{bmatrix}
\frac{1+k^2}{4} & \frac{1+k^2}{4} & \frac{1}{2} & 0 & 0 & 0 \\
0 & 0 & 0 & 1-k^2 & 0 & 0 \\
\frac{1+k^2}{4} & \frac{1}{2} & \frac{1+k^2}{4} & 0 & 0 & 0 \\
0 & 0 & 0 & 0 & 0 & 1-k^2 \\
\frac{1+k^2}{4} & \frac{3+k^2}{8} & \frac{3+k^2}{8} & 0 & 0 & 0 \\
0 & 0 & 0 & 0 & 1-k^2 & 0 \\
0 & 0 & 0 & \sqrt{2}(1-k^2) & 0 & 0 \\
0 & 0 & 0 & 0 & 0 & -\sqrt{2}(1-k^2)
\end{bmatrix}
\circ
\begin{bmatrix}
(U_1+u_1')^2 \\
(U_2+u_2')^2 \\
(U_3+u_3')^2 \\
(U_1+u_1')(U_2+u_2') \\
(U_2+u_2')(U_3+u_3') \\
(U_3+u_3')(U_1+u_1')
\end{bmatrix}
=
\begin{bmatrix}
\frac{1}{4}(e_2^2+e_1^2) \\
\frac{1}{2}(e_2^2-e_1^2) \\
\frac{1}{4}(e_4^2+e_3^2) \\
\frac{1}{2}(e_4^2-e_3^2) \\
\frac{1}{8}(e_8^2+e_7^2+e_6^2+e_5^2) \\
\frac{1}{2}(e_8^2+e_7^2-e_6^2-e_5^2) \\
\frac{1}{2}(e_8^2-e_7^2+e_6^2-e_5^2) \\
\frac{1}{2}(e_8^2-e_7^2-e_6^2+e_5^2)
\end{bmatrix}
$$

See (6.1) to (6.4)

Appendix B: Proof that System of Equations (5) cannot be solved formally /11
for the Six Unknowns $u_l u_m$ $(l,m=1,2,3)$, when $\alpha = \text{const.}$

The question is whether there are six directions (α,θ_i), $i=1,\dots,6$ so that:

$$DET = \det\left[\left(1+(k^2-1)\cos^2\alpha,\ 1+(k^2-1)\sin^2\alpha\cos^2\theta_i,\ 1+(k^2-1)\sin^2\alpha\sin^2\theta_i,\ (k^2-1)\cos\alpha\cdot\sin\alpha\cdot\cos\theta_i,\ (k^2-1)\sin^2\alpha\cdot\cos\theta_i\cdot\sin\theta_i,\ (k^2-1)\cos\alpha\cdot\sin\alpha\cdot\sin\theta_i\right)_{i=1,\dots,6}\right] \neq 0$$

Without affecting the universality, we can set $\theta_1=0$. Then we have:

$$DET = (k^2-1)\cos\alpha\cdot\sin\alpha\cdot(k^2-1)\sin^2\alpha\cdot(k^2-1)\cos\alpha\sin\alpha\cdot\left(1+(k^2-1)\cos^2\alpha\right)\cdot$$

$$\cdot\det\begin{bmatrix} 1 & 1+(k^2-1)\sin^2\alpha & 1 & 1 & 0 & 0 \\ \left(0,\ (k^2-1)\sin^2\alpha(\cos^2\theta_i-1),\ (k^2-1)\sin^2\alpha\sin^2\theta_i,\ \cos\theta_i-1,\ \cos\theta_i\sin\theta_i,\ \sin\theta_i\right)_{i=2,\dots,6} \end{bmatrix} =$$

$$= (k^2-1)\cos\alpha\cdot\sin\alpha\cdot(k^2-1)\sin^2\alpha\cdot(k^2-1)\cos\alpha\sin\alpha\cdot\left(1+(k^2-1)\cos^2\alpha\right)\cdot(k^2-1)\sin^2\alpha\cdot(k^2-1)\sin^2\alpha\cdot$$

$$\cdot\det\left[\left(-\sin^2\theta_i,\ \sin^2\theta_i,\ \cos\theta_i-1,\ \cos\theta_i\sin\theta_i,\ \sin\theta_i\right)_{i=2,\dots,6}\right] = 0,$$

since the first and second columns of the last matrix are identical except for the sign, thus they are linearly dependent.

Appendix C: Calculation of Coefficients $b_{lm}(\alpha_i,\theta_i)$ of equations (7.1) to (7.6) for k=0. /117

If we select the orientations $(\alpha,\theta) = (\frac{\pi}{6}, 0), (\frac{\pi}{3}, \pi), (\frac{\pi}{6}, \frac{\pi}{2}), (\frac{\pi}{3}, -\frac{\pi}{2}), (\frac{\pi}{6}, \frac{\pi}{4}), (\frac{\pi}{3}, -\frac{3\pi}{4})$ and denote the corresponsing signals as e_1 to e_6, then for k=0 we have:

$$\begin{pmatrix} \frac{1}{4} & \frac{3}{4} & 1 & -\frac{\sqrt{3}}{2} & 0 & 0 \\ \frac{3}{4} & \frac{1}{4} & 1 & \frac{\sqrt{3}}{2} & 0 & 0 \\ \frac{1}{4} & \frac{7}{8} & \frac{7}{8} & -\frac{\sqrt{3}}{2\sqrt{2}} & \frac{1}{4} & \frac{\sqrt{3}}{2\sqrt{2}} \\ \frac{3}{4} & \frac{5}{8} & \frac{5}{8} & \frac{\sqrt{3}}{2\sqrt{2}} & \frac{3}{4} & -\frac{\sqrt{3}}{2\sqrt{2}} \\ \frac{1}{4} & \frac{7}{8} & \frac{7}{8} & -\frac{\sqrt{3}}{2\sqrt{2}} & -\frac{1}{4} & -\frac{\sqrt{3}}{2\sqrt{2}} \\ \frac{3}{4} & \frac{5}{8} & \frac{5}{8} & \frac{\sqrt{3}}{2\sqrt{2}} & -\frac{3}{4} & \frac{\sqrt{3}}{2\sqrt{2}} \end{pmatrix} \circ \begin{pmatrix} u_1^2 \\ u_2^2 \\ u_3^2 \\ u_1u_2 \\ u_2u_3 \\ u_3u_1 \end{pmatrix} = \begin{pmatrix} e_1^2 \\ e_2^2 \\ e_3^2 \\ e_4^2 \\ e_5^2 \\ e_6^2 \end{pmatrix}$$

By addition and subtraction of rows, we obtain:

$$\begin{pmatrix} -1 & 1 & 0 & 0 & 0 & 0 \\ 1 & 1 & 2 & 0 & 0 & 0 \\ 0 & 1 & -1 & 0 & 0 & 0 \\ 0 & 0 & 0 & 1 & 0 & 0 \\ 0 & 0 & 0 & 0 & 1 & 0 \\ 0 & 0 & 0 & 0 & 0 & 1 \end{pmatrix} \circ \begin{pmatrix} u_1^2 \\ u_2^2 \\ u_3^2 \\ 2u_1u_2 \\ 2u_2u_3 \\ 2u_3u_1 \end{pmatrix} =$$

/118

$$= \begin{pmatrix} \frac{1}{2}\left[(4-\frac{12}{2-\sqrt{2}})e_1^2 - (4-\frac{4}{2-\sqrt{2}})e_2^2 + \frac{2}{2-\sqrt{2}}(3e_3^2 - e_4^2 + 3e_5^2 - e_6^2)\right] \\ \frac{1}{2}\left[\,2e_1^2 + 2e_2^2\,\right] \\ \left[\,-2e_1^2 - 2e_2^2 + e_3^2 + e_4^2 + e_5^2 + e_6^2\,\right] \\ \frac{1}{(2-\sqrt{2})\sqrt{3}}\left[\,-6e_1^2 + 2e_2^2 + 3e_3^2 - e_4^2 + 3e_5^2 - e_6^2\,\right] \\ \left[\,e_3^2 + e_4^2 - e_5^2 - e_6^2\,\right] \\ \frac{1}{\sqrt{6}}\left[\,3e_3^2 - e_4^2 - 3e_5^2 + e_6^2\,\right] \end{pmatrix}$$

and furthermore:

$$\begin{pmatrix} u_1^2 \\ u_2^2 \\ u_3^2 \\ 2u_1u_2 \\ 2u_2u_3 \\ 2u_3u_1 \end{pmatrix} = \begin{pmatrix} \frac{9}{4}\left(\frac{2}{2-\sqrt{2}}-1\right) & -\frac{9}{4}\left(\frac{4}{3(2-\sqrt{2})}-1\right) & -\frac{1}{2}\left(\frac{9}{2-\sqrt{2}}-1\right) \\ -\frac{1}{4}\left(\frac{6}{2-\sqrt{2}}+1\right) & \frac{7}{4}\left(\frac{4}{7(2-\sqrt{2})}-1\right) & \frac{1}{2}\left(\frac{3}{2-\sqrt{2}}+1\right) \\ -\frac{7}{4}\left(\frac{6}{7(2-\sqrt{2})}-1\right) & \frac{1}{4}\left(\frac{4}{2-\sqrt{2}}+1\right) & \frac{1}{2}\left(\frac{3}{2-\sqrt{2}}-1\right) \\ -\frac{6}{\sqrt{3}(2-\sqrt{2})} & \frac{2}{\sqrt{3}(2-\sqrt{2})} & \frac{3}{\sqrt{3}(2-\sqrt{2})} \\ 0 & 0 & 1 \\ 0 & 0 & \frac{3}{\sqrt{6}} \end{pmatrix}$$

$$\begin{pmatrix} \frac{1}{2}\left(\frac{3}{2-\sqrt{2}}+1\right) & -\frac{1}{2}\left(\frac{9}{2-\sqrt{2}}-1\right) & \frac{1}{2}\left(\frac{3}{2-\sqrt{2}}+1\right) \\ -\frac{1}{2}\left(\frac{1}{2-\sqrt{2}}-1\right) & \frac{1}{2}\left(\frac{3}{2-\sqrt{2}}+1\right) & -\frac{1}{2}\left(\frac{1}{2-\sqrt{2}}-1\right) \\ -\frac{1}{2}\left(\frac{1}{2-\sqrt{2}}+1\right) & \frac{1}{2}\left(\frac{6}{2-\sqrt{2}}-1\right) & -\frac{1}{2}\left(\frac{1}{2-\sqrt{2}}+1\right) \\ -\frac{1}{\sqrt{3}(2-\sqrt{2})} & \frac{3}{\sqrt{3}(2-\sqrt{2})} & -\frac{1}{\sqrt{3}(2-\sqrt{2})} \\ 1 & -1 & -1 \\ -\frac{1}{\sqrt{6}} & -\frac{3}{\sqrt{6}} & -\frac{1}{\sqrt{6}} \end{pmatrix} \cdot \begin{pmatrix} e_1^2 \\ e_2^2 \\ e_3^2 \\ e_4^2 \\ e_5^2 \\ e_6^2 \end{pmatrix}.$$

Appendix D: Hot Wire Analysis without Root Expansion, Derivation and Handling of Equation (42) /119

Let $U_2=U_3=0$ and presume $U \gg |u_1'|$. From eq. (27) it follows without any approximation:

$$e_{1/2}^2 = a_{11} U_1^2 \cdot \Big[1 + \Big(2\frac{u_1'}{U_1} \pm 2\frac{a_{12}}{a_{11}}\cdot\frac{u_2'}{U_1} \pm 2\frac{a_{13}}{a_{11}}\cdot\frac{u_3'}{U_1} \Big) + \Big(\frac{u_1'^2}{U_1^2} + \frac{a_{22}}{a_{11}}\cdot\frac{u_2'^2}{U_1^2} + \frac{a_{33}}{a_{11}}\frac{u_3'^2}{U_1^2} \pm 2\frac{a_{12}}{a_{11}}\frac{u_1'u_2'}{U_1^2} + 2\frac{a_{23}}{a_{11}}\frac{u_2'u_3'}{U_1^2} \pm 2\frac{a_{13}}{a_{11}}\frac{u_1'u_3'}{U_1^2} \Big) \Big] ;$$

and in consistent expansion out to the second order:

$$\overline{e_{1/2}^2}^2 = (a_{11}U_1^2)^2 \cdot \Big[1 + 2\frac{\overline{u_1'^2}}{U_1^2} + 2\frac{a_{22}}{a_{11}}\frac{\overline{u_2'^2}}{U_1^2} + 2\frac{a_{33}}{a_{11}}\frac{\overline{u_3'^2}}{U_1^2} \pm 4\frac{a_{12}}{a_{11}}\frac{\overline{u_1'u_2'}}{U_1^2} + 4\frac{a_{23}}{a_{11}}\frac{\overline{u_2'u_3'}}{U_1^2} \pm 4\frac{a_{13}}{a_{11}}\frac{\overline{u_1'u_3'}}{U_1^2} \Big],$$

$$\overline{e_{1/2}^4} = (a_{11}U_1^2)^2 \cdot \Big[1 + 6\frac{\overline{u_1'^2}}{U_1^2} + \Big(2\frac{a_{22}}{a_{11}} + 4\Big(\frac{a_{12}}{a_{11}}\Big)^2\Big)\frac{\overline{u_2'^2}}{U_1^2} + \Big(2\frac{a_{33}}{a_{11}} + 4\Big(\frac{a_{13}}{a_{11}}\Big)^2\Big)\frac{\overline{u_3'^2}}{U_1^2} \pm 12\frac{a_{12}}{a_{11}}\frac{\overline{u_1'u_2'}}{U_1^2} + \Big(8\frac{a_{12}a_{13}}{a_{11}^2} + 4\frac{a_{23}}{a_{11}}\Big)\frac{\overline{u_2'u_3'}}{U_1^2} \pm 12\frac{a_{12}}{a_{11}}\frac{\overline{u_1'u_3'}}{U_1^2} \Big],$$

$$\overline{e_1^2 e_2^2} = (a_{11}U_1^2)^2 \Big[1 + 6\frac{\overline{u_1'^2}}{U_1^2} + \Big(2\frac{a_{22}}{a_{11}} - 4\Big(\frac{a_{12}}{a_{11}}\Big)^2\Big)\frac{\overline{u_2'^2}}{U_1^2} + \Big(2\frac{a_{33}}{a_{11}} - 4\Big(\frac{a_{13}}{a_{11}}\Big)^2\Big)\frac{\overline{u_3'^2}}{U_1^2} + \Big(4\frac{a_{23}}{a_{11}} - 8\frac{a_{12}a_{13}}{a_{11}^2}\Big)\frac{\overline{u_2'u_3'}}{U_1^2} \Big]$$

From this follows equation (42):

/120

$$\begin{bmatrix} a_{11}^2, & 2a_{11}^2, & 2\,a_{11}\,a_{22}, & 2\,a_{11}\,a_{33}, & 4\,a_{11}\,a_{12}, \\ a_{11}^2, & 2\,a_{11}^2, & 2\,a_{11}\,a_{22}, & 2\,a_{11}\,a_{33}, & -4\,a_{11}\,a_{12}, \\ a_{11}^2, & 6\,a_{11}^2, & (2\,a_{11}\,a_{22}+4\,a_{12}^2), & (2\,a_{11}\,a_{33}+4\,a_{13}^2), & 12\,a_{11}\,a_{12}, \\ a_{11}^2, & 6\,a_{11}^2, & (2\,a_{11}\,a_{22}+4\,a_{12}^2), & (2\,a_{11}\,a_{33}+4\,a_{13}^2), & -12\,a_{11}\,a_{12}, \\ a_{11}^2, & 6\,a_{11}^2, & (2\,a_{11}\,a_{22}-4\,a_{12}^2), & (2\,a_{11}\,a_{33}-4\,a_{13}^2), & 0, \end{bmatrix}$$

$$\begin{bmatrix} 4\,a_{11}\,a_{23}, & 4\,a_{11}\,a_{13} \\ 4\,a_{11}\,a_{23}, & -4\,a_{11}\,a_{13} \\ (8\,a_{12}\,a_{13}+4\,a_{11}\,a_{23}), & 12\,a_{11}\,a_{13} \\ (8\,a_{12}\,a_{13}+4\,a_{11}\,a_{23}), & -12\,a_{11}\,a_{13} \\ (-8\,a_{12}\,a_{13}+4\,a_{11}\,a_{23}), & 0 \end{bmatrix} \circ \begin{bmatrix} U_1^4 \\ U_1^2 \cdot \overline{u_1'^2} \\ U_1^2 \cdot \overline{u_2'^2} \\ U_1^2 \cdot \overline{u_3'^2} \\ U_1^2 \cdot \overline{u_1' u_2'} \\ U_1^2 \cdot \overline{u_2' u_3'} \\ U_1^2 \cdot \overline{u_3' u_1'} \end{bmatrix} = \begin{bmatrix} \overline{e_1^2}^2 \\ \overline{e_2^2}^2 \\ \overline{e_1^4} \\ \overline{e_2^4} \\ \overline{e_1^2\,e_2^2} \end{bmatrix}$$

and furthermore:

$$\begin{bmatrix} 0, & 0, & 0, & 0, & a_{11}\,a_{22}, & 0, & a_{11}\,a_{13} \\ a_{11}^2, & 2\,a_{11}^2, & 2\,a_{11}\,a_{22}, & 2\,a_{11}\,a_{33}, & 0, & 4\,a_{11}\,a_{23}, & 0 \\ 0, & 0, & 0, & 0, & a_{11}\,a_{22}, & 0, & a_{11}\,a_{13} \\ 0, & a_{11}^2, & 0, & 0, & 0, & 0, & 0 \\ 0, & 0, & a_{12}^2, & a_{13}^2, & 0, & 2\,a_{11}\,a_{23}, & 0 \end{bmatrix} \circ \begin{bmatrix} U_1^4 \\ U_1^2 \cdot \overline{u_1'^2} \\ U_1^2 \cdot \overline{u_2'^2} \\ U_1^2\,\overline{u_3'^2} \\ U_1^2\,\overline{u_1' u_2'} \\ U_1^2\,\overline{u_2' u_3'} \\ U_1^2\,\overline{u_3' u_1'} \end{bmatrix} =$$

/121

$$= \begin{bmatrix} \frac{1}{8}\,(\overline{e_1^2}^2 - \overline{e_2^2}^2) \\ \frac{1}{2}\,(\overline{e_1^2}^2 + \overline{e_2^2}^2) \\ \frac{1}{16}\,(\overline{e_1^4} - \overline{e_1^2}^2) - \frac{1}{16}\,(\overline{e_2^4} - \overline{e_2^2}^2) \\ \frac{1}{8}\,(\overline{e_2^4} - \overline{e_2^2}^2) + \frac{1}{8}\,(\overline{e_1^4} - \overline{e_1^2}^2) + \frac{1}{8}\,\overline{e_1^2 e_2^2} - \frac{1}{16}\,(\overline{e_1^4} + \overline{e_2^4}) \\ \frac{1}{16}\,(\overline{e_1^4} + \overline{e_2^4}) - \frac{1}{8}\,\overline{e_1^2 e_2^2} \end{bmatrix}$$

If the quadratic ("squared") signals are designated as 'c':

$$e^2 =: c = \bar{c} + c'$$

then:

$$\frac{1}{2}\left(\overline{e_1^2}^2 \pm \overline{e_2^2}^2\right) = \frac{1}{2}\left(\bar{c}_1^2 \pm \bar{c}_2^2\right),$$

$$\frac{1}{16}\left(\overline{e_1^4} - \overline{e_1^2}^2\right) - \frac{1}{16}\left(\overline{e_2^4} - \overline{e_2^2}^2\right) = \frac{1}{16}\left(\overline{c_1'^2} - \overline{c_2'^2}\right),$$

$$\frac{1}{8}\left(\overline{e_1^4} - \overline{e_1^2}^2\right) + \frac{1}{8}\left(\overline{e_2^4} - \overline{e_2^2}^2\right) + \frac{1}{8}\overline{e_1^2 e_2^2} - \frac{1}{16}\left(\overline{e_1^4} + \overline{e_2^4}\right) =$$

$$= \frac{1}{16}\overline{(c_1' + c_2')^2} - \frac{1}{16}(\bar{c}_1 - \bar{c}_2)^2,$$

$$\frac{1}{16}\left(\overline{e_1^4} + \overline{e_2^4}\right) - \frac{1}{8}\overline{e_1^2 e_2^2} = \frac{1}{16}\overline{(c_1' - c_2')^2} + \frac{1}{16}(\bar{c}_1 - \bar{c}_2)^2$$

and thus:

$$\begin{bmatrix} 0 & 0 & 0 & 0 & a_{11}a_{12} & 0 & a_{11}a_{13} \\ a_{11}^2 & 2a_{11}^2 & 2a_{11}a_{22} & 2a_{11}a_{33} & 0 & 4a_{11}a_{23} & 0 \\ 0 & 0 & a_{12}^2 & a_{13}^2 & 0 & 2a_{12}a_{13} & 0 \\ 0 & 0 & 0 & 0 & a_{11}a_{12} & 0 & a_{11}a_{13} \\ 0 & a_{11}^2 & 0 & 0 & 0 & 0 & 0 \end{bmatrix} \cdot \begin{bmatrix} U_1^4 \\ U_1^2\,\overline{u_1'^2} \\ U_1^2\,\overline{u_2'^2} \\ U_1^2\,\overline{u_3'^2} \\ U_1^2\,\overline{u_1'u_2'} \\ U_1^2\,\overline{u_2'u_3'} \\ U_1^2\,\overline{u_3'u_1'} \end{bmatrix} =$$

$$= a_{11}\cdot\left(\frac{1}{4a_{11}}\right)\cdot\begin{bmatrix} \frac{1}{2}\left(\bar{c}_1^2 - \bar{c}_2^2\right) \\ 2\left(\bar{c}_1^2 + \bar{c}_2^2\right) \\ \frac{1}{4}\overline{(c_1' - c_2')^2} + \frac{1}{4}(\bar{c}_1 - \bar{c}_2)^2 \\ \frac{1}{4}\left(\overline{c_1'^2} - \overline{c_2'^2}\right) \\ \frac{1}{4}\overline{(c_1' + c_2')^2} - \frac{1}{4}(\bar{c}_1 - \bar{c}_2)^2 \end{bmatrix}. \qquad /122$$

There is a very great formal similarity of this equation system with equation system (32). For the usual eight orientations of the hot-wires, the following equations result:

$$\overline{u_1'^2}\,U_1^2 = \frac{1}{(1+k^2)^2}\cdot\left[\frac{\overline{(c_1'+c_2')^2}}{4} - \frac{(\bar{c}_1-\bar{c}_2)^2}{4}\right] = \frac{1}{(1+k^2)^2}\cdot\left[\frac{\overline{(c_3'+c_4')^2}}{4} - \frac{(\bar{c}_3-\bar{c}_4)^2}{4}\right],$$

$$\overline{u_2'^2}\,U_1^2 = \frac{1}{(1+k^2)^2}\left(\frac{1+k^2}{1-k^2}\right)^2\cdot\left[\frac{\overline{(c_1'-c_2')^2}}{4} + \frac{(\bar{c}_1-\bar{c}_2)^2}{4}\right],$$

$$\overline{u_3'^2}\,U_1^2 = \frac{1}{(1+k^2)^2}\left(\frac{1+k^2}{1-k^2}\right)^2\cdot\left[\frac{\overline{(c_3'-c_4')^2}}{4} + \frac{(\bar{c}_3-\bar{c}_4)^2}{4}\right],$$

$$\overline{u_1'u_2'}\,U_1^2 = \frac{1}{(1+k^2)^2}\left(\frac{1+k^2}{1-k^2}\right)\cdot\frac{(\overline{c_2'^2}-\overline{c_1'^2})}{4},$$

$$\overline{u_2'u_3'}\,U_1^2 = \frac{1}{(1+k^2)^2}\left(\frac{1+k^2}{1-k^2}\right)^2\cdot\frac{\overline{(c_5'-c_6')^2}+(\bar{c}_5-\bar{c}_6)^2-\overline{(c_7'-c_8')^2}-(\bar{c}_7-\bar{c}_8)^2}{8},$$

$$\overline{u_3'u_1'}\,U_1^2 = \frac{1}{(1+k^2)^2}\left(\frac{1+k^2}{1-k^2}\right)\cdot\frac{(\overline{c_4'^2}-\overline{c_3'^2})}{4},$$

$$\left(\frac{1+k^2}{2}\right)^2\cdot(U_1^4+2\,\overline{u_1'^2}\,U_1^2)+2\left(\frac{1+k^2}{2}\right)^2\cdot\overline{u_2'^2}\,U_1^2+2\,\frac{1+k^2}{2}\,\overline{u_3'^2}\cdot U_1^2 = \frac{1}{2}(\bar{c}_1^2+\bar{c}_2^2),$$

$$\left(\frac{1+k^2}{2}\right)^2\cdot(U_1^4+2\overline{u_1'^2}\,U_1^2)+2\left(\frac{1+k^2}{2}\right)^2\overline{u_3'^2}\,U_1^2+2\,\frac{1+k^2}{2}\,\overline{u_2'^2}\,U_1^2 = \frac{1}{2}(\bar{c}_3^2+\bar{c}_4^2),$$

$$\left(\frac{1+k^2}{2}\right)^2\cdot(U_1^4+2\,\overline{u_1'^2}\,U_1^2)+2\,\frac{1+k^2}{2}\,\frac{3+k^2}{4}\,(\overline{u_2'^2}\,U_1^2+\overline{u_3'^2}\,U_1^2)\mp$$
$$\mp 4\,\frac{1+k^2}{2}\cdot\frac{1-k^2}{4}\cdot\overline{u_2'u_3'}\,U_1^2 = \frac{1}{2}(\bar{c}_{5/7}^2+\bar{c}_{6/8}^2).$$

Appendix E: Properties of the Step Function $g(t',s,\theta)$

/123

$$g(t',s,\sigma) = \begin{cases} a = \sqrt{\frac{1}{s} - \frac{1}{\sigma}} \;, & 0 \le t' \le s \;, \\ -b = -\frac{1/\sigma}{\sqrt{\frac{1}{s} - \frac{1}{\sigma}}} \;, & s \le t' < \sigma \;, \\ 0 \;, & \sigma \le t' < 1 \;, \end{cases}$$

continues periodically on the t'-axis

$$0 < s < \sigma < 1 \;.$$

1) $$\overline{g} = \int_0^1 dt'\, g(t',s,\sigma) = a \cdot s - b(\sigma - s) =$$

$$= s\sqrt{\frac{1}{s} - \frac{1}{\sigma}} - \frac{\frac{1}{\sigma}(\sigma - s)}{\sqrt{\frac{1}{s} - \frac{1}{\sigma}}} = s\sqrt{\frac{1}{s} - \frac{1}{\sigma}} - \frac{\sigma s}{\sigma}\frac{\frac{1}{s} - \frac{1}{\sigma}}{\sqrt{\frac{1}{s} - \frac{1}{\sigma}}} =$$

$$= s\sqrt{\frac{1}{s} - \frac{1}{\sigma}} - s\sqrt{\frac{1}{s} - \frac{1}{\sigma}} = 0 \;.$$

2) $$\overline{g^2} = \int_0^1 dt'\, g^2(t',s,\sigma) = a^2 \cdot s + b^2(\sigma - s) =$$

$$= s\left(\frac{1}{s} - \frac{1}{\sigma}\right) + \frac{1}{\sigma^2}\frac{\sigma - s}{\frac{1}{s} - \frac{1}{\sigma}} = s\left(\frac{1}{s} - \frac{1}{\sigma}\right) + \frac{\sigma s}{\sigma^2}\frac{\frac{1}{s} - \frac{1}{\sigma}}{\frac{1}{s} - \frac{1}{\sigma}} =$$

$$= 1 - \frac{s}{\sigma} + \frac{s}{\sigma} = 1 \;.$$

3) $$\overline{g^n} = \left(\sqrt{\frac{1}{s} - \frac{1}{\sigma}}\right)^n \cdot s + \left(\frac{-1/\sigma}{\sqrt{\frac{1}{s} - \frac{1}{\sigma}}}\right)^n (\sigma - s) \;;$$

$$\Gamma = \frac{\overline{g^4}}{\overline{g^2}^2} = \overline{g^4} = s\left(\frac{1}{s} - \frac{1}{\sigma}\right)^2 + (\sigma - s)\frac{1/\sigma^4}{\left(\frac{1}{s} - \frac{1}{\sigma}\right)^2} =$$

$$= \sigma / (s(\sigma - s)) - 3/\sigma \;.$$

4) Assuming that $2s \le \theta \le 1/2$

a) for $0 \le r \le s$:

/124

$$\overline{g(t',s,\sigma) \cdot g(t'-r,s,\sigma)} = (s-r)a^2 - r\,ab + (\sigma - r - s)b^2 =$$

$$= 1 - r(a^2 + ab + b^2) \;;$$

b) for $s \le r \le \sigma - s$:

$$\overline{g(t',s,\sigma)\cdot g(t'-r,s,\sigma)} = -s\,ab + (\sigma - s - r)\,b^2 = 1 - [s(a^2+ab) + r\,b^2];$$

c) for $\sigma - s \le r \le \sigma$:

$$\overline{g(t',s,\sigma)\cdot g(t'-r,s,\sigma)} = -(\sigma - r)\cdot ab = 1 - [s\,a^2 + (\sigma - r)\,ab + (\sigma - s)\,b^2];$$

d) for $\sigma \le r \le \frac{1}{2}$:

$$\overline{g(t',s,\sigma)\cdot g(t'-r,s,\sigma)} = 0;$$

e) $$\overline{g(t',s,\sigma)\cdot g(t'-r,s,\sigma)} = \overline{g(t'+r,s,\sigma)\cdot g(t',s,\sigma)} = \overline{g(t',s,\sigma)\cdot g(t'+r,s,\sigma)}.$$

Thus, together we have: /125

$$\overline{g(t',s,\sigma)\cdot g(t'-r,s,\sigma)} = \begin{cases} 1 - [|r|(a^2+ab+b^2)], & 0 \le |r| \le s; \\ 1 - [s(a^2+ab) + |r|^2 b^2], & s \le |r| \le \sigma - s; \\ 1 - [s\,a^2 - (\sigma - |r|)\,ab + (\sigma - s)\,b^2], & \sigma - s \le |r| \le \sigma; \\ 0, & \sigma \le |r| \le \frac{1}{2}; \end{cases}$$

and continues periodically.

If we substitute in a,b, then we obtain:

$$\overline{g(t',s,\sigma)\cdot g(t'-r,s,\sigma)} = \begin{cases} 1 - \frac{|r|}{\sigma}\left(\frac{\sigma}{s} + \frac{1/6}{1/s - 1/6}\right), & 0 \le |r| \le s; \\ -\frac{|r|}{\sigma}\cdot\frac{1/6}{1/s - 1/6}, & s \le |r| \le \sigma - s; \\ -1 + \frac{|r|}{\sigma}, & \sigma - s \le |r| \le \sigma; \\ 0, & \sigma \le |r| \le \frac{1}{2}; \end{cases}$$

and continues periodically.

Appendix F: Computer Program to Check the Conventional Analysis and the Analysis without Root Expansion

/126

Nomenclature:

Name in computer program	normal quantity designation
K	k
S	s
T	σ
GAM	Γ
C2	C_2
C3	C_3
SA1	$\text{sign}(A_1)$
SA2	$\text{sign}(A_2)$
SA3	$\text{sign}(A_3)$
C(1)	C_{12}
C(2)	C_{13}
C(3)	C_{23}
Q(1,N)	$(\bar{e}_1-\bar{e}_2)/(\bar{e}_1+\bar{e}_2)$
Q(2,N)	$(\bar{e}_3-\bar{e}_4)/(\bar{e}_3+\bar{e}_4)$
Q(3,N)	$(\bar{e}_5-\bar{e}_6)/(\bar{e}_5+\bar{e}_6)$
Q(4,N)	$(\bar{e}_7-\bar{e}_8)/(\bar{e}_7+\bar{e}_8)$
LAM( )	λ
MY( )	μ
NY( )	ν
W1	$\overline{u_1'^2}/U^2$
W2	$\overline{u_2'^2}/U^2$
W3	$\overline{u_3'^2}/U^2$
W4	$\overline{u_1'u_2'}/U^2$
W5	$\overline{u_1'u_3'}/U^2$
W6	$\overline{u_2'u_3'}/U^2$
W7	$\overline{u_2'u_3'}/U^2$
F2( )	F^2
E2	$\epsilon_{1/2}^2$
EPS1	$\dfrac{\overline{(c_2'+c_1')^2}-\overline{d}_{1/2}^2}{16\bar{c}_{1/2}^2}$
EPS2	$\dfrac{\overline{(c_2'-c_1')^2}+\overline{d}_{1/2}^2}{16\bar{c}_{1/2}^2}$
F2Q( )	F_q^2

```
                MNF.
                C     Analysis of hot wire signals of turbulent flows          /127
                C
                C     Type and dimension instructions
 1.   0000008         INTEGER O
 2.   0000108         REAL K,LAM(11),MY(11),NY(11),KAP,K2,LAMQ(11),MYQ(11),NYQ(11)
 3.   0000208         DIMENSION R(3),AL(8),C(3),ALM(5,8),G(8,17),GM(8),
                     1  GS(4),GQ(4),Q(4,11),GA(8,17),EP(7),W(7,8,11),F2(11),
                     2  TE(8),F(3,17),X(18),DX(17),XM(17),GQ(8,17),F2Q(11)
                C     Input of parameters and calculations of signals E
                C
                C     Isotropic turbulence (beginning )                        ( )
 4.   0002318         T=1./3.
 5.   0046458         R(1)=T
 6.   0046408         R(2)=0.
 7.   0046478         R(3)=2.*T
 8.   0046508         DO 25 LS=1,2
 9.   0046538         S=1./6.-FLOAT(LS-1)*(1./6.-0.0555)
                C
10.   0046568         ALP12=1.0
11.   0046578         ALP13=1.0
12.   0046578         SA1=-1.0
                C     Isotropic turbulence (end)                               (end)
13.   0046618         SA2=SIGN(1.,ALP12)*SA1
14.   0046638         SA3=SIGN(1.,ALP13)*SA1
15.   0046668         DO 3  L=1,3
16.   0046718         X(L)=S-R(L)
17.   0046728         X(3+L)=T-R(L)
18.   0046758         X(6+L)=1.-R(L)
19.   0047008         X(9+L)=1.+S-R(L)
20.   0047038       3 X(12+L)=1.+T-R(L)
21.   0047078         X(16)=0.0
22.   0047078         X(17)=1.0
23.   0047108         X(18)=1.0
24.   0047118         CALL AMON(X,18)

                                                                               /128
25.   0047148         DO 16  M=1,18
26.   0047158         IF(X(M).LT.0.0)  X(M)=0.0
27.   0047218         IF(X(M).GT.1.0)  X(M)=1.0
28.   0047248      16 CONTINUE
29.   0047268         DO 15  M=1,17
30.   0047308         DX(M)=X(M+1)-X(M)
31.   0047318      15 XM(M)=(X(M+1)+X(M))/2.
32.   0047358         DO 25  LK=1,2
33.   0047368         K=0.2*FLOAT(LK-1)
34.   0047408         C2=ALP12**2
35.   0047418         C3=ALP13**2
36.   0047428         PI=4.*ATAN(1.)
37.   0047468         DO 1 I=1,8
38.   0047518       1 AL(I)=PI/4.
39.   0047548         TE(1)=0.0
40.   0047548         TE(2)=PI
41.   0047558         TE(3)=PI/2.
42.   0047578         TE(4)=-PI/2.
43.   0047608         TE(5)=PI/4.
44.   0047618         TE(6)=-3.*PI/4.
45.   0047638         TE(7)=-PI/4.
46.   0047648         TE(8)=3.*PI/4.
47.   0047668         GAM=1/(S*(T-S))-3./T
                C
48.   0047718         DO 4 I=1,8
49.   0047738         A=AL(I)
50.   0047738         TH=TE(I)
51.   0047758         K2=K**2-1.
52.   0050008         ALM(1,I)=1.+K2*(COS(A))**2
53.   0050078         ALM(2,I)=1.+K2*(SIN(A)*COS(TH))**2
54.   0050178         ALM(3,I)=1.+K2*(SIN(A)*SIN(TH))**2
55.   0050278         ALM(4,I)=K2*COS(A)*SIN(A)*COS(TH)
56.   0050408         ALM(5,I)=K2*COS(A)*SIN(A)*SIN(TH)
57.   0050528         ALM(6,I)=K2*(SIN(A))**2*COS(TH)*SIN(TH)
58.   0050648       4 CONTINUE
```

/129

```
      DO 2  L=1,3
    2   C(L)=0.0
        DO 5  M=1,17
        DO 55  L=1,3
        F(L,M)=FF(S,T,P(L),XM(M))
   55   CONTINUE
        C(1)=C(1)+DX(M)*F(1,M)*F(2,M)
        C(2)=C(2)+DX(M)*F(1,M)*F(3,M)
    5   C(3)=C(3)+DX(M)*F(2,M)*F(3,M)
        C(1)=SIGN(1.,ALP12)*C(1)
        C(2)=SIGN(1.,ALP13)*C(2)
        C(3)=SIGN(1.,ALP12)*SIGN(1.,ALP13)*C(3)
        DO 26 N=1,21
        A1=SA1*SQRT(0.125*FLOAT(N-1))
        A2=ALP12*A1
        A3=ALP13*A1
        DO 6  I=1,8
        DO 6  M=1,17
        G2=ALM(1,I)*(1.+A1*F(1,M))**2+ALM(2,I)*(A2*F(2,M))**2
       1+ALM(3,I)*(A3*F(3,M))**2
       2+2.*ALM(4,I)*(1.+A1*F(1,M))*A2*F(2,M)
       3+2.*ALM(5,I)*(1.+A1*F(1,M))*A3*F(3,M)
       4+2.*ALM(6,I)*A2*F(2,M)*A3*F(3,M)
        GQ(I,M)=G2
    6   G(I,M)=SQRT(G2)
C
C     Calculation of time history  averages
        DO 7 I=1,5
        P=1.0
        DO 8  M=1,17
    8   P=P+DX(M)*G(I,M)
    7   GM(I)=P
        DO 9 J=1,4
        GD(J)=(GM(2*J-1)-GM(2*J))/2.
        GS(J)=(GM(2*J-1)+GM(2*J))/2.
    9   A(J,N)=GD(J)/GS(J)
        EA(N)=GS(2)/GS(1)
        EY(N)=GS(3)/GS(1)
        EY(N)=GS(4)/GS(1)
```

/130

```
        DO 10 I=1,8
        DO 10  M=1,17
   10   GA(I,M)=G(I,M)-GM(I)
        DO 11 J=1,7
   11   EP(J)=0.0
        DO 12  M=1,17
        EP(1)=EP(1)+(GA(2,M)+GA(1,M))**2   * DX(M)
        EP(2)=EP(2)+(GA(2,M)-GA(1,M))**2   * DX(M)
        EP(3)=EP(3)+(GA(4,M)-GA(3,M))**2   * DX(M)
        EP(4)=EP(4)+(GA(2,M)**2-GA(1,M)**2)*DX(M)
        EP(5)=EP(5)+(GA(4,M)**2-GA(3,M)**2)*DX(M)
        EP(6)=EP(6)+(GA(6,M)-GA(5,M))**2   * DX(M)
   12   EP(7)=EP(7)+(GA(8,M)-GA(7,M))**2   * DX(M)
        E1=EP(1)/(800.*GS(1)**2)     *200.
        E2=EP(2)/(800.*GS(1)**2)     *200.
        E3=EP(3)/(800.*GS(2)**2)     *200.
        E4=EP(4)/(800.*GS(1)**2)     *200.
        E5=EP(5)/(800.*GS(2)**2)     *200.
        D6=EP(6)/(1600.*GS(3)**2)    *200.
        D7=EP(7)/(1600.*GS(4)**2)    *200.
        E6=D6-D7
        E7=MY(N)**2*D6-NY(N)**2*D7
        E8=(1.-K**2)/4.*(NY(N)**2-MY(N)**2)
        KAP=(1.+K**2)/(1.-K**2)
C       Exact quantities
        W(1,1,N)=A1**2
        W(1,2,N)=A2**2
        W(1,3,N)=A3**2
        W(1,4,N)=C(1)*ABS(A1*A2)
        W(1,5,N)=C(2)*ABS(A1*A3)
        W(1,6,N)=C(3)*ABS(A2*A3)
        W(1,7,N)=W(1,6,N)
        W(1,8,N)=S2
```

/131

```
C     First approximation
      W(2,1,N)=E1
      W(2,2,N)=KAP**2*E2
      W(2,3,N)=KAP**2*E3
      W(2,4,N)=KAP*E4
      W(2,5,N)=KAP*E5
      W(2,6,N)=KAP**2*E6
      W(2,7,N)=W(2,5,N)
      W(2,8,N)=E2
C     Second approximation
      F2(N)=1./(1.+(LAM(N)**2-1.)*KAP-2.*(1.+3.*K**2)*E2/((1.-K**2)**2))
      W(3,1,N)=W(2,1,N)*F2(N)
      W(3,2,N)=W(2,2,N)*F2(N)
      W(3,3,N)=W(2,3,N)*F2(N)*LAM(N)**2
      W(3,4,N)=W(2,4,N)*F2(N)
      W(3,5,N)=W(2,5,N)*F2(N)*LAM(N)**2
      W(3,6,N)=KAP**2*E7*F2(N)
      W(3,7,N)=KAP**2*E8*F2(N)
      W(3,8,N)=E6
C     VALUE OF PARAMETER
      IF(E1.EQ.0.) GOTO17
      W(4,1,N)=E1*(1.+E2*(1.-(GA1-1.)/2.*E3/E1))**2
      GOTO 14
   13 W(4,1,N)=1.0
   14 W(4,2,N)=E2*(1.+2.*K**2+E2)**2
      W(4,3,N)=W(4,2,N)
      W(4,4,N)=E4*(1.+2.*K**2+2.*E2)
      W(4,5,N)=0.0
      W(4,6,N)=0.0
      W(4,7,N)=1.0
      W(4,8,N)=E6
C
C     Analysis by means of the squared signals
      DO 27  I=1,8
      P=0.0
      DO 28  M=1,17
   28 P=P+DX(M)*GJ(I,M)
   27 GM(I)=P
      DO 29  J=1,4
      GS(J)=GM(2*J-1)-GM(2*J)
      GS(J)=SQRT((GM(2*J-1)**2.+GM(2*J)**2.)/2.)
   29 CONTINUE
      LAMQ(N)=GS(2)/GS(1)
      MYQ(N)=GS(3)/GS(1)
      NYQ(N)=GS(4)/GS(1)
      DO 30  I=1,8
      DO 30  M=1,17
   30 GA(I,M)=GJ(I,M)-GM(I)
      DO 31  J=1,7
   31 EP(J)=0.0
      DO  32  M=1,17
      EP(1)=EP(1)+(GA(2,M)+GA(1,M))**2*DX(M)
      EP(2)=EP(2)+(GA(2,M)-GA(1,M))**2*DX(M)
      EP(3)=EP(3)+(GA(4,M)-GA(3,M))**2*DX(M)
      EP(4)=EP(4)+(GA(2,M)**2-GA(1,M)**2)*DX(M)
      EP(5)=EP(5)+(GA(4,M)**2-GA(3,M)**2)*DX(M)
      EP(6)=EP(6)+(GA(6,M)-GA(5,M))**2*DX(M)
   32 EP(7)=EP(7)+(GA(8,M)-GA(7,M))**2*DX(M)
      E1=EP(1)/(16.*GS(1)**2)
      E2=EP(2)/(16.*GS(1)**2)
      E3=EP(3)/(16.*GS(2)**2)
      E4=EP(4)/(16.*GS(1)**2)
      E5=EP(5)/(16.*GS(2)**2)
      D6=EP(6)/(32.*GS(3)**2)
      D7=EP(7)/(32.*GS(4)**2)
      E6=D6-D7
      E7=MYQ(N)**2*(D6+GJ(3)**2/(32.*GS(3)**2))
     1   -NYQ(N)**2*(D7+GJ(4)**2/(32.*GS(4)**2))
```

/132

```
C     Linear approximation, squared signal                              /133
      EPS1=E1-GD(1)**2/(16.*GS(1)**2)
      EPS2=E2+GD(1)**2/(16.*GS(1)**2)
      W(5,1,N)=E1
      W(5,2,N)=KAP**2*E2
      W(5,3,N)=KAP**2*E3
      W(5,4,N)=KAP*E4
      W(5,5,N)=KAP*E5
      W(5,6,N)=KAP**2*E6
      W(5,7,N)=EPS1
      W(5,8,N)=EPS2
C
C     Quasilinear approximation, squared signal
      W(6,1,N)=EPS1
      W(6,2,N)=KAP**2*EPS2
      W(6,3,N)=W(5,3,N)+KAP**2*G*(2)**2/(16.*GS(2)**2)
      W(6,4,N)=W(5,4,N)
      W(6,5,N)=W(5,5,N)
      W(6,6,N)=KAP**2*E7
      W(6,7,N)=EPS1
      W(6,8,N)=EPS2
C
C     Second approximation, squared signal
      F2Q(N)=1./(1.+2./(1.-K**2)*(LAMQ(N)**2-1.)-2.*EPS1
     1  -(3.+K**2)*(1.+K**2)/(1.-K**2)**2*2.*EPS2)
      W(7,1,N)=W(6,1,N)*F2Q(N)
      W(7,2,N)=W(6,2,N)*F2Q(N)
      W(7,3,N)=W(6,3,N)*F2Q(N)*LAMQ(N)**2
      W(7,4,N)=W(6,4,N)*F2Q(N)
      W(7,5,N)=W(6,5,N)*F2Q(N)*LAMQ(N)**2
      W(7,6,N)=W(6,6,N)*F2Q(N)
      W(7,7,N)=F2Q(N)
      W(7,8,N)=F2Q(N)
    2 CONTINUE                                                          /134
      WRITE(6,200) K,S,T,GAM,C2,C3,SA1,SA2,SA3,C(1),C(2),C(3)
  200 FORMAT(1H1,53H Analysis of hot-wire signals of turbulent flows
     1 //////10X,54H Isotropic turbulence
     2 ///10X,21H Input parameters//11X,9(6H   K      S      T
     3  GAM     C2      C3      SA1     SA2     SA3     C(1)    C(2)
     4 C(3)  //11X,12F8.4//)
      WRITE(6,250)
  250 FORMAT(//10X,11H Averages///10X,104H      Q(1,N)      Q(2,N)
     1    Q(3,N)      Q(4,N)      LAM(N)      MY(N)       NY(N)
     2    F2(N) /)
      DO 300 N=1,11
  300 WRITE(6,350)Q(1,N),Q(2,N),Q(3,N),Q(4,N),LAM(N),MY(N),NY(N),F2(N)
  350 FORMAT(10X,9E13.3/)
      WRITE(6,370)
  370 FORMAT(///10X,96H Precise fluc. quantities
      WRITE(6,380)
  380 FORMAT(10X,10(2H      W1      W2      W3      W4
     1      W5      W6      W7      E2    /)
      WRITE(6,350) ((W(I,J,N),J=1,8),N=1,11)
      WRITE(6,270)
  270 FORMAT(///10X,15H First approx.)
      WRITE(6,380)
      WRITE(6,350)((W(2,J,N),J=1,8),N=1,11)
      WRITE(6,470)
  470 FORMAT(///10X,17H Second  approx.)
      WRITE(6,380)
      WRITE(6,350)((W(3,J,N),J=1,8),N=1,11)
      WRITE(6,570)
  570  FORMAT(///10X,27H Special fourth approx.)
      WRITE(6,380)
      WRITE(6,350)((W(4,J,N),J=1,8),N=1,11)
      WRITE(6,670)
  670 FORMAT(///10X,37H Linear approx., squared signal
      WRITE(6,680)
  680 FORMAT(12X,10(2H      W1      W2      W3      W4
     1      W5      W6      EPS1    EPS2  /)
```

```
242.  0064248        WRITE(6,350)((W(5,O,N),O=1,8),N=1,11)
243.  0064458        WRITE(6,770)
244.  0064508    770 FORMAT(///10X,42HQuasilinear approx., squared signal
245.  0064508        WRITE(6,680)
246.  0064538        WRITE(6,350)((W(6,O,N),O=1,8),N=1,11)
247.  0064748        WRITE(6,870)
248.  0064778    870 FORMAT(///10X,37HSecond approx., squared signal
249.  0064778        WRITE(6,680)
250.  0065028    880 FORMAT(12X,10HW1          W2          W3          W4
     1          W5          W6          F2Q         F2Q   /)
251.  0065028        WRITE(6,350) ((W(7,O,N),O=1,8),N=1,11)
252.  0065238     25 CONTINUE
253.  0065278        END

  1.  0000008        FUNCTION FF(S,T,R,X)
                C     Definition only for non-negative X+R
  2.  0000008        Y=X+R-AINT(X+R)
  3.  0000058        IF(Y.LT.S)  FF=SQRT(1./S-1./T)
  4.  0000158        IF(Y.GE.S.AND.Y.LT.T)  FF=-(1./T)/SQRT(1./S-1./T)
  5.  0000308        IF(Y.GE.T)  FF=0.0
  6.  0000338        RETURN
  7.  0000368        END

  1.  0000008        SUBROUTINE AMON(A,N)
  2.  0000058        DIMENSION A(N)
  3.  0000078        DO 1  L=1,N-1
  4.  0000098        DO 1  M=1,N-L
  5.  0000378        B=AMIN1(A(M),A(M+1))
  6.  0000118        C=AMAX1(A(M),A(M+1))
  7.  0000138        A(M)=B
  8.  0000148        A(M+1)=C
  9.  0000148      1 CONTINUE
 10.  0000208        RETURN
 11.  0000228        END
```

Appendix G: The Second Approximation for the Hot Wire not Aligned in the Main Direction of Flow

/136

According to (27), as a second approximation, we have:

$$(G1)\quad e_{1/2} = \sqrt{a_{11}}\,U_1\Big[\,1 + 2\frac{u_1'}{U_1} \pm 2\frac{a_{12}}{a_{11}}\frac{U_2+u_2'}{U_1} \pm 2\frac{a_{13}}{a_{11}}\frac{U_3+u_3'}{U_1} + \\ + \frac{u_1'^2}{U_1^2} + \frac{a_{22}}{a_{11}}\frac{(U_2+u_2')^2}{U_1^2} + \frac{a_{33}}{a_{11}}\frac{(U_3+u_3')^2}{U_1^2} \pm \\ \pm 2\frac{a_{12}}{a_{11}}\frac{u_1'(U_2+u_2')}{U_1^2} \pm 2\frac{a_{13}}{a_{11}}\frac{u_1'(U_3+u_3')}{U_1^2} + 2\frac{a_{23}}{a_{11}}\frac{(U_2+u_2')(U_3+u_3')}{U_1^2}\Big].$$

From this follows:

$$a_{11}\overline{e_{1/2}^2} = a_{11}^2U_1^2 + a_{11}a_{22}U_2^2 + a_{11}a_{33}U_3^2 \pm 2a_{11}a_{12}U_1U_2 \pm 2a_{11}a_{13}U_1U_3 + \\ + 2a_{11}a_{23}U_2U_3 + (a_{11}a_{22} - a_{12}^2)\overline{u_2'^2} + (a_{11}a_{33} - a_{13}^2)\overline{u_3'^2} + \\ + 2(a_{11}a_{23} - a_{12}a_{13})\overline{u_2'u_3'},$$

$$a_{11}\overline{e_{1/2}^2} = a_{11}^2U_1^2 + a_{11}a_{22}U_2^2 + a_{11}a_{33}U_3^2 \pm 2a_{11}a_{12}U_1U_2 \pm 2a_{11}a_{13}U_1U_3 + \\ + 2a_{11}a_{23}U_2U_3 + a_{11}^2\overline{u_1'^2} + a_{11}a_{22}\overline{u_2'^2} + a_{11}a_{33}\overline{u_3'^2} \pm \\ \pm 2a_{11}a_{12}\overline{u_1'u_2'} \pm 2a_{11}a_{13}\overline{u_1'u_3'} + 2a_{11}a_{23}\overline{u_2'u_3'},$$

$$a_{11}\overline{e_1e_2} = a_{11}^2U_1^2 + (a_{11}a_{22} - 2a_{12}^2)U_2^2 + (a_{11}a_{33} - 2a_{13}^2)U_3^2 + \\ + 2(a_{11}a_{23} - 2a_{12}a_{13})U_2U_3 + \\ + a_{11}^2\overline{u_1'^2} + (a_{11}a_{22} - 2a_{12}^2)\overline{u_2'^2} + (a_{11}a_{33} - 2a_{13}^2)\overline{u_3'^2} \\ + 2(a_{11}a_{23} - 2a_{12}a_{13})\overline{u_2'u_3'}.$$

With the usual X-wire orientations, we thus obtain a linear equation system of 20 equations for the (formal) 12 unknowns $U_1^2, U_2^2, U_3^2, U_1U_2, U_2U_3, U_3U_1, \overline{u_1'^2}, \overline{u_2'^2}, \overline{u_3'^2}, \overline{u_1'u_2'}, \overline{u_2'u_3'}, \overline{u_3'u_1'}$.
From these equations follows:

$$\overline{u_1'^2} - \left(\frac{1-k^2}{1+k^2}\right)^2U_2^2 = \frac{2}{1+k^2}\left[\frac{\overline{(e_2'+e_1')^2}}{4} - \frac{(\overline{e_2}-\overline{e_1})^2}{4}\right],$$

$$\overline{u_1'^2} - \left(\frac{1-k^2}{1+k^2}\right)^2 U_3^2 = \frac{2}{1+k^2}\left[\frac{\overline{(e_4'+e_3')^2}}{4} - \frac{(\bar{e}_4-\bar{e}_3)^2}{4}\right],$$

$$\overline{u_2'^2} + U_2^2 = \frac{2}{1+k^2}\left(\frac{1+k^2}{1-k^2}\right)^2\left[\frac{\overline{(e_2'-e_1')^2}}{4} + \frac{(\bar{e}_2-\bar{e}_1)^2}{4}\right] =$$
$$= \frac{2}{1+k^2}\left(\frac{1+k^2}{1-k^2}\right)^2\left[\frac{\overline{(e_2-e_1)^2}}{4}\right],$$

$$\overline{u_3'^2} + U_3^2 = \frac{2}{1+k^2}\cdot\left(\frac{1+k^2}{1-k^2}\right)^2\left[\frac{\overline{(e_4'-e_3')^2}}{4} + \frac{(\bar{e}_4-\bar{e}_3)^2}{4}\right] =$$
$$= \frac{2}{1+k^2}\cdot\left(\frac{1+k^2}{1-k^2}\right)^2\left[\frac{\overline{(e_4-e_3)^2}}{4}\right],$$

$$\overline{u_1'u_2'} = \frac{2}{1+k^2}\,\frac{1+k^2}{1-k^2}\left[\frac{\overline{(e_2'^2-e_1'^2)}}{4}\right],$$

$$\overline{u_1'u_3'} = \frac{2}{1+k^2}\,\frac{1+k^2}{1-k^2}\left[\frac{\overline{(e_4'^2-e_3'^2)}}{4}\right],$$

$$\overline{u_2'u_3'} + U_2U_3 = \frac{2}{1+k^2}\left(\frac{1+k^2}{1-k^2}\right)^2\cdot\left[\frac{\overline{(e_6'-e_5')^2}}{8} + \frac{(\bar{e}_6-\bar{e}_5)^2}{8} - \right.$$
$$\left. - \frac{\overline{(e_8'-e_7')^2}}{8} - \frac{(\bar{e}_8-\bar{e}_7)^2}{8}\right],$$

$$U_1U_2 = \frac{2}{1+k^2}\cdot\frac{1+k^2}{1-k^2}\cdot\frac{\bar{e}_2^2-\bar{e}_1^2}{4},$$

$$U_1U_3 = \frac{2}{1+k^2}\cdot\frac{1+k^2}{1-k^2}\cdot\frac{\bar{e}_4^2-\bar{e}_3^2}{4},$$

$$\frac{1+k^2}{2}U_1^2 + \frac{1+k^2}{2}U_2^2 + U_3^2 + \frac{2k^2}{1+k^2}\overline{u_2'^2} + \overline{u_3'^2} = \frac{\bar{e}_1^2+\bar{e}_2^2}{2},$$

$$\frac{1+k^2}{2}U_1^2 + U_2^2 + \frac{1+k^2}{2}U_3^2 + \overline{u_2'^2} + \frac{2k^2}{1+k^2}\overline{u_3'^2} = \frac{\bar{e}_3^2+\bar{e}_4^2}{2},$$

and other equations which will not be needed. From the given equations, the final result can be derived:

$$(G2.1)\quad \overline{u_1'^2} = \frac{2}{1+k^2} s_{1/2}^2 \cdot \left[\frac{\overline{(e_2' + e_1')^2}}{4 s_{1/2}^2} - (1 - F_d^{-2}) \cdot \frac{d_{1/2}^2}{s_{1/2}^2} \right] =$$

$$= \frac{2}{1+k^2} s_{1/2}^2 \cdot \left[\frac{s_{3/4}^2}{s_{1/2}^2} \cdot \frac{\overline{(e_4' + e_3')^2}}{4 s_{3/4}^2} - (1 - \frac{s_{3/4}^2}{s_{1/2}^2} F_d^{-2}) \frac{d_{3/4}^2}{s_{1/2}^2} \right] ,$$

$$(G2.2)\quad \overline{u_2'^2} = \frac{2}{1+k^2} s_{1/2}^2 \cdot \left(\frac{1+k^2}{1-k^2}\right)^2 \cdot \left[\frac{\overline{(e_2' - e_1')^2}}{4 s_{1/2}^2} + \right.$$

$$\left. + (1 - F_d^{-2}) \cdot \frac{d_{1/2}^2}{s_{1/2}^2} \right] ,$$

$$(G2.3)\quad \overline{u_3'^2} = \frac{2}{1+k^2} s_{1/2}^2 \cdot \left(\frac{1+k^2}{1-k^2}\right)^2 \cdot \left[\frac{s_{3/4}^2}{s_{1/2}^2} \frac{\overline{(e_4' - e_3')^2}}{4 s_{3/4}^2} + \right.$$

$$\left. + (1 - \frac{s_{3/4}^2}{s_{1/2}^2} F_d^{-2}) \frac{d_{3/4}^2}{s_{1/2}^2} \right] ,$$

$$(G2.3)\quad \overline{u_1' u_2'} = \frac{2}{1+k^2} s_{1/2}^2 \cdot \frac{1+k^2}{1-k^2} \cdot \frac{\overline{(e_2'^2 - e_1'^2)}}{4 s_{1/2}^2} ,$$

$$(G2.4)\quad \overline{u_2' u_3'} = \frac{2}{1+k^2} \cdot s_{1/2}^2 \cdot \left(\frac{1+k^2}{1-k^2}\right)^2 \cdot \left[\frac{\overline{(e_6' - e_5')^2}}{8 s_{5/6}^2} \cdot \frac{s_{5/4}^2}{s_{1/2}^2} - \right.$$

$$- \frac{\overline{(e_8' - e_7')^2}}{8 s_{7/8}^2} \cdot \frac{s_{7/8}^2}{s_{1/2}^2} + \frac{1}{2} \left(\frac{d_{5/4}^2}{s_{1/2}^2} - \frac{d_{7/8}^2}{s_{1/2}^2} \right) -$$

$$\left. - \frac{s_{3/4}}{s_{1/2}} \cdot \frac{d_{1/2}}{s_{1/2}} \cdot \frac{d_{3/4}}{s_{1/2}} F_d^{-2} \right] ,$$

$$(G2.5)\quad \overline{u_3' u_1'} = \frac{2}{1+k^2} s_{1/2}^2 \frac{1+k^2}{1-k^2} \frac{\overline{(e_4'^2 - e_3'^2)}}{4 s_{3/4}^2} \cdot \frac{s_{3/4}^2}{s_{1/2}^2} ,$$

$$(G2.6)\quad U_1^2 = \frac{2}{1+k^2} s_{1/2}^2 \cdot F_d^2 ,$$

$$(G2.7)\quad U_2^2 = \frac{2}{1+k^2} \left(\frac{1+k^2}{1-k^2}\right)^2 d_{1/2}^2 \cdot F_d^{-2} ,$$

$$(G2.8)\quad U_3^2 = \frac{2}{1+k^2} \left(\frac{1+k^2}{1-k^2}\right)^2 d_{3/4}^2 F_d^{-2}$$

with: /139

$$(G2.9)\quad F_d^2 = \frac{1}{2}\left[1 + \frac{1+k^2}{1-k^2}\left(\frac{s_{3/4}^2}{s_{1/2}^2} - 1\right) - 2\,\frac{1+3k^2}{(1-k^2)^2}\,\varepsilon_{1/2}^2 + \right.$$

$$\left. + \frac{1+k^2}{1-k^2}\,\frac{d_{3/4}^2}{s_{1/2}^2} - \frac{2(1+4k^2-k^4)}{(1-k^2)^2}\cdot\frac{d_{1/2}^2}{s_{1/2}^2}\right] +$$

$$+ \sqrt{\frac{1}{4}[\ldots]^2 + \frac{2k^2}{1-k^2}\,\frac{d_{1/2}^2}{s_{1/2}^2} - \frac{1+k^2}{1-k^2}\,\frac{d_{3/4}^2}{s_{1/2}^2}\cdot\frac{s_{3/4}^2}{s_{1/2}^2}} \quad ,$$

$$s_{1/m} = (\bar{e}_m + \bar{e}_1)/2 \quad , \qquad (1, m = 1, \ldots, 8)$$

$$d_{1/m} = (\bar{e}_m - \bar{e}_1)/2 \quad ,$$

$$\varepsilon_{1/2}^2 = \frac{\overline{(e_2' - e_1')^2}}{4\, s_{1/2}^2} \quad .$$

The formulas for the 1st approximation follow formally from the 2nd approximation, if we set:

$$F_d = 1 \qquad \text{and} \qquad s_{1/2} = s_{3/4} = s_{5/6} = s_{7/8}$$

It is easy to see that for the case when $U_2 = U_3$ or $d_{1/2} = d_{3/4} = d_{5/6} = d_{7/8} = 0$ the formulas (G2.1) to (G2.6) and (G2.9) are transformed into the old formulas (33.1) to (33.6) and (36) of section (4.1).
On the other hand, we have: /140

$$F_d^2 \longrightarrow 1$$

$$s_{3/4}^2,\ s_{5/6}^2,\ s_{7/8}^2 \longrightarrow s_{1/2}^2$$

for the transition from turbulent to laminar flow.

Unfortunately, the formulas are very cumbersome. In many cases, they can be made much simpler: If we can assume $U_3=0$ for symmetry reasons and by neglecting tangential cooling ($k=0$), then we have for example:

$$\overline{u_1'^2} = \frac{\overline{(e_2'+e_1')^2}}{2} - 2\,(1-F_d^{-2})\,d_{12}^2 = \frac{\overline{(e_4'+e_3')^2}}{2} ,$$

$$\overline{u_2'^2} = \frac{\overline{(e_2'-e_1')^2}}{2} + 2\,(1-F_d^{-2})\,d_{12}^2 ,$$

$$\overline{u_3'^2} = \frac{\overline{(e_4'-e_3')^2}}{2} ,$$

$$\overline{u_1'u_2'} = \frac{(\overline{e_2'^2}-\overline{e_1'^2})}{2}$$

$$\overline{u_2'u_3'} = \frac{1}{4}\left[\overline{(e_6'-e_5')^2} - \overline{(e_8'-e_7')^2}\right] + (d_{56}^2 - d_{78}^2) ,$$

$$\overline{u_3'u_1'} = \frac{1}{2}\cdot(\overline{e_4'^2}-\overline{e_3'^2}) ,$$

$$U_1^2 = 2\,s_{12}^2\cdot F_d^2 ,$$

$$U_2^2 = 2\,d_{12}^2\,F_d^{-2} ,$$

$$F_d^2 = \left[1+\left(\frac{s_{34}^2}{s_{12}^2}-1\right)-2\,\varepsilon_{12}^2-2\,\frac{d_{12}^2}{s_{12}^2}\right] .$$

We see that changes compared to the aligned X-wire occur only in the equations for $\overline{u_1'^2}$, $\overline{u_2'^2}$, $\overline{u_2'u_3'}$ and F_d^2, where the correction terms for $\overline{u_1'^2}$, $\overline{u_2'^2}$ are of fourth order, and are thus negligible.

Afterword:

/141

These investigations were performed during my employ at the Institute (now Department) for Turbulence Research of the German Research and Test Center for Air and Space Travel e.V. (DFVLR), which is researching with the Hermann-Föttinger Institute for Thermo- and Fluid Dynamics (HFI) of the Technical University of Berlin, the Problems of turbulent flows*. All my collegues of both institutions who provided direct or indirect support in this work are due my sincere gratitude, namely:

Prof. H. Fiedler Ph.D.
J.D. Vagt Ph.D

for their interest, participation, literature hints and criticism,

B. Lehmann for his unpublished (at that time) measured results,

Mrs. I. Gereke, Mrs. H. Walthelm and Mrs. C. King for preparation of the drawings and figures and for typing this quite difficult text.

Manfred Bartenwerfer, Dipl. Phys.
Institute for Experimental Flow Mechanics of the DFVLR,
Dept. of Turbulence Research
Müller-Breslau Str. 8
1000 Berlin 12

*Within the framework of this cooperation, the numerical results were computed in the computer center of the Technical University Berlin.

RESUME

Name: Manfred Rüdiger Bartenwerfer

Date of birth: [redacted] in [redacted]

Citizenship: German

Family status: Married, one child

Education: Entered school in 1949, 4 years grammar school, 6 years public school, 3 years mathematics-science high school, graduation in February 1962 from the Max-Lanck High School in Bielfeld.

Professional training: From 1962, study of physics at the University of Göttingen, advancement to candidacy November 1964, diploma work in the technical area of theoretical physics (under Prof. M. Kohler)*, diploma exam in February 1969.

Occupation: 1969 to 1972, employed at the Institute for Theoretical Physics of the University of Göttingen, from March 1973 to December 1974, employed at the Hermann Föttinger Institute for Thermo- and Fluid Dynamics of the Technical University of Berlin, since January 1975, employed at the Institute (now Department) for Turbulence Research of the German Research and Test Center for Air and Space Travel e.V. (DFVLR).

*On spin polarization of slow electrons in elastic scattering on periodic structures.